UNIVERSITY OF SIENA

UNIVERSITÀ
DI SIENA
1240

DEPARTMENT OF MEDICAL BIOTECHNOLOGIES

PhD PROGRAM IN MEDICAL BIOTECHNOLOGY

SECTION OF MICROBIOLOGY AND VACCINE

XXXIII CYCLE

IDENTIFICATION OF NEUTRALIZING EPITOPES OF TOSV: A MOUSE MODEL

SHIBILY PRATHYUMNAN

Signed 28/04/2021

Supervisor: **Prof.ssa Maria Grazia Cusi**

Student: **Shibily Prathyumnan**

2021

ACKNOWLEDGEMENT

Undertaking this PhD has been a truly life-changing experience for me and it would not have been possible to do without the support and guidance that I received from many people.

Firstly, I would like to express my sincerest gratitude to my supervisor **Prof.ssa Maria Grazia Cusi** for the continuous support of my PhD study and related research, for her patience, motivation, and immense knowledge. Her guidance helped me in all the time of research and writing of this thesis. I appreciate her contributions of time, ideas, and support to make this thesis productive and stimulating. I could not have imagined having a better advisor and mentor for my PhD study.

I thank my fellow lab mates of Molecular Virology Lab, University of Siena, especially **Dr. Gianni Gori Savellini, Dr.ssa Claudia Gandolfo, Dr.ssa Chiara Terrosi** and **Dr.Gabriele Anichini** for the stimulating discussions, for the most cherished time we were working together before deadlines, and for all the fun we have had.

A special word of gratitude to my dearest friend **Dr.ssa Valeria Fox**, LAMMB, University of Siena, for her relentless encouragement and the quality time she spent with me.

I owe a big hug to my queen, **Dr.ssa Karthika Sundaran Shibily** for being my side throughout this course and living every minute of it, without whom I would not have the courage to embark on this journey in first place. A kiss to my little prince, **Aadi** for being such a good little boy and making it possible for me to complete what I started.

My greatest thanks and love to my parents, **Dr. Prathyumnan** and **Mrs. Girija Kumari** and also my in-laws, **Mr. Sundaresan** and **Mrs. Remani** for their endless support. I could not have reached this far without their prayers and sacrifice. I am forever grateful and indebted for their kindness and generosity.

As everything begins and ends in **GOD**, I conclude this acknowledgement by thanking **HIM** for eternal love, care and blessings.

Shibily Prathyumnan

CONTENTS

ABSTRACT

Emerging and re-emerging viral infections have been an important public health problem in recent years. The Bunyavirales order is one of the largest groups of segmented negative-sense single-stranded RNA viruses, which includes many pathogenic strains that cause severe human diseases. Toscana virus (TOSV), a Phlebovirus belonging to the *Phenuiviridae* family, is considered an emergent pathogen associated with acute neurological disease, such as meningitis, meningoencephalitis and encephalitis, occurring in the Mediterranean countries (principally Italy, Spain, France) during the summer months (Valassina *et al*., 2003 a; Valassina *et al*., 2003 b; Charrel *et al*., 2005; Sanbonmatsu –Gàmez *et al*., 2009; Cusi *et al*., 2010).

The mechanisms of protection against natural infection of Phlebovirus are not known, however it is supposed that a virus neutralizing antibody response against the viral glycoproteins could be needed to block the first stages of infection. Neutralizing antibody responses are critical components of the host defense against viral infections and are recognized as a key element in the protective immune response against infection elicited by many prophylactic vaccines (Burton *et al*., 2012; Corti *et al*., 2013). In this setting, we focused our attention on TOSV glycoproteins (Gn and Gc). In a previous work, Prof. Cusi's group was able to localize three neutralizing epitopes on Gn glycoprotein using human mAbs obtained by immortalization of B cells from a subject infected with TOSV. It was postulated that these 3 aminoacid sequences, separated in the primary structure of the protein, had probably a neutralizing activity in the tridimensional structure, in which peptides 1- 2 could be part of a conformational epitope without peptide 3; which instead, is necessary to

strengthen the neutralizing activity and hinder the virus replication, by blocking the binding of Gn to the receptor.

The present study was aimed to confirm *in vivo* the immunogenic efficacy of these three epitopes in various combinations in mouse model and to test if the mice serum obtained show any cross reactivity with other members of Phlebovirus (such as SFNV, PUNV, SNVF, CYPR) and eventually, to evaluate if these cross-reactive sera are also neutralizing against other Phlebovirus. Moreover, these results could be used to design epitopes that can serve as potential targets for the production of epitope-based diagnostics and vaccines against TOSV and other related Phlebovirus.

The study also developed monoclonal antibodies against TOSV NSs protein by immortalization of human B cells by a modified methodology. These monoclonals could be used for better understanding the role of NSs in viral infection of the host and eventually in passive immunization.

CHAPTER 1

1.1 Arbovirus

Newly emerging or re-emerging infections continue to pose significant global public health threats. Arthropod-borne pathogens account more than 17% of infectious diseases, affect millions of people around the world each year, causing over 700,000 deaths annually and comprise a significant proportion of emerging human pathogens (Jones *et al.,* 2008; Woolhouse *et al.,* 2008; Rosenberg *et al.,* 2013; WHO Fact Sheet 2020).

A high proportion of arboviruses associated with human and animal disease circulate in tropical and subtropical regions, where arthropods tend to be abundant. However, many arboviruses also circulate among wildlife species in temperate regions of the world. Despite the global distribution of viruses such as West Nile virus (WNV), Dengue Virus (DENV) and Chikungunya Virus (CHIKV), most of the arboviruses are generally endemic but limited to specific regions of the world. Nevertheless, even within this relatively localized distribution, diffusion to distant locations can occur via animal or vector migration (Liang *et al.,* 2015).

Arboviruses already have a well-known history of emergence and will undoubtedly continue to emerge in the future. There are many unidentified arboviruses that, due to their high mutation rates, may emerge as pathogens although they are not present as epidemic strains in the wild environment (Marchi *et al.,*2018) yet. Considering the history of emergence of some arboviruses, these epidemics have occurred globally as a result of climate and socio-economic changes that have allowed the spread to new geographical areas of viruses previously confined to specific ecological niches. Usually, their dissemination is linked to the natural geographic distribution of the vector, nevertheless climate change and the increasing globalization and habitat modifications, are already resulting in changing

epidemiology of a variety of arboviruses and facilitate their spreading to new geographic locations (Whitehorn *et al.,*2019). Through spillover transmission from enzootic amplification cycles, humans can be infected as incidental and dead-end hosts. By contrast, some arboviruses undergo urban cycle involving humans as amplifying hosts and causing several epidemics in urban areas (Weaver *et al.,* 2010; Coffey *et al.,* 2013; Agarwal *et al.,* 2017).

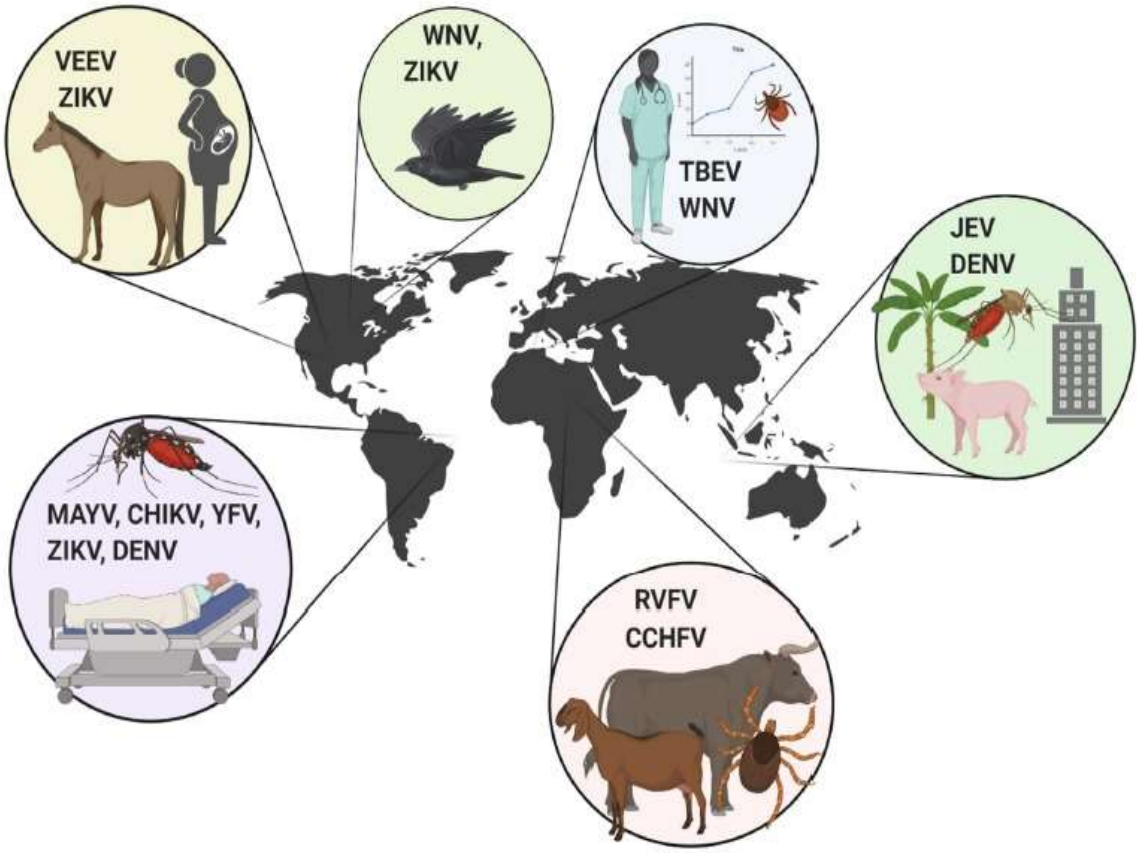

Figure 1: Arbovirus Outbreak. Venezuelan equine encephalitis virus (VEEV), Zika virus (ZIKV), West Nile virus (WNV), tick-borne encephalitis virus (TBEV), Japanese encephalitis virus (JEV), dengue virus (DENV), Rift Valley fever virus (RVFV), Crimean-Congo hemorrhagic fever virus (CCHV), Mayaro virus (MAYV), Chikungunya virus (CHIKV), and Yellow fever virus (YFV).

The majority of arboviruses circulate in nature between an amplifying vertebrate host and a vector arthropod without causing harm to either of them. More than 100 arboviruses are known to infect humans and over 40 to infect domestic animals. In general, these represent 'dead-end infections' in unnatural vertebrate hosts. Examples of important human pathogens include the four dengue viruses (dengue virus 1–4), West Nile virus, Rift Valley fever, Yellow fever virus, and Japanese encephalitis virus. Nairobi sheep disease, Venezuelan equine encephalitis, and Bluetongue virus are examples of veterinary diseases caused by infection with arboviruses. With the single exception of African swine fever virus, arboviruses have RNA genomes consisting of linear or segmented, positive-sense or negative-sense, and single- or double-stranded molecules. (Miller, 2008).

Although some arboviral infections are asymptomatic or cause mild influenza-like illness, many arboviruses are important human and veterinary pathogens causing serious illness ranging from rash and arthritis to encephalitis and hemorrhagic fever (Hollidge *et al.,* 2010). Arthropod-borne viruses (arboviruses) are transmitted biologically among vertebrate hosts by hematophagous (blood feeding) arthropod vectors such as mosquitoes and other biting flies, and ticks. Biological transmission can be vertical, involving the passage of the virus from an infected female vector to both male and female offspring. Horizontal transmission can be from a vector to a vertebrate host via the saliva during blood feeding. This transmission is the most common for the majority of arboviruses and involves infection of the vector alimentary tract following a viremic blood meal, dissemination of the virus in the vector, and eventual virus replication in the salivary glands (Serena *et al.,* 2018).

Most of the arboviruses that cause human/animal diseases belong to four virus families: *Togaviridae* (genus *Alphavirus*), *Flaviviridae* (genus *Flavivirus*), *Bunyaviridae* (genera *Orthobunyavirus, Phlebovirus* and *Nairovirus*) and *Reoviridae* (genera *Coltivirus* and *Orbivirus*) (Agarwal *et al.,* 2017; Powers 2009). In 2016, the family of *Bunyaviridae* was changed to Bunyavirales order (Virus Taxonomy: 2016 Release, EC 48, Budapest, Hungary, August 2016; Virus Taxonomy) to accommodate related viruses with segmented, linear, single-stranded,

negative-sense or ambisense RNA genomes and classified into twelve families (ICTV 2019 release, https://talk.ictvonline.org/taxonomy/).

1.2 Bunyavirales

The Bunyavirales order is one of the largest groups of segmented negative-sense single-stranded RNA viruses, which includes many pathogenic strains that cause severe human diseases**.** It is subdivided into 12 families: *Arenaviridae*, *Cruliviridae*, *Fimoviridae*, *Hantaviridae*, *Leisbuviridae*, *Mypoviridae*, *Nairoviridae*, *Peribunyaviridae*, *Phasmaviridae*, *Phenuiviridae*, *Tospoviridae* and *Wupedeviridae* comprising of 46 genera. Four families contain members that cause life-threatening diseases in humans: *Hantaviridae*, *Nairoviridae*, *Peribunyaviridae* and *Phenuiviridae* (Wichgers *et al.,* 2018; Abudurexiti *et al.,* 2019). These families include the species Bunyamwera virus (BUNV), Crimean-Congo haemorrhagic fever virus (CCHFV), Hantaan virus (HTNV), La Crosse virus (LACV), Rift Valley fever virus (RVFV), Severe fever with thrombocytopenia syndrome virus (SFTSV), and Sin Nombre virus (SNV). Three families within Bunyavirales contain members that infect plants as their primary host: *Fimoviridae*, *Phenuiviridae*, and *Tospoviridae*. Within these families, there is one genus of plant infecting viruses: Emaravirus, Tenuivirus, and Orthotospovirus respectively (Herath *et al.,* 2020). Most bunyaviruses are transmitted by insects or ticks, with the exception of members from the family *Hantaviridae* that are entirely rodent borne (Zhang, 2014).

Viruses in the order Bunyavirales infect arthropods, plants, protozoans, and vertebrates. Their RNA genomes are segmented and exhibit negative or ambisense polarity. Depending on the family and genus, bunyaviruses (now referring to all members of the Bunyavirales) has a fixed number of genome segments which range from two to eight, with plant viruses having the largest numbers of segments. (Herath *et al.,* 2020).

The viral particles have a diameter of 80 to 120 nm and are composed of helicoidal nucleocapsids containing three RNA segments that code for a minimum of four structural proteins in a negative-sense orientation named small (S), medium (M) and

large (L), reflecting their relative nucleotide length. Viruses within each genus share similar overall segment length and a generally common expression strategy for their encoded protein products (Schmaljohn & Nichol, 2006). The genetic organization of the segments is similar across all genera; each template strand further contains conserved complementary oligonucleotide sequences at their 5'- and 3'-ends (NTRs), allowing the formation of "panhandle" structures and noncovalently closed circular RNAs (Schmaljohn & Elliott 2014). These terminal nucleotide sequences, which surround a single transcriptional unit, are highly conserved among viruses within a genus, but differ from those of viruses in other genera. These structures seem to be important for transcription mechanisms and genome replication or for genome packaging and for virion assembly (Valassina *et al.,*2003). There are differences in the patterns of sizes of the viral RNAs and structural proteins between the different genera, and the expression strategy of non-structural proteins also differs between different genera. (Elliot *et al.,* 2014).

The coding regions of each genome segment lie between terminal non-translated sequences that vary in length. The 3' and 5' genomic RNA termini are essential for RNA synthesis and are typically invariant.

A major difference between bunyaviruses from other enveloped viruses is that the virions are devoid of any classical matrix or capsid protein. The matrix function is performed by the cytoplasmic tail of Gn, one of the two glycoproteins, that not only contains a Golgi localization signal but is also involved in the initiation of the budding process and the packaging of ribonucleoproteins (RNPs) into virus particles (Spiegel *et al.,* 2016).

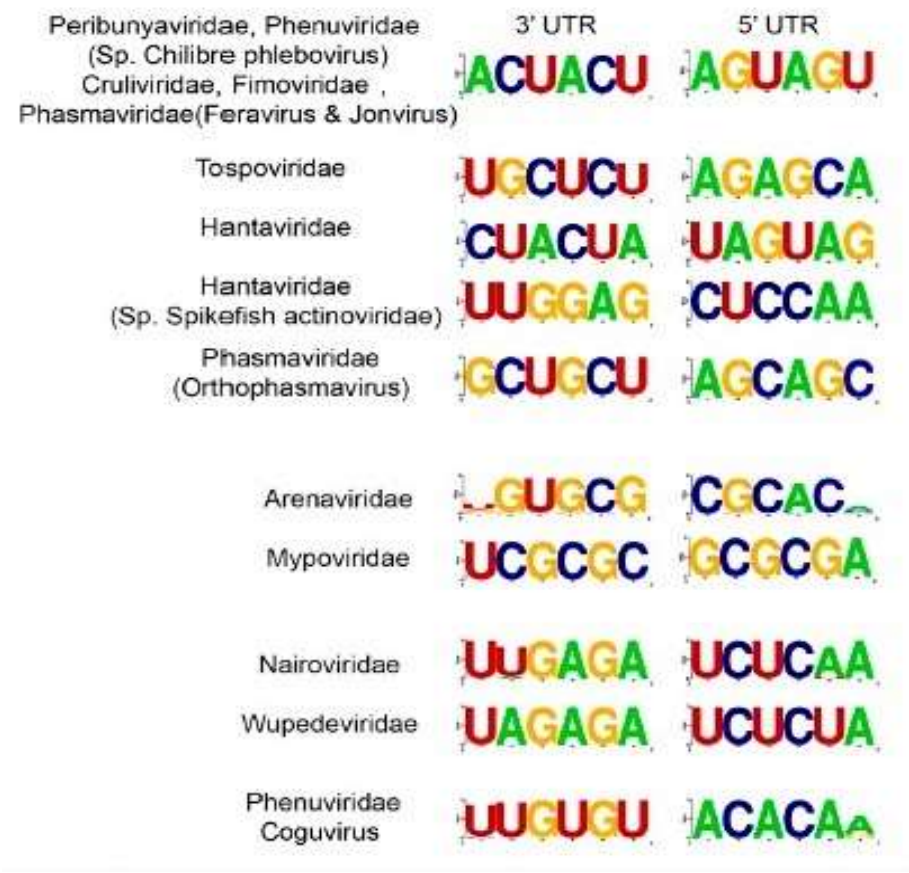

Figure 2: Consensus nucleotide sequence of the 3' and 5' termini for each genomic segment of Bunyaviriales.

The S segment (1869 nucleotides) of all bunyaviruses encodes the nucleocapsid (N) protein, whose primary role is to encapsidate the viral RNA-replication products and forms the ribonucleoprotein (RNP) complex. The N protein is the most abundant viral product in virions and infected cells. The S segments of most members of the genera Orthobunyavirus, Tospovirus and Phlebovirus also encode a non-structural protein called NSs, that shows a low conservation across the Phlebovirus genus compared to other viral proteins, with sequence similarities ranging only from approximately 10% to 30% (Bichaud *et al.,* 2016; Yu *et al.,* 2011). The NSs protein is an important virulence determinant, acting as an inhibitor of the antiviral type I IFN system of the mammalian host (Boshra *et al.,* 2011; Weber *et al.,* 2014 a; Weber *et al.,*2014 b). Hantaviruses and Nairoviruses use the negative-sense coding RNA to

express a single protein N from their virion complementary-sense RNA (cRNA) (Schmaljohn & Hooper 2001).

The N and NSs proteins of Orthobunyaviruses are translated from the same mRNA encoded by the S segment genome, whereas the Phlebovirus and Tospovirus N and NSs proteins are translated from separate mRNAs transcribed from the genomic and antigenomic strands, respectively (ambisense gene expression) (Walter & Barr 2011). In particular, a viral complementary, subgenomic mRNA corresponding to the 3' half of the viral S RNA codes for the N protein, and the viral subgenomic mRNA corresponding to the 5' half of the viral S RNA codes for the NSs proteins.

Among phleboviruses, there is a short intergenic region (IR), a sequence stretch that is proposed to form an irregular double-stranded RNA (dsRNA) structure in the region between the two ORFs (Boshra *et al.,* 2011). Formation of the RNP (ribonucleoprotein) depends on the association of viral RNA with multiple copies of the N protein so that the RNA becomes encapsidated along its entire length (Walter & Barr 2011). Whilst the primary role of the N protein is to provide structural uniformity to the RNA genome, the additional roles include interaction with membrane glycoproteins (Hepojoki *et al.,* 2010; Overby *et al.,* 2007; Ribeiro *et al.,*2009; Shi *et al.,* 2007; Snippe *et al.,* 2007) and interaction with the viral RNA dependent RNA polymerase (RdRp) to allow access to the RNP during RNA synthesis (Walter & Barr 2011).

The M segment (ranging from 3,600 to 4,900 nucleotides) of all members of the *Phenuiviridae* family encodes, in a single open reading frame (ORF) of cRNA, a polyprotein precursor, that is processed into the glycoproteins Gn and Gc (referring to the amino-terminal or carboxy-terminal coding of the proteins) (Walter & Barr 2011).The Gn/Gc precursor is translocated, due to a signal sequence preceding Gn, from the cytoplasm into the membrane of the endoplasmic reticulum (ER), where it is cleaved into Gn and Gc components by host-cell proteases (Schmaljohn & Elliott 2014). In the ER, Gn and Gc are glycosylated with N-linked glycans (Kuismanen *et al.,* 1984;Matsuoka *et al.,* 1988) of the high-mannose type, which can be processed

into hybrid and complex forms upon import of the two glycoproteins into the Golgi apparatus (Kuismanen *et al.,* 1984; Matsuoka *et al.,* 1988; Madoff *et al.,* 1982; Shi *et al.,* 2005). By virtue of a retention signal, the heavily glycosylated Gn– Gc heterodimer is retained in the Golgi, where it associates with RNPs to mediate assembly and budding of mature virus particles, that are released from infected cells by exocytosis. The Gn–Gc heterodimer performs critical roles in mediating virus assembly, formation of the virus particle and attachment to new target cells (Schmaljohn & Nichol 2006).

Most members of the genera Orthobunyavirus, Phlebovirus and Tospovirus also encode an NSm protein. The Tospovirus NSm protein is translated from a separate mRNA encoded by the antigenome, whereas the Orthobunyavirus and Phlebovirus NSm is cleaved by cellular proteases from the same polyprotein precursor that yields the Gn and Gc proteins (Walter & Barr 2011). Bunyavirus NSm protein is thought to play a role in virus assembly (Shi *et al.,* 2007). In contrast, the Phlebovirus NSm has been shown to be non-essential (Gerrard *et al.,* 2007), but may play accessory roles in the regulation of apoptosis (Won *et al.,* 2007). The M segment of Tospoviruses uses an ambisense coding strategy. The cRNA has a gene order of 5'-Gn-Gc-3', and the vRNA encodes NSm. There are separate, subgenomic messages for the Gc–Gn precursor and for NSm (Law *et al.,* 1992; Kormelink *et al.,* 1992). Hantaviruses have an M segment cRNA gene order of 5'-Gc-Gn-3' (Schmaljohn *et al.,* 1987), while a gene order of 5'-Gn-Gc-3' was determined for the Nairovirus (Marriott *et al.,* 1992).

The M segment gene order and the coding strategy varies among viruses in the Phlebovirus genus (Schmaljohn & Elliott 2014). For Rift Valley fever virus (RVFV) and Toscana virus (TOSV), the cRNA gene order of M fragment is 5'-NSm-Gn-Gc-3' (Collett *et al.,* 1985; Valassina *et al.,* 2003). In general, M-segment gene products have a cysteine content of approximately 4% to 7%. Positions of these residues are highly conserved in the M-segment products of related viruses, suggesting that the positions may be crucial for determining correct polypeptide folding. In the case of TOSV, there are nine sites of glycosylation (Valassina *et al.,* 2003). All M-segment

polyproteins display variable numbers of predicted transmembrane regions, and a hydrophobic sequence at the carboxy-terminus, indicative of a membrane anchor region. Therefore, the M segment translation products of viruses in the *Phenuiviridae* family are typical class I membrane proteins, with the amino terminus exposed on the surface of the virion and the carboxy-terminus anchored in the membrane (Schmaljohn & Elliott, 2014).

The L segment (range in size from about 237kD for Phleboviruses, to 459kD for Nairoviruses) contains a single open reading frame (ORF) that encodes the viral polymerase. The L ORF is expressed via a viral-complementary mRNA (Valassina M. *et al.,* 2003). All L segments of viruses of the family use conventional negative sense coding strategies (Schmaljohn & Elliott 2014). Bunyavirus L proteins perform several complex functions that together result in the generation of RNA-replication and mRNA-transcription products from their respective viral templates (Walter & Barr 2011). Primary transcription of negative-sense viral RNA to mRNA is initiated by interaction of the virion-associated polymerase (L) and the three viral RNA templates (Bouloy & Hannoun 1976; Ranki & Pettersson 1975). Members of the *Phenuiviridae* family use primers cleaved from cytoplasmic host-cell mRNAs for extension. Cleavage of the capped primers is accomplished by endonucleolytic activity associated with virions (Patterson JL. *et al.,* 1984). Alignments with homologues of other members of the *Phenuiviridae* family indicate that L protein-associated endonuclease domain is well-conserved, containing metal-binding and catalytic lysine residues, and shows a high degree of sequence similarity to putative endonuclease motifs of L proteins from other segmented, negative-stranded RNA viruses such as Arenaviruses, Emaraviruses and Tenuiviruses (Walter & Barr 2011).

1.3 *Phenuiviridae*

Phenuiviridae is a virus family belonging to the order Bunyavirales established in 2016. Members of *Phenuiviridae* are enveloped viruses with helical capsid morphology. Envelope glycoproteins of these viruses are distributed with icosahedral symmetry (T=12) [http://viralzone.expasy.org/7101?outline=all_by_species]. *Phenuiviridae* is a

negative single stranded RNA (-ssRNA) virus family [https://www.uniprot.org/taxonomy/1980418]. *Phenuiviridae* family members include human and animal pathogenic viruses transmitted by arthropod vectors, including phlebotomine sandflies, mosquitos and ticks (Matsuno *et al.,* 2015; Palacios *et al.,* 2013). They can cause a variety of clinical syndromes ranging from a brief, self-limiting febrile illness, to retinitis, encephalitis, meningoencephalitis and fatal haemorrhagic fever (Liu *et al.,* 2003).

Replication begins with the attachment of viral proteins to host receptors and entry of virus by endocytosis. Acidification of endocytic vesicles causes uncoating of the virus which is followed by fusion of viral membranes with that of the host endosomes. Primary transcription of viral complementary mRNA occurs and the L, M and S mRNAs are translated. Transcription starts by viral RNA dependent RNA polymerase (L) binding to a promoter on each encapsidated segment, and is terminated by a strong hairpin sequence at the end of each gene. These are capped by L protein during synthesis using cap snatching, but are not polyadenylated. S-segment uses ambisense strategy to encode for several proteins: both genomic and antigenomic RNA are transcribed. The hairpin sequence is a stop polymerase signal which prevents ambisense transcription from producing dsRNA. M segment encodes for several polyproteins by leaky scanning, which are cleaved by host protease into Nsm, Gn and Gc proteins. This is followed by RNA replication and morphogenesis. Mature virions are released by fusion of virus-containing cytoplasmic vesicles with the plasma membrane and budding. (David *et al.,*2007; https://viralzone.expasy.org/7101?outline=all_by_species)

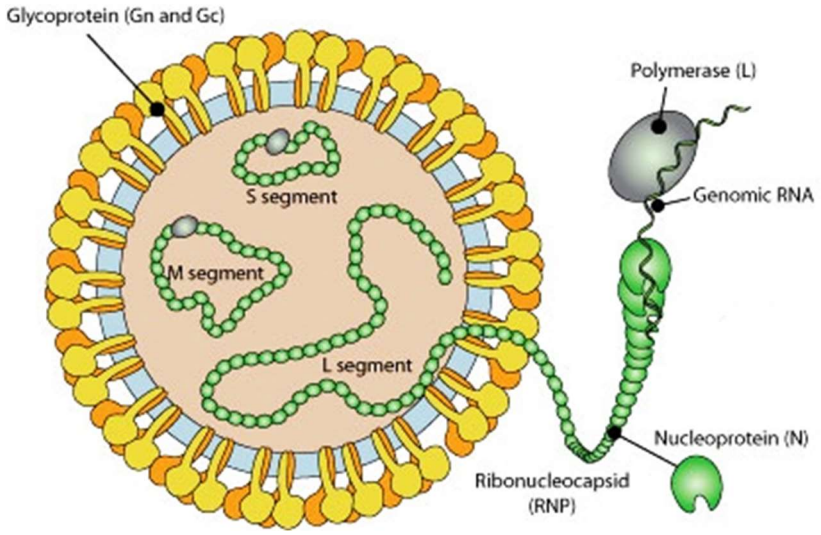

Figure:3 Structure of a Phenuiviridae virion *(https://viralzone.expasy.org)*

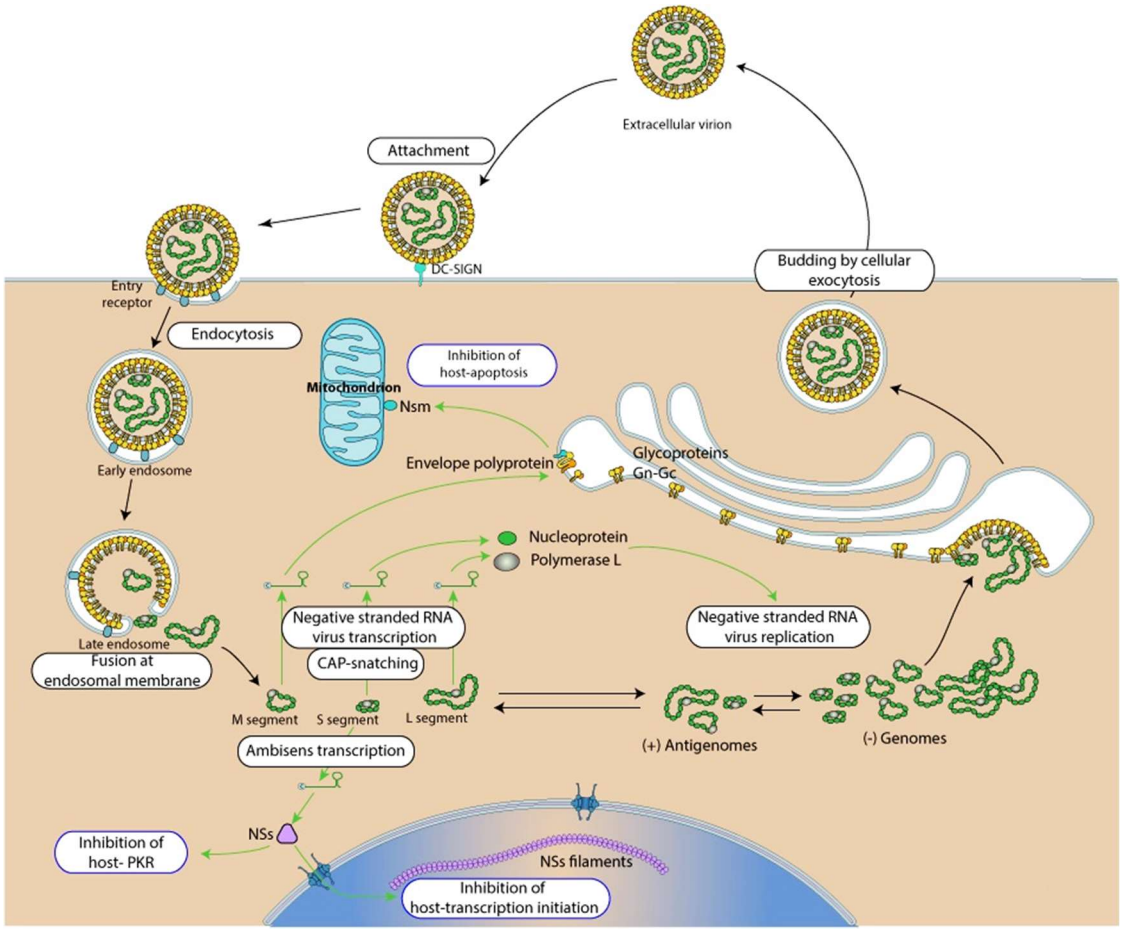

Figure:4 Replicative cycle of a Phenuiviridae virion

(https://viralzone.expasy.org)

Table:1 Taxonomical Classification of *Phenuiviridae* family

Family *Phenuiviridae*		
Genus	**Species**	**Notable Viruses**
Banyangvirus	Guertubanyangvirus	Guertu virus (GTV)
	Heartland banyangvirus	Heartland virus (HRTV)
	Huaiyangshanbanyangvirus	Severe Fever with Thrombocytopenia Syndrome Virus (SFTSV)
Beidivirus	Dipteran beidivirus	Húběidiptera virus 3 (HbDV-3)
Goukovirus	Cumutogoukovirus	Cumuto virus (CUMV)
	Gouleakogoukovirus	Gouléako virus (GOLV)
	Yichang insect goukovirus	Yíchāng insect virus (YcIV)
Horwuvirus	Horsefly horwuvirus	Wǔhàn horsefly virus (WhHV)
Hudivirus	Dipteran hudivirus	Húběidiptera virus 4 (HbDV-4)
Hudovirus	Lepidopteran hudovirus	Húběi lepidoptera virus 1 (HbLV-1)
Kabutovirus	Huangpikabutovirus	Huángpí tick virus 2 (HpTV-2)
	Kabuto mountain kabutovirus	Kabuto mountain virus (KAMV)
Laulavirus	Laurel Lake laulavirus	Laurel Lake virus (LLV)
Mobuvirus	Mothramobuvirus	Mothra virus (MTHV)
Phasivirus	Badu phasivirus	Badu virus (BADUV)
	Phasi Charoen-like phasivirus	PhasiChaeron-like virus (PCLV)
	Wutai mosquito phasivirus	Wǔtái mosquito virus (WtMV)
Phlebovirus	Bujaruphlebovirus	Bujaru virus (BUJV)
		Munguba virus (MUNV)
	Candiru phlebovirus	Alenquer virus (ALEV)
		Ariquemes virus (ARQV)
		Candirú virus (CDUV)

		Itaituba virus (ITAV)
		Jacundá virus (JCNV)
		Maldonado virus (MLOV)
		Morumbi virus (MR(M)BV)
		Mucura virus (MCRV/MRAV)
		Nique virus (NIQV)
		Oriximiná virus (ORXV)
		Serra Norte virus (SRNV)
		Turuna virus (TUAV)
	Chilibrephlebovirus	Cacao virus (CACV)
		Chilibre virus (CHIV)
	Frijoles phlebovirus	Frijoles virus (FRIV)
		Joá virus (JOAV)
	Mukawaphlebovirus	Mukawa virus (MKWV)
	Punta Toro phlebovirus	Buenaventura virus (BUEV)
		Campana virus (CMAV)
		Capira virus (CAPIV)
		Coclé virus (CCLV)
		Leticia virus (LTCV)
		Punta Toro virus (PTV)
	Rift Valley fever phlebovirus	Rift Valley fever virus (RVFV)
	Salehabadphlebovirus	Adana virus (ADAV)
		Adria virus (ADRV)
		Alcube virus
		Arbia virus (ARBV)
		Arumowot virus (AMTV)

		Bregalaka virus (BREV)
		Medjerda Valley virus (MVV)
		Odrénisrou virus (ODRV)
		Olbia virus (OLBV)
		Salehabad virus (SALV)
		Zaba virus (ZABAV)
	Sandfly fever Naples phlebovirus	Arrábida virus (ARRV)
		Balkan virus (BALKV)
		Fermo virus (FERV)
		Gordil virus (GORV)
		Granada virus (GRV = GRAV)
		Massilia virus (MASV)
		Punique virus (PUNV)
		Saddaguia virus (SADV)
		Saint-Floris virus (SAFV)
		Sandfly fever Naples virus (SFNV)
		Tehran virus (THEV)
		Toscana virus (TOSV)
		Zerdali virus (ZERV)
	Uukuniemi phlebovirus	Chizé virus (CHZV)
		EgAN 1825–61 virus (EGAV)
		Fin V 707 virus (FINV)
		Oceanside virus (OCV = OCEV)
		Pontevès virus (PTVV)
		St. Abbs Head virus (SAHV)
		Uukuniemi virus (UUKV)

		ZalivTerpenyia virus (ZTV)
Pidchovirus	Pidgeypidchovirus	Pidgey virus (PGYV)
Tenuivirus	Echinochloa hoja blancatenuivirus	Echinochloa hoja blanca virus (EHBV)
	Iranian wheat stripe tenuivirus	Iranian wheat stripe virus (IWSV)
	Maize stripe tenuivirus	Maize stripe virus (MStV = MSpV)
	Rice grassy stunt tenuivirus	Rice grassy stunt virus (RGSV)
	Rice hoja blancatenuivirus	Rice hoja blanca virus (RHBV)
	Rice stripe tenuivirus	Rice stripe virus (RSV = RStV)
	Urochloa hoja blancatenuivirus	Urochloa hoja blanca virus (UHBV)
Wenrivirus	Shrimp wenrivirus	Wēnzhōu shrimp virus 1 WzSV-1
Wubeivirus	Dipteran wubeivirus	Húběidiptera virus 5 (HbDV-5)
	Fly wubeivirus	Wǔhàn fly virus 1 (WhFV-1)

1.4 Toscana Virus

Within the *Phenuiviridae* family of Bunyavirales order, Phlebovirus genus contains more than 80 viruses, with about half classified into nine antigenic complexes that are regarded as species, whereas 33 are considered as tentative species in the genus. The viruses of the genus Phlebovirus are present throughout the world and their name is associated with their principal vector, phlebotomine sandflies, however there are prominent exceptions, such as RVFV which is primarily associated with Aedes species mosquitoes and Uukuniemi virus (UUKV), which is associated with the tick Ixodesricinus (Schmaljohn& Elliott 2014).

Among sandfly-transmitted viruses, three serotypes have been identified: Naples, Sicilian and Toscana serocomplex. Naples and Sicilian serotypes have the widest geographical distribution which is related to the distribution of the vector (*P. pappatasi*) and they have been isolated from sandflies in Africa, central Asia, the Americas and Europe.

Toscana Virus (TOSV) was first isolated in 1971 in central Italy (in Monte Argentario, Grosseto Province) from two different species of sandflies, *Phlebotomus perniciosus* (*P. perniciosus*) and *Phlebotomus perfiliewi* (*P. perfiliewi*) (Verani *et al.,* 1982; Verani *et al.,* 1984; Verani *et al.,*1988); and it was registered in the International Catalogue of Arbovirus, belonging to the Phlebovirus genus, in 1980. Other strains of Toscana virus were isolated from *P. perfiliewi*, in other parts of Italy where the insect vectors were present (Verani *et al.*, 1982, 1984a, 1988; Ciufolini *et al.,* 1985). The virus can be transmitted transovarially in the insect vectors, but its animal reservoir has not been identified yet. TOSV isolation from the brain of a bat (*Pipistrellus kuhli*) has been the only evidence of the possible involvement of this species in the ecology of the virus (Verani *et al.,* 1982, Verani *et al.,* 1984, Ciufolini *et al.,* 1985). However, serological investigations have shown that anti-TOSV specific IgG has been detected in some

animal species, indicating that this virus can also infects animals (Ciluna *et al.,* 2007).

TOSV belongs to the Naples serocomplex and is the only virus associated with neuroinvasive infections.

1.4.1 Epidemiology

TOSV is widespread in the Mediterranean basin, and evidence of human infection has been found in Italy, France, Spain, Portugal, Cyprus, and Turkey. Phylogenetic analysis has distinguished two genotypes of TOSV, A and B; the first is circulating mainly in Italy, France, Algeria, Tunisia, Turkey, and the second in Spain, France, Portugal, Morocco, Turkey indicating a different geographic distribution possibly related to the vector. A third lineage, C, has been recently added and identified in a strain circulating in Croatia and Greece (Punda-Polić *et al.,* 2012). As already seen for other arbo-bunyavirus, the diffusion of TOSV is expanding with the geographic distribution of its vector, leading to a higher pathogenicity in non-exposed populations of areas outside the current prevalence (Mediterranean basin) (Collao *et al.,*2009). This distribution, evolving with the climate, globalization and habitat modification, has implications for the epidemiology of TOSV.

TOSV represents an important emerging pathogen in Europe and Northern Africa (Charrel *et al.,* 2012).The first case of TOSV infection reported from Spain occurred in a Swedish tourist after a visit to Catalonia and was documented by plaque reduction neutralization test (PRNT) (Eitrem *et al.,* 1991), whereas the presence of the virus in Portugal was suspected on the basis of a strain isolated from the cerebrospinal fluid (CSF) of a Swedish patient who was returning to his home country from Portugal (Ehrnst *et al.,* 1985). A large epidemiological study conducted in the province of Granada by a Spanish group (Sanbonmastu *et al.,* 2005) established TOSV as one of the most important etiological agents of CNS diseases. The first case of TOSV infection acquired in France was reported in a German traveler who was returning from southern France (Dobler *et al.,* 1997). An

interesting study on seroprevalence was conducted in volunteer blood donors in France, showing that 12% of sera from healthy donors and 18.9% of sera from patients hospitalized for CNS infection were IgG positive for TOSV, confirming that TOSV circulates in southeastern France and that a significant proportion of healthy blood donors has a history of TOSV infection (De Lamballerie *et al.,* 2007).

Seroconversion to TOSV was observed in Swedish United Nations soldiers based in Cyprus without any clinical manifestations (Eitrem *et al.,* 1990). Similarly, populations living on the Ionian Islands and western mainland of Greece also showed a seroprevalence of 60% and 35% respectively (Charrel *et al.,* 2005). Although the seroprevalence of antibodies to TOSV was found to be low in Germany, TOSV infection could be considered in patients returning from virus-endemic areas who had fever and headaches or symptoms of meningitis (Schwarz *et al.,* 1995). Some infections imported into Germany by people returning from a vacation in Tuscany, France, Spain or Portugal have been reported (Dobler *et al.,* 1997; Ehrnst *et al.,* 1985; Schwarz *et al.,* 1995; Imirzalioglu *et al.,* 2006; Kuhn *et al.,* 2005; Defuentes *et al.,* 2005; Schwarz *et al.,* 1996). Another case of imported TOSV infection has been recorded in the Netherlands, where a patient with meningoencephalitis was hospitalized after a vacation in central Italy during the summer (Beersma *et al.,* 2004). Other imported TOSV infections acquired by travelers have been reported during the past few years. In Switzerland, a case of meningitis due to TOSV infection was reported in a tourist who had stayed on the coast of Tuscany (Elba Island) during August (Sonderegger *et al.,* 2008). The presence of sandfly fever virus was also investigated in Bosnia and Herzegovina in a serological study of the local population. The presence of specific anti-TOSV antibodies was revealed in a group of patients during 2006-2008 (Hukic *et al.,* 2009).

In Italy, clinical and epidemiological studies have demonstrated human infection by TOSV in Tuscany (Braito *et al.,* 1998; Nicoletti *et al.,* 1991; Terrosi *et al.,* 2009; Valassina *et al.,* 2003; Cusi *et al.,* 2010; Valassina *et al.,*1996), Marches (Nicoletti

et al., 1991), Sicily (Amodio *et al.,* 2012; Calamusa *et al.,* 2012; Colomba *et al.,* 2012; Valassina *et al.,* 1996), Emilia Romagna (Portolani *et al.,*2002; Vocale *et al.,* 2012), Piedmont (Valassina *et al.,* 2003), Umbria (Baldelli *et al.,* 2004; Francisci *et al.,* 2003), Campania (Di Nicuolo *et al.,* 2005), Sardinia (Venturi *et al.,* 2007), Elba island (Gabriel *et al.,* 2010; Sonderegger *et al.,* 2009), and Calabria (Greco *et al.,* 2012).The rate of TOSV associated meningitis during summer in Italy was demonstrated by an epidemiological study conducted on hospitalized patients residing in Tuscany during the 1995-1998 period. About eighty percent of cases of aseptic meningitis were due to TOSV infection during summer period (Valassina *et al.,* 2000).

All studies agree regarding the monthly distribution of human cases of TOSV infections: the highest risk of acquiring TOSV is in August, then July and September, and finally June and October. Populations living in rural areas and with high levels of outdoor activity are at the greatest risk of TOSV infection. Seroprevalence studies performed in southern Europe indicate that a significant proportion of the exposed population (5 to 50%, depending on the studies and on the regions) possess antibodies that react with Toscana virus. According to these data, TOSV is the most prevalent arthropod-borne virus in Europe far ahead of tick-borne encephalitis virus, West Nile virus, or dengue virus. Hence there is a great need to draw attention to TOSV (Charrel *et al.,* 2005).

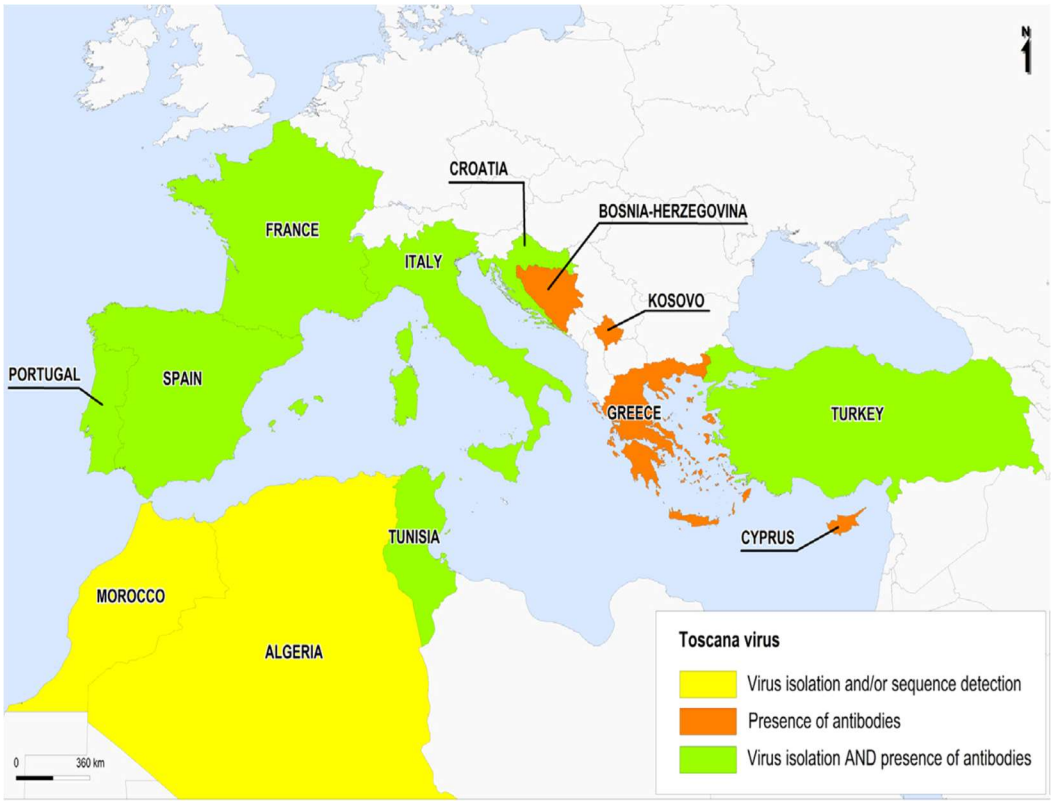

Figure:5 Toscana Virus in the Mediterranean Basin (Charrel, 2014)

1.4.2 Clinical manifestations of TOSV infection

TOSV infections have an incubation period of three to six days (Sonderegger *et al.,* 2009). The clinical picture is variable. In addition to meningitis and meningoencephalitis, few cases of encephalitis without meningitis have been described (Dioniso *et al.,* 2001). The high seroprevalence suggests that asymptomatic infection is rather common and TOSV therefore is probably under-recognized. In a study performed in the area around Florence, Siena and Arezzo, forestry workers with high occupational risk of TOSV infection showed a seropositivity rate of over 75% with negative history of neurological symptoms (Valassina *et al.,* 2003). This confirms that TOSV infection can be very mild or even completely free of symptoms. TOSV is the major cause of aseptic meningitis (95%) and meningoencephalitis (4.5%) and influenza-like illness during the summer season, especially in July, August and September when the maximum

activity of the sandfly vector occurs (Hemmersbach-Miller *et al.,* 2004; Sanbonmatsu –Gàmez *et al.,* 2009).

TOSV was recognized as a causative agent of neurological disease in humans only in 1983, when it was isolated for the first time from a young woman with lymphocytic meningitis (Nicoletti *et al.,* 1991). The most documented clinical form of TOSV infection consists of neuro-invasive cases which are generally hospitalized (Charrel *et al.,* 2012). A wider clinical spectrum of TOSV-associated diseases is now documented, including asymptomatic or mild disease without CNS involvement, such as febrile erythema or influenza-like illness, as well as unusual clinical manifestations or severe sequelae of the neurological infection (Bartels *et al.,* 2011; Brisbarre *et al.,*2011; Serata *et al.,* 2011). The clinical manifestations of meningitis from TOSV is quite similar to that caused by other viral agents; however, it is found that levels of anti-inflammatory and antiviral mediators were significantly higher in cerebrospinal fluid (CSF) of TOSV-infected patients as compared to patients with other infectious or noninfectious neurological diseases (Varani *et al.,* 2015).

In any case, it is not possible to define a characteristic symptomatology for neurological infections caused by TOSV (Dionisio *et al.,* 2003). Generally, incubation period is influenced by the virus load, ranging from few days to 2 weeks. Disease onset is intense with headache (100%, 18h–5 days), fever (76%–97%), nausea and vomiting (67%–88%) and myalgias (18%). Physical examination may show neck rigidity (53%–95%), Kernig signs (87%), poor levels of consciousness (12%), tremors (2.6%), paresis (1.7%), nystagmus (5.2%). In most cases CSF contained more than 5–10 cells with normoglycorrachia and normoproteinorrachia (Charrel *et al.,* 2012). It is also possible to have abnormal CT or MRI (Rinaldi *et al.,* 2011). Blood samples may show leukocytosis (29%) or leukopenia (6%) (Charrel *et al.,* 2005). The mean duration of the disease is 7 days, and the outcome is usually favorable (Charrel *et al.,* 2012).

Although TOSV infection consists of a mild disease with a favorable outcome in most cases, an outcome with severe complications is possible, but only a small number of severe cases have been reported in the literature. Two young brothers and a sister living in Umbria experienced TOSV infection in the form of severe meningoencephalitis with stiff neck, deep coma, maculopapular rash, diffuse lymphadenopathy, hepatosplenomegaly, renal involvement, skin rash with lamellar desquamation, a tendency to bleed, and diffuse intravascular coagulopathy. CNS manifestations occurred after 3 weeks of fever (Baldelli *et al.,* 2004). One case of meningitis, complicated by abducens nerve palsy, was reported (Schwarz *et al.,* 1995). Two cases of ischemic complication followed diagnosis of TOSV infection were reported (Klugman *et al.,* 2009). A case of deafness as a sequela of TOSV infection was also described (Martínez-García *et al.,* 2008). A case in which lymphadenopathy was the main clinical finding at the presentation of symptoms and preceded the onset of meningitis was documented (Rinaldi *et al.,* 2011). Serata *et al.,* 2011 reported a case of psychiatric sequelae following encephalitis due to TOSV infection in a patient without personal or family psychiatric history. Severe and lethal encephalitis was also reported (Bartels & Boni, 2011).

A retrospective study on the antibody prevalence rates of Toscana virus (TOSV) among children and adults was performed in a population living in Tuscany during 1999-2006. The seroprevalence rate was 19.8% in adults and 5.8% in children, showing an age-dependent increase in TOSV specific immunity. Moreover, correlating seroprevalence to the clinical profile, the study indicated that asymptomatic TOSV infection is more frequent in young people (91%) than in adults (31.4%), in whom a higher incidence of severe signs of neurological disorders correlated to TOSV infection are present (Terrosi *et al.,* 2009).

Although the vast majority of cases have a favorable outcome, some severe cases of TOSV infections were described (Depaquit *et al.,* 2010; Charrel *et al.,* 2005; Baldelli *et al.,* 2004; Cusi *et al.,* 2010; Vocale *et al.,* 2012). Various studies have reported a larger extent for neurological symptoms than initially identified. Other

neurological manifestations such as deafness, (Martinez-Garcia *et al.,* 2008; Paul *et al.,* 1995) persistent personality alterations (Serata *et al.,* 2011), fasciitis and myositis (Doudier *et al.,* 2011) and speech disorders and paresis (Sanbonmastu-Gamez *et al.,* 2009) were also reported.

1.4.3 TOSV infection and role of glycoproteins

TOSV virus genome is composed of three single-strand RNA segments named S, M and L. The S segment is 1869 nucleotides long and codes for a 253 aminoacid protein, the N protein, in viral complementary sense and for a 316 amino acid protein, a non-structural protein, NSs, in analogy to other members of the same genus (Giorgi *et al.,* 1991). The M segment is 4215 nucleotides long, it has only one open reading frame (ORF) in the viral complementary sense, coding for a putative protein of 1339 amino acid (Gro *et al.,* 1997) co-translationally processed in three proteins: the 30 kDa non structural protein, NSm, and the envelope glycoproteins, Gn and Gc (Di Bonito *et al.,* 1997). Sequence analysis of the L segment showed that it is 6404 nucleotides long and it contains a single ORF, in the viral complementary sense, coding for a protein of 2095 amino acids with a deduced molecular mass of 239 kDa (Accardi *et al.,* 1993) supposed to be the viral polymerase.

TOSV like Phleboviruses and other bunyaviruses use their envelope proteins, Gn and Gc, for entry into target cells and for assembly of progeny particles in infected cells. The glycoproteins are involved in the first step of the bunyavirus replication cycle mediating the viral entry into host cells and are the targets for neutralizing antibodies. Once inside the target cell, exposure to endosomal low pH induces Gc-driven fusion of the viral envelope with the vesicle membranes, leading the release of viral genome in the cytoplasm where the replication cycle starts. Moreover, Gn and Gc also facilitate virion incorporation of the viral genome via their intracellular domains and Gn and Gc interactions allow the formation of a highly ordered glycoprotein lattice on the virion surface. (Spiegel *et al.,* 2016).

Gn and Gc are synthesized as a precursor protein, in the secretory pathway of infected cells. The cleavage step is executed by a cellular enzyme, signal peptidase (Lober *et al.,* 2001; Gerrard *et al.,* 2007; Andersson *et al.,* 1997), during import of the Gn/Gc precursor into the endoplasmic reticulum (ER). In the ER, both Gn and Gc are decorated with N-linked glycans (Kuismanen *et al.,* 1984; Matsuoka *et al.,* 1988) of the high-mannose type, which can be processed into hybrid and complex forms upon import into the Golgi apparatus (Kuismanen *et al.,* 1984; Shi *et al.,* 2005; Madoff *et al.,* 1982) which is the site of bunyavirus budding (Kuismanen *et al.,* 1982; Fontana *et al.,* 2008; Smith *et al.,* 1982; Salanueva *et al.,* 2003; Murphy *et al.,* 1973). This process is facilitated by Gn and Gc, which play a key role in particle morphogenesis and genome incorporation (Piper *et al.,* 2011; Overby *et al.,* 2006; Novoa *et al.,* 2005; Spiropoulou *et al.,* 2001; Cifuentes *et al.,* 2014). Finally, infectious particles with Gn and Gc are released from the infected cell by exocytosis.

Considerable progress has been made over the last three decades in understanding the role of the glycoproteins in phlebovirus entry. Although the processing of phlebovirus glycoproteins by signal peptidase is a pivotal step of glycoprotein maturation, only limited experimental data concerning this process is currently available. The subsequent steps in phlebovirus glycoprotein maturation, i.e., disulfide bond formation and N-glycosylation are even less well characterized. Furthermore, the mechanism of how glycoproteins and RNPs interact during virus assembly is poorly understood.

In some phleboviruses, antigenic sites involved in virus neutralization *in vitro* have been mapped on the envelope glycoproteins and are thought to be conformational (Pifat *et al.,* 1988; Besselaar and Blackburn,1991). The human antibody response against linear epitopes of the envelope glycoproteins has not been studied extensively. In the infection of humans by Sin Nombre hantavirus, an IgG and IgM response is directed almost exclusively against a linear epitope of 31 amino acids

of G1, the glycoprotein located at the 3' end of the M genomic segment (Hjelle *et al.,*1994).

Usually, the neutralizing activity is a property of the anti Gn-Gc antibodies, as shown for other viruses of this family, like RVFV, La Crosse virus (LACV) and Hantaan virus (HTNV) (Saluzzo *et al.,* 1989a, b; Gonzalez-Scarano *et al.,* 1982; Grady & Kinch 1985; Arikawa *et al.,* 1989). Various studies have been attempted to identify the immunodominant antigen involved in the human immune response against TOSV. The important role of N protein in human infections has been demonstrated by the presence of a strong cytotoxic T cell response against N in patients affected by viral associated meningitis (Cusi *et al.,*2002). The N protein is considered an important immunogenic antigen, with a partial neutralizing activity of anti-N antibodies (Cusi *et al.,* 2001) but also the anti-glycoproteins response plays a fundamental role to develop a protective immune response, although it apparently seems short lived (Cusi *et al.,* 2002; Di Bonito P. *et al.,* 2002). Despite this, a study (Gori Savellini *et al.,* 2008) demonstrated that a combination of TOSV protein N-Gc, used as vaccine, was able to protect 100% of animals from a lethal intracranial challenge with a neurovirulent strain of the virus.

The mechanisms of protection against TOSV natural infection are not known, however it could be supposed that a virus-neutralizing antibody response against viral glycoproteins would be useful to block the first stages of infection. For these reasons, we decided to focus our attention not only on the N protein, but also on the Gn viral glycoprotein and to identify possible conserved epitopes that can induce a neutralizing activity.

CHAPTER 2
AIM OF THE THESIS

Emerging and re-emerging viral infections have been an important public health problem in recent years. The pathogenesis of the Toscana virus (TOSV), circulating in the Mediterranean area, which is responsible for aseptic meningitis, meningoencephalitis and encephalitis is still largely unclear and the mechanisms of protection against this natural infection are still not known, but despite this, the humoral response is thought to help with the cell mediated immune response in order to fight the infection. In particular, a virus-neutralizing antibody response against viral glycoproteins, which are involved in the initial stages of Phlebovirus entry, replication cycle and release, would be necessary to inhibit the first steps of infection.

In a previous work carried out in Prof. Cusi's laboratory, it was possible to localize three neutralizing epitopes on Gn glycoprotein using human mAbs obtained by immortalization of B cells from a subject infected with TOSV. It was hypothesized that these 3 aminoacid sequences, which are separated in the primary structure of the protein, had probably a neutralizing activity once exposed near one another as a conformational epitope in the natural structure of the protein.

Based on this idea, the aim of this thesis was to *in vivo* evaluate the immunogenic efficacy of the three peptides in various combinations in a mouse model. The study also aimed at determining the possible cross reactivity of the mice sera immunized with different combinations of the peptides, against viruses such as SFNV, PUNV, SNSV, CYPR which are antigenically related to TOSV. These results could be used to design epitopes that can serve as potential targets for the production of epitope-based diagnostic tools. In addition, the analysis of the possible cross-reactivity with other viruses could be exploited for the design of a vaccine against TOSV and antigenically related other Phleboviruses.

Finally, the study also aimed at producing monoclonal antibodies against TOSV NSs protein by a modified EBV immortalization protocol. These monoclonal antibodies could be useful for a better characterization of the NSs protein.

CHAPTER 3

MATERIALS AND METHODS

3.1 Cells and Viruses

Vero cells (ATCC CCL-81) were grown as a monolayer in Dulbecco's modified Eagle's medium (DMEM) (Lonza, Milan, Italy) supplemented with 5% heat inactivated fetal calf serum (FCS) (Lonza) and 100 U/ml penicillin-streptomycin (HyCloneEurope, Milan, Italy) at 37°C. Toscana virus (TOSV) strain 1812 cultured on Vero cells (isolated from a clinical specimen S.Maria alle Scotte Hospital, Siena, Italy) was plaque purified and propagated for viral stocks preparation. B95.8 cells were grown in RPMI 1640 (Hyclone, Cramligton, UK) supplemented with 10% FBS (Lonza) and 100 U/ml penicillin-streptomycin at 37°C with 5% CO_2. The supernatant containing Epstein Barr Virus (EBV) was collected, centrifuged at 1800 rpm for 10 min to remove the cells and filtered through a 0.22μ filter. The filter sterile EBV was then stored at -80°C until further use.

3.2 Human PBMC Isolation

PBMCs were isolated from human blood, diluted in an equal volume of phosphate buffered saline (PBS) and further separated on Ficoll-Hypaque gradient by centrifugation at 1800 rpm for 20 minutes at RT. Cells were collected from the plasma/Ficoll interface and resuspended in PBS and centrifuged at 1300 rpm for 10min. at RT. Cells were finally resuspended in RPMI 1640 medium and counted. The cells were either cultured or freezed in liquid nitrogen in 10% DMSO.

3.3 Plasmid Construction

Viral RNA was extracted from TOSV-infected Vero cells using a QIAamp viral RNA minikit (Qiagen). Plasmid vector pGex-2T (Amersham Biosciences) was used for the construction of a plasmid containing the peptide 1 and peptide 2

sequences of TOSV Gn glycoprotein. The gene sequence was amplified from the purified viral RNA by reverse transcriptase PCR (RT-PCR) using specific primers. The reaction was carried out using the Super Script III one-step RT-PCR mix (Invitrogen) by one cycle of reverse transcription at 50°C for 30 min and 94°C for 2 min, followed by 40 cycles of PCR (15 min at 94°C, 30 s at 56°Cand 1 min at 68°C) and 5 min at 68°C. The primers used were:

Forward Primer: 5'- AAGGATCCGGAAGTGATATGTCG - 3'
Reverse Primer: 5'- GGGGAATTCTCATCTTCATCTGCTC- 3'

The amplified gene was then cloned into pGex-2T vector linearized with Bam HI and EcoRI. The plasmid was named as GC683.

Another plasmid named GC727 containing peptide 1, 2 and 3 sequences of TOSV Gn glycoprotein was constructed by fusing peptide 3 sequence with GC683. Infusion cloning was performed as per the manufacturer's instructions (Takara Bio Inc). Briefly, the GC683 was linearized with EcoRI restriction enzyme and the linearized vector was gel eluted using E.Z.N.A.® MicroElute Gel Extraction Kit (Omega Bio-tek), following manufacturer's instructions. The sequence shown below, used for Infusion cloning, was purchased from Integrated DNA Technologies. The sequence was designed in such a way to introduce a 5 alanine sequence (highlighted) upstream of peptide 3 that was fused with the linearized vector.

5'- GAG CAG ATG AAG ATG AGA ATT CAT GCG GCGGCGGCGGCG TCC TGT GAG GTT AGC AGC TGC CTA TTC TGT GTG CAC GGA CTG CTT AAC TAC CAG TGC CAC ACC TGA CTC GAG GAA TTC ATC GTG ACT GAC TGA CGA - 3'

The fused construct was obtained by PCR using a mix of the digested plasmid, In-Fusion HD Enzyme Premix (Takara bio) and the DNA sequence encoding peptide 3. The reaction mix was incubated for 15 min at 50 °C and then placed in ice for 15 min.

3.4 Plasmid Transformation

The GC683 and GC727 plasmids were respectively transformed in XL10 Gold and Top10 competent cells via the heat shock procedure (Froger *et al.,* 2007) and screened for selection. The integrity of the sequence of both constructs was confirmed by sequencing (Sanger *et al.,* 1977).

Protein expression was induced by 1mM IPTG (Thermo Fisher Scientific), until the cultures reached an optical density of 0.5-0.6 at 600 nm measured with the spectrophotometer (Ultrospec 2100 pro, Amersham Biosciences). Cultures were allowed to grow for 3 h, and the cells were harvested by centrifugation at 4500 rpm, for 20 minutes and stored at -80°C.

3.5 Protein Purification from Inclusion Bodies

The protein was isolated from the pellet of IPTG induced cells. The cell pellets were resuspended in STE (50 mM Tris, 150 mM NaCl, 1 mM EDTA) containing 0.1% Triton Buffer and incubated for 30 minutes, with in-between sonications and then centrifuged at 5000 rpm for 15 minutes. Supernatant was discarded while the pellets were resuspended in STE Buffer containing 4 M UREA pH 8.0 (Panreac AppliChem) and incubated for 40 minutes. The supernatant obtained following centrifugation of the incubated mixture was removed, while the pellet was resuspended in STE + 1% Triton Buffer and incubated for 30 minutes. The supernatant obtained after centrifugation was discarded and the pellet was washed with dH_2O until the supernatant became clear. The pellet was then resuspended in 10 ml of STE Buffer containing 8M UREA (pH 8.0) and incubated overnight.

The overnight sample was then filtered through a 30 kDa cutoff filter (Millipore Sigma) by centrifugation at 10,000 rpm for 15min; the flowthrough was discarded and the filtered protein was washed twice with PBS. The purified protein obtained was then quantified by Bradford reagent (Avantor®) in a spectrophotometer at 595 nm. All the incubations were made in ice and the centrifugations set at 4°C in order to guarantee protein stability.

SDS PAGE was then performed to evaluate the purity of the protein by staining the gel with Coomassie Brilliant Blue (CBB) (Bio-rad). The specificity of the protein was confirmed by Western-blot analysis. Protein was then stored at -80°C until further use.

3.6 Western Blot

The proteins separated in the gel were transferred onto a nitrocellulose membrane by electroblotting (Trans-Blot® TurboTM Transfer System, Bio-Rad) with Transfer Buffer 1X (25 mM Tris, 192 mM glycine, 10% methanol) containing 20% ethanol. The nitrocellulose membrane (Santa Cruz Bio- technology, Heidelberg, Germany) was then blocked with 5% milk (in PBS) at room temperature for 1 hour to block the possible non-specific interactions.

Anti- Goat-GST (Sigma, Milan, Italy), diluted 1:1000, was used as primary antibody and incubated with the membrane overnight. Subsequently, the membrane was washed 3 times with PBS-Tween 0.1% and incubated for 1 hour in dark with the secondary antibody, anti-Goat HRP-conjugated, (Santa Cruz Bio- technology, Heidelberg, Germany), diluted 1:2000. After washing off the unbound secondary antibody, the substrate (TMB One Component HRP Membrane Substrate, Tebu-Bio laboratories) was added and the presence of specific band was evaluated.

3.7 Animal Studies

Four-week-old female BALB/c mice (Charles River, Milan, Italy) were used in the immunization experiments. Each experiment was repeated three times to assess the reproducibility of results. Twelve groups of five mice each were immunized every 2 weeks with four intraperitoneal (IP) injections of 100 μg/mice of Gn peptides in different combinations. All animal experiments were approved by the local Ethics Committee and carried out in strict compliance with the Institutional Animal Care and Use Committee (IACUC) guidelines and in accordance with the 2010/63/EUDirective of the European Parliament and the Council for the Protection of Animals Used for Scientific Purposes.

(http://eurlex.europa.eu/LexUriServ/LexUriServ.do?uri=OJ:L:2010:276:0033:0079:EN:PDF)

Peptide 1, 2 and 3 as single units conjugated with the KLH carrier were purchased from Peptide Facility (CRIBI – Centro di Biotecnologie Università di Padova). Peptides 1 and 2 were expressed and purified in a prokaryotic system by a plasmid named GC683 whereas peptides 1, 2 and 3 by a plasmid named GC727. All the combinations of antigens as described in Table 2 contained an equal volume of Montanide as adjuvant. Two weeks after the last immunization, all mice were sacrificed, blood was drawn and serum o was collected and stored at -20 °C for further analysis.

Table: 2 Mice Immunization Chart

Groupof mice	**Antigens injected for immunization**
Group 1	Peptide 1-KLHas a single peptide
Group 2	Peptide 2-KLH as a single peptide
Group 3	Peptide 3-KLH as a single peptide
Group 4	Peptide 1-KLH and peptide 2-KLH as a single peptide alternatively
Group 5	Peptide 1-KLH and peptide 3-KLH as a single peptide alternatively
Group 6	Peptide 2-KLH and peptide 3-KLH as a single peptide alternatively
Group 7	Peptide 1-KLH, peptide 2-KLH and peptide 3-KLH as a single peptide combined
Group 8	Pep GC683purified
Group 9	Pep GC683 purified + Peptide 3-KLH as single peptide
Group 10	GC727purified
Group 11	rGn
Group 12	PBS

100µg of each antigen was used for immunization at two weeks interval with Montanide as adjuvant.

3.8 Enzyme Linked Immunosorbent Assay (ELISA)

Microtiter plates (Labsystem, Helsinki, Finland) were coated with 100µl per well of either purified whole TOSV or purified TOSV Gn glycoprotein protein (1µg/ml conc) in 0.1 M carbonate buffer (pH 9.6) and incubated overnight at 4°C. After three washing steps with phosphate buffer solution (PBS)containing 0.05% Brij, either 100µl of mice sera diluted 1:50 in dilution buffer (PBS + 0.05% Brij + 10% FBS) or 100µl of supernatant from EBV immortalized PBMC diluted 1:2 in dilution buffer (for mAbs screening), were added to each well and the plates were incubated at 37°C for one hour.

After washing, 100µl of either peroxidase conjugated anti-mouse IgG (diluted 1:333) (Sigma-Aldrich) or anti-human IgG + IgM (diluted 1:8000) were added followed by incubation at 37°C for one hour in dark. The plates were then washed and 100µl of 3,3',5,5'-tetramethylbenzidine (TMB One Component HRP Microwell Substrate, tebu-bio laboratories) was added to each well for 15 min. The reaction was stopped by adding $1NH_2SO_4$ solution and the plates were read immediately at 450 nm. Dilution buffer was used as negative control and human serum from a positive TOSV patient (diluted 1:20 in dilution buffer) was used as a positive control.

3.9 Neutralization Test

Virus neutralization was carried out on Vero cells in a 96 well microplate. Briefly, two-fold serial dilutions (25µl) of mouse sera were added to an equal volume of a TOSV dilution containing 200 TCID50 and incubated for 90 min at 37°C, then 30 min at 4°C. Fifty microliters of cells (10^6/ml) suspended in MEM (InVitrogen, Milan, Italy) with 5% FCS was added to each well. Five days after incubation at 37°C, the cultures were examined microscopically for the presence of cytopathic effect. The 50% end point titer of the serum neutralizing dose was calculated using the Reed and Muench method (Reed & Muench, 1938).

3.10 Indirect Immunofluorescence Assay

Cells infected with TOSV strain 1812 were spotted on slides and fixed for 10 min at room temperature with cold methanol/acetone. Mice sera diluted 1:50 were added and the slides were incubated for 30 minutes at 37°C. Subsequently, the slides were washed with PBS + 20% Tween for 5 minutes to remove the unbound primary antibody in the mouse sera. FITC-conjugated anti-mouse secondary antibody (Sigma, Milan, Italy) diluted 1:320 was added to the slides and then incubated for 20 minutes at 37°C in dark. After the final wash, immunofluorescence was visualized using a Diaplan microscope (Leica Microsystems, Milan, Italy).

3.11 Cross reactivity Analysis

The cross reactivity of mouse sera was tested using a commercially available kit "Sandfly fever virus Mosaic 1 types: Sicilian, Naples, Toscana, Cyprus IFA" (EUROPattern) following the manufacturer's instructions. Briefly, the mouse sera were diluted 1:50 and added to the titer plane slides. The Biochips provided with the test fields coated with the 4 viruses, were positioned above and incubated for 30 minutes at room temperature. After a PBS-Tween wash, the attached antibodies were stained with FITC conjugated anti-mouse secondary antibody for 30 minutes at room temperature in dark. Followed by washing, the results were then evaluated by a Diaplan microscope (Leica Microsystems, Milan, Italy).

3.12 Immortalization of PBMC

PBMC was isolated upon informed consent, from the blood of a patient with meningitis, infected by TOSV. Using a modified standardized protocol (Steinitz *et al.,* 1977; Corti *et al.,* 2014), Epstein Barr Virus (EBV) was used to immortalize B cells. Isolated PBMC was cultured overnight on a 6 well plate at a cell density of $4x10^6$ cells per well in RPMI supplemented with 10% heat inactivated serum supplemented with cyclosporin (Sigma) at a concentration of 1µg/ml. The supernatant cells were then collected and resuspended in filter purified B95.8 supernatant containing EBV and incubated for one hour at 37ºC with 5% CO_2.

Following incubation, RPMI medium supplemented with 10% heat inactivated serum was added to the cell suspension containing EBV and plated onto a 96 well plate at a cell density of $5x10^5$ cells per well. The cells were then incubated for three weeks at 37ºC with 5% CO_2 and were routinely monitored for the formation of clones.

After three weeks, the supernatant was tested for the presence of specific antibodies by ELISA. The cells from the ELISA positive wells were then serially diluted and plated on to a 96 well plate at a cell density of 1 cell per well. Following incubation at 37ºC with 5% CO_2 for another three weeks, the supernatant from each well was again tested for specific monoclonal antibodies by ELISA.

3.13 Statistical Analysis

All experiments were carried out in triplicate. The statistical analysis of differences between means was performed using Stat View statistical software (AbacusConcepts, Berkeley, CA, USA). Neutralization titers are presented as geometric mean±standard deviation. $P<0.05$ was considered significant.

CHAPTER 4

RESULTS AND DISCUSSION

4.1 Expression and Purification of GC683 and GC727

Previous studies (Gandolfo *et al.,* 2019) have identified three regions on TOSV Gn glycoprotein recognized by most of the neutralizing monoclonal antibodies isolated from a patient who was serologically positive to TOSV for both IgM and IgG. The first two regions, Pep 1 and Pep 2, are localized in the amino-terminal of the Gn glycoprotein, while the third region, Pep 3, is positioned close to the transmembrane region, as in Fig.7

The immunogenicity of these three identified peptide sequences were tested *in vivo* in different combinations either as a single peptide or in combinations. To this aim, Peptide 1 and Peptide 2 were cloned into a prokaryotic expression vector system and named as GC683. Similarly, Peptides 1, 2 and 3 were cloned into another prokaryotic expression vector named GC727. Both the vectors had GST as a carrier sequence. Both the plasmids were expressed in XL10 Gold and Top10 E-*coli* cells respectively, and proteins were isolated. The concentration of the isolated proteins determined by Bradford method was 5.1µg/µl for Pep-GC683 and 576ng/µl for Pep-GC727. The specificity of the isolated protein was analyzed by western blot using either anti-goat GST or TOSV positive human sera (Fig.8).

Figure: 7 The three peptide regions of TOSV Gn protein

1NHLLNWPGNG AYTLSDFAES TCTLAYGSEC KSWEHQLDEL SFPFFHSNLD KYSMLEAATE

61 TIPILNKSSA VCTISPSTHS SNACGREASL IKKKCGSDMS AFFYVNLAGQ ITVVKCDTNH

121 VLSNDCGNCI SKTLSGQKIY TPVQDMFCQK GWSESIPSTR YSKDLCSIGL HTVKECKIGT

181 TNFERVGFIV VKGRKMYIEQ MKMRSRQEFS EDQFLCYKSE GSSGSSVKLK KVKVESCKGV

241 TTSSASKCSG DEYFCSRYPC ETANVEAHCI LRRHSAVIEV NVNGVWVVPR CIGYEEVLVR

301 RTSLKVEDTS SRECDTCLWE CGKNKLIVKT HGPKIVYATA CSHGSCKSVM QKPATFVYLP

361 YPGNSEIVGG DIGVHMTEES SPSNIHMVAH CPAKDSCEVS SCLFCVHGLL NYQCHTLFSA

421 LLISTTVMSI LTLLLLLVKG AKDLVKRLFY WLITPLCWLS VFCGWMIRSW KKRVGSAISR

481 TNDTIGWRDN SRRGQDIERA QYTGGAPGAK YSFYGVMILG LLGNVHS

GSDM - *Peptide 1*

HTVK - *Peptide 2*

- *Peptide 3*

- *Transmembrane Region*

Figure: 8 Western Blot Analysis of the purified proteins.

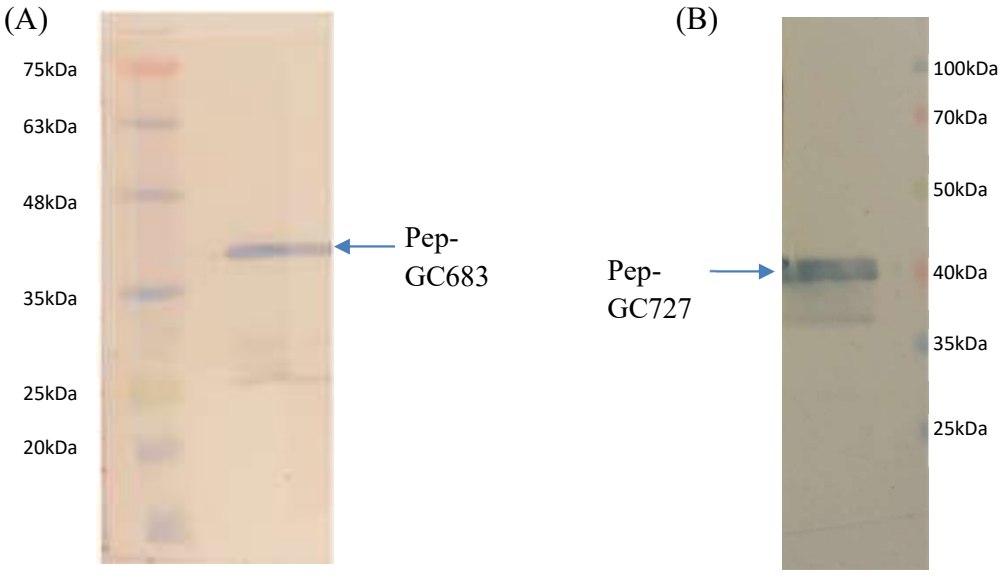

(A) Pep-GC683 (39kDa) (peptide 1-2)

(B) Pep-GC727 (42kDa) (peptides 1-2-3)

4.2 Humoral Immune response elicited to the peptides *in vivo*

Peptides 1, 2 and 3 either as a single peptide coupled with KLH as carrier or purified proteins as Pep-GC683 and Pep-GC727 or a combination of both were used to immunize 4 weeks-old female BALB/c mice intraperitoneally. Four consecutive immunizations of 5 mice/group were performed at two weeks interval with the peptides and constructs as described in table 2.

Two weeks after the last immunization, mice were sacrificed and the antibody response to the different combinations of peptides were evaluated. Sera obtained from each group were tested for the presence of antibodies against both Gn protein and purified whole TOSV by ELISA. All the mice elicited, at a different extent, an antibody response to Gn after immunization with most of the combinations of the peptides; only pep1-KLH developed a low level of antibodies, while pep2-KLH or other combinations of peptides containing peptide 2 were able to induce a high amount of antibodies reacting with Gn. ELISA results, using the purified whole TOSV as antigen, showed positivity for all the immunized mice groups, although at varying levels. Moreover, the mice group immunized with Pep-GC683 and the combination of Pep-GC683 + Peptide 3-KLH showed a comparatively better response than mice immunized with single combination of peptides or with the recombinant Gn. Immunized mice sera from each group were also tested by immunofluorescence on TOSV infected Vero cells. All the mice immunized with different combinations of peptides elicited antibodies recognizing the Gn glycoprotein in TOSV infected cells, by immunofluorescence.

A neutralization assay was also performed to determine the specific neutralizing activity against TOSV. The mice groups immunized with the single peptides 1, 2 and 3 showed low neutralization titers of 1/10, 1/23 and 1/5 respectively. Similarly, the groups immunized with a combination of all the three single peptides also produced a titer value of 1/8. The mice group immunized with a combination of peptide 2-KLH + peptide 3-KLH showed a titer of 1/24. Likewise, sera from the mice immunized with Pep GC727 containing the sequence of peptides 1, 2 and 3

showed a titer of 1/28, letting us suppose that peptide 2 and 3 are necessary to induce neutralizing antibodies. Indeed, the mice group immunized with a combination of pep-GC683 (sequence of peptides 1 and 2) and peptide 3-KLH (as a single peptide) showed a significantly higher titer of 1/183, supporting the hypothesis that for inducing a neutralization response, a proper conformation of the epitope was required. We could infer from these results that pep-GC683 containing peptide 1 and peptide 2 was able to elicit a low neutralizing antibody titer (1/10), but the titer was strongly increased, up to 1/183, with the addition of peptide 3-KLH to pep-GC683. This result was presumably due to the conformation of the protein, in particular, peptides 1 and 2 seemed to constitute a conformational epitope recognized by NT antibodies, but not sufficient to block the virus. On the contrary, the addition of peptide 3 allowed the block of the virus (NT Ab titer 1/183), probably hindering the binding site to the cell receptor. Indeed, antibodies to peptide 3, located close to the protein transmembrane fragment, recognized both the Gn and the whole virus very well, but did not show NT activity (NT titre 1/5) by themselves.

Thus, it appeared that the two identified regions, peptide 1 and peptide 2 could be part of a conformational epitope capable to induce neutralizing antibodies, and Pep 3 could strengthen this activity, contributing to enhance the neutralizing response *in vivo*. In particular, they might act in synergy reacting with distinct domains of the Gn glycoprotein and induce a steric hindrance at the binding site with the receptor, a phenomenon already proven (Hlavacek *et al.,* 1999). Thus, this event could block the virus entry into the cell and consequently, the viral replication. The mean values of the results of ELISA, immunofluorescence and neutralization assay are shown below in the table 3.

Table: 3 Evaluation of humoral response in mice immunized with different peptides

GROUPS	ELISA (MEAN±SD)		IFA	NT (GMT)
	Gn	TOSV		
Group 1 (peptide 1-KLH)	0.676±0.15	0.860±0.12	+	1/10
Group 2 (peptide 2-KLH)	2.745±0.26	0.653±0.05	+	1/23
Group 3 (peptide 3-KLH)	1.149 ±0.55	1.542±0.02	+	1/5
Group 4 (peptide 1-KLH + peptide 2-KLH)	1.793 ±0.54	0.998±0.17	+	1/10
Group 5 (peptide 1-KLH + peptide 3-KLH)	1.070 ±0.74	1.256±0.07	+	1/8
Group 6 (peptide 2-KLH + peptide 3-KLH)	2.658±0.41	0.904±0.10	+	1/24
Group 7 (peptide 1-KLH + peptide 2-KLH + peptide 3-KLH)	2.683±0.46	0.624±0.03	+	1/8
Group 8 (Pep-Gc 683)	1.519±0.37	2.305±0.16	+	1/10
Group 9 (Pep-Gc 683+peptide 3-KLH)	1.764±0.64	2.115±0.06	+	1/183
Group 10 (Pep-Gc 727)	2.330±0.66	1.191±1.01	+	1/28
Group 11 (rGn)	>3.00	0.798±0.05	+	1/660
Group 12 (PBS)	0.101±0.006	0.056±0.001	-	< 1/4

Values of ELISA are given as Mean±SD. Neutralisation titer is represented as geometric Mean Titre (GMT).

4.3 Serological cross reactivity of immunized mice with other Phleboviruses

Cross-reactivity is often seen among phleboviruses, particularly between viruses belonging to the same complex, and especially when ELISA or immunofluorescence assays are used (De Lamballarie *et al.,* 2007). Schwartz *et al.,* demonstrated that TOSV-specific IgG cross-react with other members of the genus Phlebovirus, and Tesh *et al.,* showed that TOSV is recognized by SFNV-specific antibodies in the complement fixation test (Schwartz *et al.,* 1996; Tesh *et al.,* 1982). Cross reactivity is associated with linear as well as conformational epitopes (Rizk *et al.,* 2008). The well documented serological relationships among viruses of the same genus provides the rationale to identify conserved epitope regions on viral proteins (Elliot *et al.,* 2014) and their use for diagnostic as well as treatment purposes. Considering the fact that cross-reactivity among the phlebovirus genus is generally known/frequent (Cleton *et al.,* 2012), the possible cross-reactivity of

immunized mice sera with other viruses belonging to the Phlebovirus genus was also evaluated in the study.

The sera of all the groups of mice were tested by immunofluorescence to assess the cross-reactivity with some viruses of this genus, such as Sandfly Fever Naples Virus (SFNV), Sandfly Fever Sicilian Virus (SFSV), Sandfly fever Cyprus virus (CYPR) and Punique Virus (PUNV).

From the results of the cross reactivity (Table 4), it is evident that considerable cross reactivity existed among the members of the Phlebovirus. Since SFNV shows more than 90% sequence similarity with all the three peptides, it was cross reacting with all the different combinations of immunized mice sera. Punique virus has 70% sequence similarity with peptide 3. This could explain its cross reactivity with only the mice sera immunized either with peptide 3 alone or its combinations. Although SFSV and CYPR do not show a considerable sequence similarity among all the three peptides, we could see cross reactivity with mice sera immunized with peptide 1.

However, this cross-reactivity was random, since it was not revealed in all the peptide combinations containing peptide 1, thus it seems that the reactivity was aspecific. It would be interesting to study further whether these cross-reacting sera could neutralize different members of the phlebovirus group in order to find, in addition to a valid diagnostic tool for many members of the phlebovirus genus, the epitopes useful to produce a polyvalent vaccine.

Table: 4 Cross-reactivity among mice sera with Phleboviruses

Groups	Cross-Reactivity			
	SFNV	SFSV	CYPR	PUNV
Group 1 (peptide 1)	+	-	+	-
Group 2 (peptide 2)	+	-	-	-
Group 3 (peptide 3)	+	-	-	+
Group 4 (peptide 1+peptide 2)	+	+	+	-
Group 5 (peptide 1+peptide 3)	+	-	-	+
Group 6 (peptide 2+peptide 3)	+	-	-	+
Group 7 (peptide 1+peptide 2+peptide 3)	+	-	-	+
Group 8 (Gc 683)	+	-	-	+
Group 9 (Gc 683+peptide 3)	+	-	-	+
Group 10 (Gc 727)	+	-	-	+
Group 11 (rGn)	-	-	-	-
Group 12 (PBS)	-	-	-	-

CHAPTER 5

ADDENDUM

Generation of Human Monoclonal antibody

Although the original hybridoma technique has proved to be extremely reproducible, new strategies were introduced to improve the production of monoclonal antibodies in general and of human monoclonal antibodies in particular.

Immortalization of B lymphocytes by Epstein-Barr virus (EBV) is an effective procedure for inducing long term growth of certain human B lymphocytes. EBV is a member of B-lymphotropic gamma herpes virus family that infects B-cells (Middeldorp *et al.,* 2003; Young and Rickinson, 2004). EBV infection leads to proliferation and transformation of B-cells into immortalized lymphoblastoid cells (LCL) (Price and Luftig, 2013). This unique ability of EBV is extensively used for the generation of immortalized B-cells that can produce antigen-specific human mAbs (Traggiai 2012; Yousefi *et al.*, 2013a, b). However, the EBV life cycle and transformation of different B-cell sub-sets progress with various efficiencies.

Only a portion of the circulating B cells (∼1 in 100) is immortalized by EBV (Sugden and Mark, 1977), and resting B lymphocytes are immortalized in preference to activated B lymphocytes (Aman *et al.,* 1984). Since T cells from EBV seropositive individuals suppress B cell immortalization by EBV in culture (Rickinson *et al.,* 1979), immortalization by EBV occurs with greater frequency when the immune T cells are either physically removed from culture or functionally inactivated; e.g., with cyclosporin A (Tosato *et al.,* 1982). EBV-immortalized B cell lines are initially polyclonal and secrete all major classes of immunoglobulins. After prolonged culture *in vitro*, EBV-immortalized cell lines become oligoclonal

or monoclonal, reflecting the outgrowth of selected cell clones (Nilsson and Klein, 1982). Typically, EBV-immortalized B cell lines are infected latently with EBV and produce little or no infectious viral particles (Sugden *et al.,* 1979).

Several methods have been reported to improve the efficiency of EBV transformation, including the use of irradiated fibroblast cells or culture medium supplemented with human plasma to improve the survival and proliferation of EBV infected B-cells (Pelloquin *et al.,* 1986; Manor 2008). Although Toll like receptor (TLR) agonists improve the efficiency of transformation in purified B-cells by a magnitude of 5–6 (Bourke *et al.,* 2003; Iskra *et al.,* 2010), the most evident enhancement of efficiency of transformation has been observed with memory B-cells treated with a TLR-9 agonist.

Younesi *et al.,* 2014 showed that EBV infection of B-cells in combination with a TLR 7/8 agonist was more efficient than CpG in producing antigen-specific human mAbs. It seemed memory B-cells are the main target of EBV and probably the most competent sub-sets for EBV transformation (Babcock *et al.*, 1998, Steinitz, 2014). A significant advantage of the EBV-based method is that the immortalized B cells secrete high amounts of antibodies but also maintain expression of BCR, although at a low and variable level. EBV immortalized B-cell clones maintain constant productivity with antibodies typically recovered in the culture supernatants at concentrations ranging from 5 to 50µg/ml in static cultures. (Corti *et al.,* 2014).

Monoclonal antibodies produced by the EBV method resemble the antibody repertoire of the donor of the lymphocytes. Human monoclonal antibodies are promising reagents for passive immunization. Hence, in the present study we decided to develop monoclonal antibodies against TOSV NSs protein with the intention to better understand the role of NSs in viral infection.

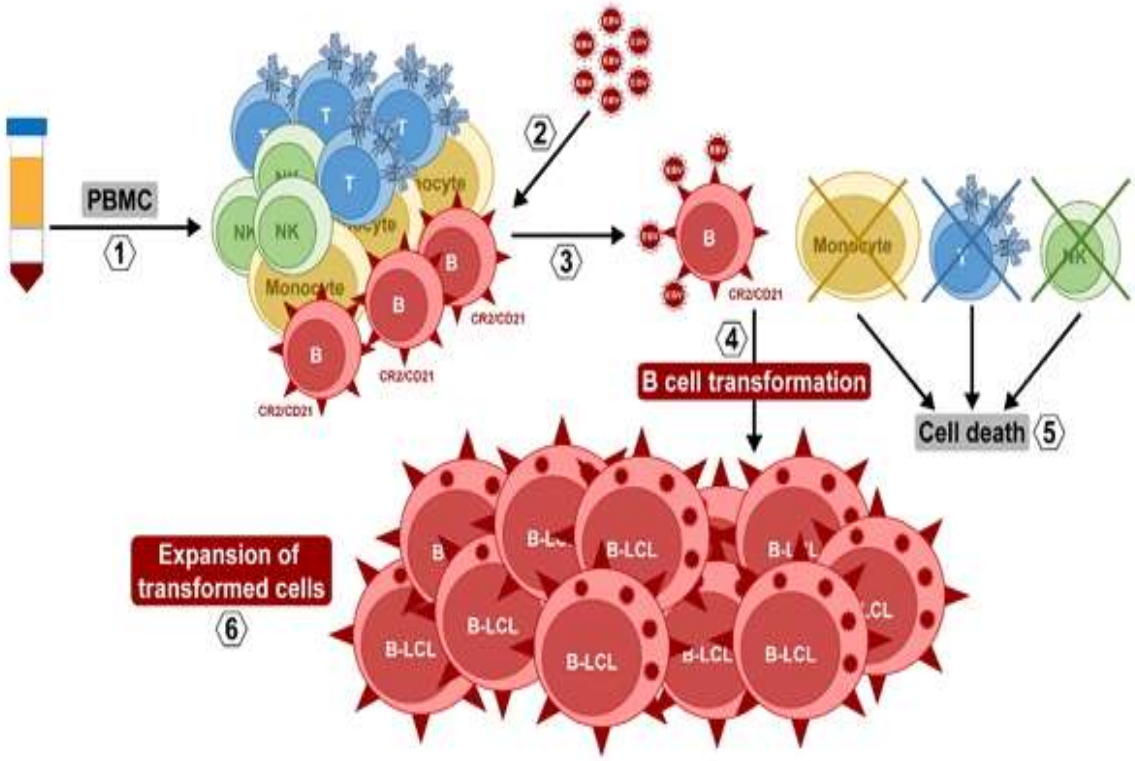

Figure:6. B cell immortalization with Epstein-Barr virus. (1) Isolation of peripheral blood mononuclear cells (PBMC) by density gradient. (2) Addition of B95-8 culture supernatant containing the EBV. (3) EBV infect B cells specifically through CR2/CD21 receptor. (4) Once inside, EBV transform B lymphocytes into B-lymphoblastoid cell lines (B-LCL). (5) The rest of PBMC that have not been infected die. (6) When they are transformed/immortalized, B-LCL proliferate, expand and produce antibodies.

RESULTS

Modified protocol for the generation of monoclonal antibodies against TOSV NSs

PBMC isolated from TOSV infected patient was cultured overnight with 1μg/ml of cyclosporin to eliminate T cells and monocytes. The B cells in suspension was immortalized with filter sterilized EBV and cultured for two weeks in a 96 well plate at a cell density of 50,000 cells per well. This protocol is a modified version of the methodology adopted by Corti *et al.,* 2014 and Steinitz *et al*., 1977. Compared with the standard protocol, CpG, which stimulates the proliferation of B cells was avoided. Also irradiated B cells which act as a feeder layer was also omitted as we saw a decrease in the viability of clones in the presence of the feeder layer debris. As the lymphoblastoid cells need to be in close proximity to grow better, the culture plate was tilted at approximately 45^0 so that the cells slide down to the corner of the plate.

After three weeks, the cell supernatant was analyzed from each well for the presence of antibodies against TOSV NSs by ELISA. The cells positive for the presence of anti NSs antibodies, were serially diluted to a density of one cell per well in a 96 well plate using JANUS automated work station. After three weeks of culture, we obtained 8 wells which were positive for NSs. These cells were then expanded and analysed. Further analyses are in course to characterize these human antibodies obtained *in vitro.*

Figure 9: EBV Immortalized B cells

DAY 1

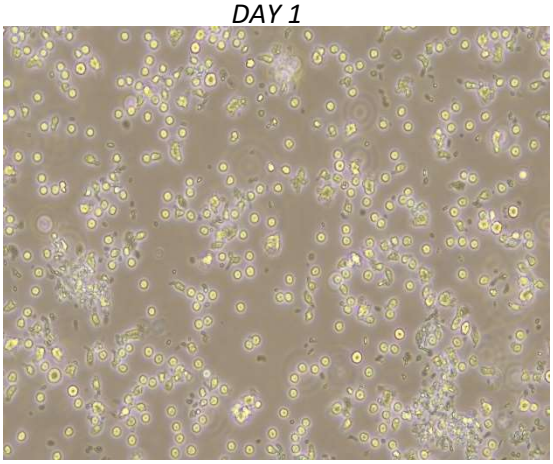

DAY 7

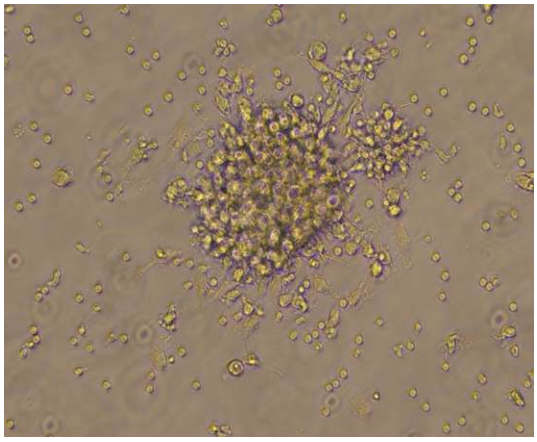

DAY 14

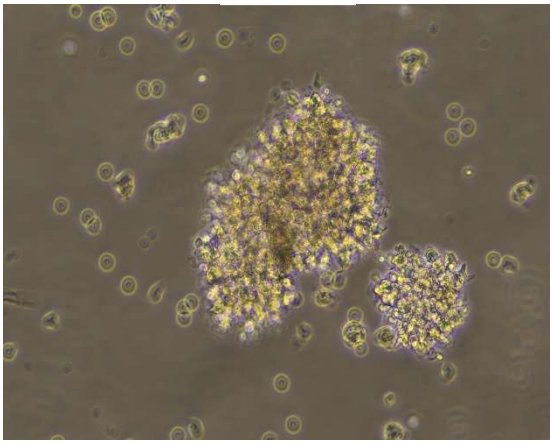

DAY 21

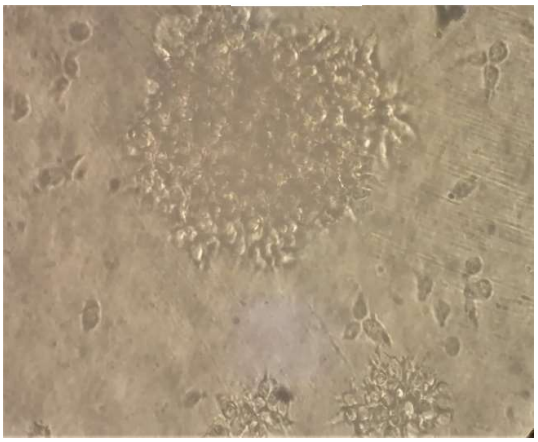

CHAPTER 6

CONCLUSIONS

Currently, the prospect of newly emerging viruses in *Phenuiviridae* family is a cause of public concern. Among the viruses belonging to Phlebovirus genus, Toscana virus is responsible for aseptic meningitis, meningoencephalitis, and encephalitis associated with fever, myalgia and severe frontal headache with usually a benign course, followed by a medium to long convalescence (Nicoletti *et al.,* 1991; Braito *et al.,* 1998; Valassina *et al.,* 1998; 2000; Dionisio *et al.,* 2001).

In subjects infected by TOSV , antibodies to glycoproteins are detected in about one third of the patients; some serum samples with neutralizing activity have even undetectable levels of antibodies to Gn and Gc (Di Bonito *et al.,* 1999). Despite their important role in viral entry and release, biological activities of TOSV Gn and Gc glycoproteins are not completely understood. These data raise some questions about antigenic variability and relevant neutralization epitopes of TOSV glycoproteins. The mechanisms of protection against phlebovirus natural infection are not known, however it could be supposed that a virus-neutralizing antibody response against viral glycoproteins would be useful to interfere with the first stages of infection and support the cell mediated immunity.

Focusing on Gn glycoprotein of TOSV, previous studies have identified three epitope regions by pepscan analysis which showed an antibody reactivity with the peptides present in the amino-terminal and near the transmembrane region of the protein, leading us to hypothesize that these sequences are part of a conformational epitope. The current study was focused on identifying the immunogenic efficacy of these peptides *in vivo* and their possible conformation to elicit a neutralizing activity.

Two weeks old female BALB/c mice were immunized with the three identified peptides either as a single antigen or as purified protein expressed in a prokaryotic

system or in a combination. Mice humoral immune response to the immunized peptides were analysed by ELISA and Neutralization Assay. The results of the study underline the hypothesis that peptides 1 and 2 could form a conformational epitope, while peptide 3 is necessary to strengthen the neutralizing activity.

Similar studies have been performed on other phleboviruses. Wu *et al.,* 2017 has deduced crystal structures of the Gn head domain from both SFTSV and RVFV, which display a similar compact triangular shape overall, while the three subdomains (domains I, II, and III) making up the Gn head display different arrangements, indicating that domain III, is an ideal region recognized by specific neutralizing antibodies, while domain II is probably recognized by broadly neutralizing antibodies. However, the arrangements of the three domains could be different among the members of the family. So far, the real pattern of the arrangement of viral glycoproteins into a functional complex on the virus surface has not been determined.

The possible serological cross-reactivity of the immunized sera against other viruses belonging to the same Sandfly Fever Naples serogroup such as SFNV, SFSV, CYPRUS, PUNV was also analysed in order to see if any of the tested combinations could act as a shared epitope for all these Phleboviruses, useful for the development of a diagnostic assay or the starting point for the development of a vaccine. The immunofluorescence results showed cross reactivity for SFNV and PUNV as they share 90% and 70% sequence similarity respectively with TOSV glycoproteins.

Moreover, the identification of shared neutralizing epitopes among them could be exploited for the development of a plurivalent vaccine protective against several sandfly viruses.

The study also developed monoclonal antibodies against TOSV NSs protein using a modified EBV mediated immortalization protocol from PBMC isolated from a patient infected with TOSV. Our modified methodology could produce efficiently TOSV NSs specific monoclonal antibodies without the use of CpG or irradiated

feeder cells. Similar methodology can also be used for the production of monoclonal antibodies against other immunogenic proteins of the virus. In recent years, passive immunization with human or humanized monoclonal antibodies (MAbs) specific to viral proteins has been tested in animal models and clinical trials, providing evidence of the effectiveness of MAbs for prophylaxis or treatment of infectious diseases (Both *et al.,* 2013). Since the emergence of SARS-CoV-2, several groups have reported the isolation of neutralizing antibodies from survivors that target the S protein (Rogers *et al*., 2020; Wec *et al.,* 2020; Zost *et al.*, 2020). However, a larger scaled up culture has to be done with the monoclonal antibody producing clones so that purified quantifiable monoclonal antibody could be obtained which can be used to better characterize the NSs protein and study its role in viral infection.

CHAPTER 7

BIBLIOGRAPHY

1. Abudurexiti, A.; Adkins, S.; Alioto, D.; Alkhovsky, S.V.; Avšič-Županc, T.; Ballinger, M.J.; Bente, D.A.; Beer, M.; Bergeron, É.; Blair, C.D.; Briese, T.; Buchmeier, M.J.; Burt, F.J.; Calisher, C.H.; Cháng, C.; Charrel, R.N.; Choi, I.R.; Clegg, J.C.S.; de la Torre, J.C.; de Lamballerie, X.; Dèng, F.; Di Serio, F.; Digiaro, M.; Drebot, M.A.; Duàn, X.; Ebihara, H.; Elbeaino, T.; Ergünay, K.; Fulhorst, C.F.; Garrison, A.R.; Gāo, G.F.; Gonzalez, J.J.; Groschup, M.H.; Günther, S.; Haenni, A.L.; Hall, R.A.; Hepojoki, J.; Hewson, R.; Hú, Z.; Hughes, H.R.; Jonson, M.G.; Junglen, S.; Klempa, B.; Klingström, J.; Kòu, C.; Laenen, L.; Lambert, A.J.; Langevin, S.A.; Liu, D.; Lukashevich, I.S.; Luò, T.; Lǔ, C.; Maes, P.; de Souza, W.M.; Marklewitz, M.; Martelli, G.P.; Matsuno, K.; Mielke-Ehret, N.; Minutolo, M.; Mirazimi, A.; Moming, A.; Mühlbach, H.P.; Naidu, R.; Navarro, B.; Nunes, M.R.T.; Palacios, G.; Papa, A.; Pauvolid-Corrêa, A.; Pawęska, J.T.; Qiáo, J.; Radoshitzky, S.R.; Resende, R.O.; Romanowski, V.; Sall, A.A.; Salvato, M.S.; Sasaya, T.; Shěn, S.; Shí, X.; Shirako, Y.; Simmonds, P.; Sironi, M.; Song, J.W.; Spengler, J.R.; Stenglein, M.D.; Sū, Z.; Sūn, S.; Táng, S.; Turina, M.; Wáng, B.; Wáng, C.; Wáng, H.; Wáng, J.; Wèi, T.; Whitfield, A.E.; Zerbini, F.M.; Zhāng, J.; Zhāng, L.; Zhāng, Y.; Zhang, Y.Z.; Zhāng, Y.; Zhou, X.; Zhū, L.; Kuhn, J.H. Taxonomy of the order Bunyavirales: update 2019. Arch Virol. 2019, 164, 1949-1965.
2. Accardi, L.; Gr´O, M.C; Di Bonito, P.; Giorgi, C. Toscana virus genomic L segment: molecular cloning, coding strategy and amino acid sequence in comparison with other negative strand RNA viruses. Virus Res 1993, 27, 119–131.
3. Agarwal, A.; Parida, M.; Dash, P.K. Impact of transmission cycles and vector competence on global expansion and emergence of arboviruses. Rev. Med. Virol. 2017, 27, 1-12.
4. Aman, P.; Ehlin-Henriksson, B.; Klein, G. Epstein-Barr virus susceptibility of normal human B lymphocyte populations. J. Exp. Med. 1984, 159, 208-220.
5. Amodio, E.; Cusi, M.G.; Valenti, R.M.; Valentini, M.; Mammina, C.; Gori-Savellini, G.; Vitale, F.; Romano, N.; Goedert, J.J.; Calamusa, G. Immunoglobulin

M seropositivity for Toscana virus in a random population sample in Sicily. Int. J. Infect Dis. 2012, 16, e633–e635.

6. Andersson, A.M.; Melin, L.; Persson, R.; Raschperger, E.; Wikstrom, L.; Pettersson, R.F. Processing and membrane topology of the spike proteins G1 and G2 of Uukuniemi virus. J. Virol. 1997, 71, 218–225.
7. Arikawa, J., Schmaljohn, A.L., Dalrymple, J.M., Schmaljohn, C.S. Characterization of Hantaan virus envelope glycoprotein antigenic determinants defined by monoclonal antibodies. J. Gen. Virol. 1989, 70, 615–624.
8. Babcock, G.J.; Decker, L.L.; Volk, M.; Thorley-Lawson, D. EBV persistence in memory B-cells in vivo. Immunity, 1998, 9:395–404.
9. Baldelli, F.; Ciufolini, M.G.; Francisci, D.; Marchi, A.; Venturi, G.; Fiorentini, C.; Luchetta, M.L.; Bruto, L.; Pauluzzi, S. Unusual presentation of life-threatening Toscana virus meningoencephalitis. Clin Infect Dis 2004, 38, 515-520
10. Bartels, S.; De Boni, L.; Kretzschmar, H.A.; Heckmann, J.G. Lethal encephalitis caused by the Toscana virus in an elderly patient. J. Neurol. 2011, 259, 175-177.
11. Beersma, M.F; Grimbergen, Y.A.; Kroon, F.P.; Veldkamp, P.J.; Meningitis caused by Toscana virus during a summer stay in Italy. Ned Tijdschr Geneeskd. 2004, 148, 286–288.
12. Besselaar, T.G.; Blackburn, N.K. Antigenic analysis of West Nile virus strains using monoclonal antibodies. Arch. Virol. 1988, 99, 75-88.
13. Bichaud, L.; Dachraoui, K.; Alwassouf, S.; Alkan, C.; Mensi, M.; Piorkowski, G.; Sakhria, S.; Seston, M.; Fares, W.; de Lamballerie, X.; Zhioua, E.; Charrel, R. N. Isolation, full genomic characterization and neutralization-based human seroprevalence of Medjerda Valley virus, a novel sandfly-borne phlebovirus belonging to the Salehabad virus complex in northern Tunisia. J. Gen. Virol. 2016, 97, 602–610.
14. Boshra, H.; Lorenzo, G.; Busquets, N.; Brun, A. Rift Valley fever: Recent insights into pathogenesis and prevention. J. Virol. 2011, 85, 6098–6105.

15. Both, L.; Banyard, A.C; van Dolleweerd, C.; Wright, E.; Ma, J.K.; Fooks, A.R. Monoclonal antibodies for prophylactic and therapeutic use against viral infections. Vaccine, 2013, 31: 1553–1559.
16. Bouloy, M.; Hannoun, C. Studies on lumbo virus replication I. RNA-dependent RNA polymerase associated with virions. Virology, 1976, 69, 258–264.
17. Bourke, E.; Bosisio, D.; Golay,. J.; Polentarutti, N.; Mantovani, A. The toll-like receptor repertoire of human B-lymphocytes: inducible and selective expression of TLR9 and TLR10 in normal and transformed cells. Blood , 2003, 102:956–963.
18. Braito, A.; Ciufolini, M.G.; Pippi, L.; Corbisiero, R.; Fiorentini, C.; Gistri, A.; Toscano L. Phlebotomustransmitted toscana virus infections of the central nervous system: a seven-year experience in Tuscany. Scand J Infect Dis 1998, 30, 505-508.
19. Brisbarre, N.; Attoui, H.; Gallian, P.; Di Bonito, P.; Giorgi, C.; Cantaloube, J.F.; Biagini, P.; Touinssi, M.; Jordier, F.; Micco, P. Seroprevalence of Toscana virus in blood donors, France, 2007. Emerg. Infect. Dis. 2011, 17, 941-943.
20. Brisbarre, N.M.; Plumet, S.; de Micco, P.; Leparc-Goffart, I., Emonet, S.F. Toscana virus inhibits the interferon beta response in cell cultures. Virology. 2013, 442, 189–194.
21. Burton, D.R.; Poignard, P.; Stanfield, R.L.; Wilson, I.A; Broadly neutralizing antibodies present new prospects to counter highly antigenically diverse viruses. Science. 2012, 337, 183–186
22. Calamusa, G.; Valenti, R.M.; Vitale, F.; Mammina, C.; Romano, N.; Goedert, J.J.; Gori- Savellini, G.; Cusi, M.G.; Amodio, E., Seroprevalence of and risk factors for Toscana and Sicilian virus infection in a sample population of Sicily (Italy). J. Infect. 2012, 64, 212–217.
23. Charrel, R.N.; Bichaud, L.; Lamballerie, De, X. Emergence of Toscana virus in the mediterranean area. 2012, 1, 135-141.
24. Charrel, R.N.; Gallian, P.; Navarro-Mari, J.M.; Nicoletti, L.; Papa, A.; Sánchez-Seco, M. P.; Tenorio, A.; Lamballerie, X. Emergence of Toscana virus in Europe. Emerg Infect Dis. 2005, 11, 1657-1663.

25. Cifuentes-Muñoz, N.; Salazar-Quiroz, N.; Tischler, N.D. Hantavirus Gn and Gc envelope glycoproteins: Key structural units for virus cell entry and virus assembly. Viruses 2014, 6, 1801–1822.
26. Ciluna, M.T.; Scaramozzino, P.; Cocumelli, C.; Cusi, M.G.; Perfetti, G.; Autorino, G.L. Preliminary observations on the potential role of some mammalian reservoirs of Toscana virus. Proceedings of the International Meeting on Emerging Diseases and Surveillance, Vienna Austria, 2007 February 23-25.
27. Ciufolini, M.G.; Maroli, M.; Verani, P. Growth of two phleboviruses after experimental infection of their suspected sand fly vector, Phlebotomus perniciosus (Diptera: Psychodidae) Am J Trop Med Hyg. 1985, 34, 174–179.
28. Cleton, N.; Koopmans, M.; Reimerink, J.; Godeke, G.J.; Reusken, C. Come fly with me: review of clinically important arboviruses for global travelers. J Clin Virol. 2012 Nov;55(3):191-203. Epub 2012 Jul 25. Erratum in: J Clin Virol. 2013 Jan;56(1):89-91.
29. Coffey, L.L.; Forrester, N.; Tsetsarkin, K.; Vasilakis, N.; Weaver, S.C. Factors shaping the adaptive landscape for arboviruses: Implications for the emergence of disease. Future Microbiology. 2013, 8,155-176.
30. Collao, X.; Palacios, G.; Sanbonmatsu-Gámez, S.; Ruiz, M. P.; Negredo, A. I.; Navarro-Marí, J. M.; Grandadam, M.; Aransay, A.M.; Lipkin, W.I.; Tenorio, A.; Sánchez-Seco, M. P. Genetic diversity of Toscana virus. Emerg Infect Dis 2009,15, 574-577.
31. Collett, M.S.; Purchio, A.F.; Keegan, K.; Frazier, S.; Hays, W.; Anderson, D.K.; Parker, M.D.; Schmaljohn, C.; Schmidt, J.; Dalrymple, J.M. Complete nucleotide sequence of the M RNA segment of Rift Valley fever virus. Virology, 1985, 144, 228–245.
32. Colomba, C.; Saporito, L.; Ciufolini, M.G.; Marchi, A.; Rotolo, V.; De Grazia, S.; Titone, L.; Giammanco, G.M.; Prevalence of Toscana sandfly fever virus antibodies in neurological patients and control subjects in Sicily. New Microbiol. 2012, 35, 161– 165.

33. Corti, D.; Bianchi, S.; Vanzetta, F.; Minola, A.; Perez, L.; Agatic, G.; Guarino, B.; Silacci, C.; Marcandalli, J.; Marsland, B.J.; Piralla, A.; Percivalle, E.; Sallusto, F.; Baldanti, F.; Lanzavecchia, A. Cross-neutralization of four paramyxoviruses by a human monoclonal antibody. Nature 2013, 501, 439–443.

34. Corti, D.; Lanzavecchia, A. Efficient methods to isolate human monoclonal antibodies from memory B cells and plasma cells. Microbiol Spectrum, 2014, 2, AID-0018-2014.

35. Cusi, M.G.; Gori Savellini, G.; Zanelli, G. Toscana virus epidemiology : from Italy to beyond. The open virology Journal 2010, 4, 22-28.

36. Cusi, M.G.; Valensin, P.E.; Donati, M.; Valassina, M. Neutralization of Toscana virus is partially mediated by antibodies to the nucleocapsid protein. J. Med. Virol. 2001, 63, 72–75.

37. Cusi, M.G.; Valentini, M.; Valensin, P.E.; Valassina, M.; 2002. Immune response to the neurotropic Toscana virus infection: preliminary data. 1st SIV International Workshop on Neurovirology. Alghero, June 23–25, Italy.

38. David, M.; Knipe, Peter M. Howley, et al. Fields' Virology. 5th edition. 2007 Lippincott Williams & Wilkins. USA.

39. De Lamballerie, X.; Tolou, H.; Durand, J.P.; Charrel, R.N. Prevalence of Toscana virus antibodies in volunteer blood donors and patients with central nervous system infections in southeastern France. Vector Borne Zoonotic Dis. 2007, 7, 275–277.

40. Defuentes, G.; Rapp, C.; Imbert, P.; Durand, J.P.; Debord, T. Acute meningitis owing to phlebotomus fever Toscana virus imported to France. J Travel Med. 2005, 12, 295–296.

41. Depaquit, J.; Grandadam, M.; Fouque, F.; Andry, P.E.; Peyrefitte, C. Arthropod-borne viruses transmitted by Phlebotomine sandflies in Europe: a review. Euro Surveill. 2010, 15(10):19507.

42. Di Bonito, P.; Bosco, S.; Mochi, S.; Accardi, L.; Ciufolini, M.G.; Nicoletti, L.; Giorgi, C.; Human antibody response to Toscana virus glycoproteins expressed by recombinant baculovirus. J. Med.Virol. 2002, 68, 615–619.

43. Di Bonito, P.; Mochi, S.; Gr´o, M.C.; Fortini, D.; Giorgi, C. Organization of the M genomic segment of Toscana phlebovirus. J Gen Virol, 1997, 78, 77–81.
44. Di Bonito, P.; Nicoletti, L.; Mochi, S.; Accardi, L.; Marchi, A.; Giorgi, C. Immunological characterization of Toscana virus proteins. Arch Virol.1999, 144,1947– 1960.
45. Di Nicuolo, G.; Pagliano, P.; Battisti, S.; Starace, M.; Mininni, V.; Attanasio, V.; Faella, F.S.; Toscana virus central nervous system infections in southern Italy. J Clin Microbiol, 2005, 43, 6186–6188.
46. Dionisio, D.; Esperti, F.; Vivarelli, A.; Valassina, M. Epidemiological, clinical and laboratory aspects of sandfly fever. Curr Opin Infect Dis. 2003,16, 383-388.
47. Dionisio, D.; Valassina, M.; Ciufolini, M.G.; Vivarelli, A.; Esperti, F.; Cusi, M.G.; Mazzoli, F.; Lupi, C. Encephalitis without meningitis due to sandfly fever virus serotype Toscana. Clin Infec Dis. 2001, 32, 1241–1248.
48. Dobler, G.; Treibl, J.; Haass, A.; Frosner, G.; Woesner, R.; Schimrigk, K. Toscana virus infection in German traveler's returning from the Mediterranean. Infection. 1997, 25, 325–328.
49. Doudier, B.; Ninove, L.; Million, M.; de Lamballerie, X.; Charrel, R.N.; Brouqui, P. Présentation inhabituelle d'une encéphalite àToscana dans le sud de la France [Unusual Toscana virus encephalitis in southern France]. Med Mal Infect. 2011, 1, 50-1.
50. Ehrnst, A.; Peters, C.J.; Niklasson, B.; Svedmyr, A.; Holmgren, B. Neurovirulent Toscana virus (a sandfly fever virus) in Swedish man after visit to Portugal. Lancet. 1985, 1,1212–1213.
51. Eitrem, R.; Niklasson, B.; Weiland, O. Sandfly fever among Swedish tourists. Scand J Infect Dis. 1991, 23, 451–457.
52. Eitrem, R.; Vene, S.; Niklasson, B. Incidence of sand fly fever among Swedish United Nations soldiers on Cyprus during 1985. Am J Trop Med Hyg. 1990, 43, 207–211.
53. Elliott, R.M.; Brennan, B. Emerging phleboviruses. Curr Opin Virol. 2014, 5, 50-57.

54. Fontana, J.; Lopez-Montero, N.; Elliott, R.M.; Fernandez, J.J.; Risco, C. The unique architecture of Bunyamwera virus factories around the Golgi complex. Cell. Microbiol. 2008, 10, 2012–2028.
55. Francisci, D.; Papili, R.; Camanni, G.; Morosi, S.; Ferracchiato, N.; Valente, M.; Ciufolini, M.G.; Baldelli, F. Evidence of Toscana virus circulation in Umbria: first report. Eur. J. Epidemiol. 2003, 18, 457 459.
56. Froger, A.; Hall, J.E. Transformation of plasmid DNA into E. coli using the heat shock method. J Vis Exp. 2007, 6, 253.
57. Gabriel, M.; Resch, C.; Gunther, S.; Schmidt Chanasit, J. Toscana virus infection imported from Elba into Switzerland. Emerg. Infect Dis. 2010, 16, 1034–1036.
58. Gandolfo Claudia, Shibily Prathyumnan, Chiara Terrosi, Gabriele Anichini, Gianni Gori Savellini, Davide Corti, Luisa Bracci, Antonio Lanzavecchia, Maria Grazia Cusi. B cell epitope mapping and selection of Toscana Virus neutralizing epitopes for vaccine design. Poster presented at the 3rd National Congress of the Italian Society for Virology "SIV-ISV", Padua, September 10-12, 2019.
59. Gerrard, S. R.; Bird, B. H.; Albarino, C. G.; Nichol, S.T. The NSm proteins of Rift Valley fever virus are dispensable for maturation, replication and infection. Virology 2007, 359, 459–465.
60. Giorgi, C.; Accardi, L.; Nicoletti, L.; Gr´o, M.C.; Takehara, K.; Hilditch, C.; Bishop, D.H. Sequences and coding strategies of the S RNAs of Toscana and Rift Valley fever viruses compared to those of Punta Toro, Sicilian Sandfly fever, and Uukuniemi Viruses. Virology 1991, 180, 738–753.
61. Gonzalez-Scarano, F.; Shope, R.E.; Calisher, C.E.; Nathanson, N. Characterization of monoclonal antibodies against GN and N proteins of La Crosse and Tahyna, two California serogroup bunyaviruses. Virology 1982, 120, 42–53.
62. Gori Savellini, G.; Anichini, G.; Gandolfo, C.; Prathyumnan, S.; Cusi, M.G. Toscana virus non-structural protein NSs acts as E3 ubiquitin ligase promoting RIG-I degradation. PLoS Pathog 2019, 15(12): e1008186.

63. Gori Savellini, G.; Di Genova, G.; Terrosi, C.; Di Bonito, P.; Giorgi, C.; Valentini, M.; Docquier, J.D.; Cusi, M.G. Immunization with Toscana virus N-Gc proteins protects mice against virus challenge. Virology 2008, 375, 521–528.
64. Gori Savellini, G.; Gandolfo, C.; Cusi, M.G. Truncation of the C-terminal region of Toscana Virus NSs protein is critical for interferon-β antagonism and protein stability. Virology. 2015, 486, 255–262.
65. Gori Savellini, G.; Valentini, M.; Cusi, M.G. Toscana virus NSs protein inhibits the induction of type I interferon by interacting with RIG-I. J Virol. 2013, 87, 6660–6667.
66. Gori Savellini, G.; Weber, F.; Terrosi, C.; Habjan, M.; Martorelli, B.; Cusi, M.G. Toscana virus induces interferon although its NSs protein reveals antagonistic activity. J Gen Virol. 2011, 92, 71–79.
67. Gr´o, M.C.; Di Bonito, P.; Fortini, D.; Mochi, S.; Giorgi, C. Completion of molecular characterization of Toscana phlebovirus genome: nucleotide sequence, coding strategy of M genomic segment and its amino acid sequence comparison to other phleboviruses. Virus Res 1997, 51, 81–91.
68. Grady, L.; Kinch,W. Two monoclonal antibodies against La Crosse virus show host dependent neutralizing activity. J. Gen. Virol. 1985, 66, 2773–2776.
69. Greco, F.; Mauro, M.V.; Tenuta, R.; Apuzzo, G.; Giraldi, C. A new case of meningitis due to Toscana virus. New Microbiol. 2012, 35, 99–100
70. Hemmersbach Miller, M.; Parola, P.; Charrel, R.N.; Paul Durand, J.; Brouqui, P. Sandfly fever due to Toscana virus: an emerging infection in southern France. Eur J Intern Med, 2004, 15, 316-317.
71. Hepojoki, J.; Strandin, T.; Wang, H.; Vapalahti, O.; Vaheri, A.; Lankinen, H. Cytoplasmic tails of hantavirus glycoproteins interact with the nucleocapsid protein. J Gen Virol, 2010, 91, 2341–2350.
72. Herath, V.; Romay, G.; Urrutia, C.D.; Verchot, J. Family level Phylogenies reveal relationships of Plant Viruses within the Order Bunyavirales. Viruses 2020, 12, 1010.

73. Hjelle, B., Chavez-Giles, F.; Torrez-Martinez, N.; Yamada, N.; Sarisky, J.; Ascher, M.; Jenison. S. Dominant glycoprotein epitope of Four Corners hantavirus is conserved across a wide geographical area. J. Gen. Virol. 1994, 75, 2881–2888
74. Hlavacek, W.S.; Posner, R.G.; Perelson A.S. Steric effects on multivalent ligand-receptor binding: Exclusion of ligand sites by bound cell surface receptors. Biophysical Journal, 1999, 76, 3031-3043.
75. Hollidge, B.S.; González-Scarano, F.; Soldan, S.S. Arboviral encephalitides: transmission, emergence, and pathogenesis. J Neuroimmune Pharmacol. 2010, 5, 428-442.
76. http://viralzone.expasy.org/7101?outline=all_by_species
77. https://www.uniprot.org/taxonomy/1980418
78. Hukić, M.; Salimović-Besić, I. Sandfly - Pappataci fever in Bosnia and Herzegovina: the new-old disease. Bosn J Basic Med Sci. 2009,9,39–43.
79. ICTV 2019 release, https://talk.ictvonline.org/taxonomy/
80. Imirzalioglu, C.; Schaller, M.; Bretzel, R.G. Sandfly fever Naples virus (serotype Toscana) infection with meningeal involvement after a vacation in Italy. Dtsch Med Wochenschr. 2006, 131, 2838–40.
81. Iskra, S.; Kalla, M.; Delecluse, H.J.; Hammerschmidt, W.; Moosmann, A. Toll-like receptor agonists synergistically increase proliferation and activation of B-cells by EBV. J Virol.2010, 84:3612–3623.
82. Jones, K.E.; Patel, N.G.; Levy, M.A.; Storeygard, A.; Balk, D.; Gittleman, J.L.; Daszak, P. Global trends in emerging infectious diseases. Nature 2008, 451, 990–993.
83. Kainulainen, M.; Habjan, M.; Hubel, P.; Busch, L.; Lau, S.; Colinge, J.; Furga, G.S.; Pichlmair, A.; Weber, F. Virulence factor NSs of rift valley fever virus recruits the F-box protein FBXO3 to degrade subunit p62 of general transcription factor TFIIH. J Virol. 2014, 88, 3464–3473.
84. Kainulainen, M.; Lau, S.; Samuel, C.E.; Hornung, V.; Weber, F. NSs Virulence Factor of Rift Valley Fever Virus Engages the F-Box Proteins FBXW11 and β-

TRCP1 To Degrade the Antiviral Protein Kinase PKR. J Virol. 2016, 90, 6140–6147.

85. Kalveram, B.; Ikegami, T. Toscana virus NSs protein promotes degradation of double-stranded RNA-dependent protein kinase. J Virol. 2013,87, 3710-3718.

86. Klugman, K.P.; Astley, M.; Lipsitch, M. Unusual Manifestation of Toscana Virus Sporadic Oropouche Virus Infection, Acre. 2009, 15, 347-348.

87. Knippenberg, V.I.; Carlton Smith, C.; Elliott, R.M. The N-terminus of Bunyamwera orthobunyavirus NSs protein is essential for interferon antagonism. J Gen Virol. 2010, 91, 2002–2006.

88. Kormelink, R.; de Haan, P.; Meurs, C. Peters, D.; Goldbach, R. The nucleotide sequence of the M RNA segment of tomato spotted wilt virus, a bunyavirus with two ambisense RNA segments. J Gen Virol 1992, 73, 2795–2804.

89. Kuhn, J.; Bewermeyer, H.; Hartmann-Klosterkoetter, U.; Emmerich, P.; Schilling, S.; Valassina, M. Toscana virus causing severe meningoencephalitis in an elderly traveler. J Neurol Neurosurg Psychiatry. 2005, 76, 1605–1606.

90. Kuismanen, E. Post translational processing of Uukuniemi virus glycoproteins G1 and G2. J. Virol. 1984, 51, 806–812.

91. Kuismanen, E.; Hedman, K.; Saraste, J.; Pettersson, R.F. Uukuniemi virus maturation: Accumulation of virus particles and viral antigens in the Golgi complex. Mol. Cell. Biol. 1982, 2, 1444–1458.

92. Lamballerie, X. D.; Tolou, H.; Durand, J.P.; Charrel, R.N. Prevalence of Toscana virus antibodies in volunteer blood donors and patients with central nervous system infections in southeastern France. Vector Borne Zoonotic Dis. 2007, 7, 275-277.

93. Law, M.D.; Speck, J.; Moyer, J.W. The M RNA of impatiens necrotic spot tospovirus (Bunyaviridae) has an ambisense genomic organization. Virology 1992, 188, 732–741.

94. Liang, G.; Gao, X.; Gould, E.A. Factors responsible for the emergence of arboviruses; strategies, challenges and limitations for their control. Emerging Microbes and Infections. 2015, 4, e18.

95. Liu, D.Y.; Tesh, R.B.; Travassos da Rosa A.P.A.; Peters, C.J.; Yang, Z.; Guzman, H. Xiao, S.Y. Phylogenetic relationships among members of the genus Phlebovirus (Bunyaviridae) based on partial M segment sequence analyses. J Gen Virol. 2003, 84, 465–73.

96. Lober, C.; Anheier, B.; Lindow, S.; Klenk, H.D.; Feldmann, H. The Hantaan virus glycoprotein precursor is cleaved at the conserved pentapeptideWAASA. Virology 2001, 289, 224–229.

97. Ly, H.J.; Ikegami, T. Rift Valley fever virus NSs protein functions and the similarity to other bunyavirus NSs proteins. Virol J 2016, 13, 1-13.

98. Madoff, D.H.; Lenard, J. A membrane glycoprotein that accumulates intracellularly: Cellular processing of the large glycoprotein of La Crosse virus. Cell 1982, 28, 821–829.

99. Manor E. 2008. Human plasma accelerates immortalization of B-lymphocytes by Epstein-Barr virus. Cell Prolif. 1986, 41:292–298.

100. Marchi, S.; Trombetta, C.M.; Montomoli, E. (November 5th 2018). Emerging and Re-emerging Arboviral Diseases as a Global Health Problem, Public Health - Emerging and Re-emerging Issues, Md. Anwarul Azim Majumder, Russell Kabir and Sayeeda Rahman, IntechOpen, DOI: 10.5772/intechopen.77382. Available from: https://www.intechopen.com/books/public-health-emerging-and-re-emerging-issues/emerging-and-re-emerging-arboviral-diseases-as-a-global-health-problem.

101. Marriott, A.C.; el Ghorr, A.A.; Nuttall, P.A. Dugbe nairovirus M RNA: Nucleotide sequence and coding strategy. Virology 1992, 190, 606–615.

102. Martínez-García, F.A.; Moreno-Docón, A.; Segovia-Hernández, M.; Fernández-Barreiro, A. Deafness as a sequela of Toscana virus meningitis. Med Clin (Barc) 2008, 130, 639.

103. Matsuno, K.; Weisend, C.; Kajihara, M.; Matysiak, C.; Williamson, B.N.; Simuunza, M. Mweene, A.S.; Takada, A.; Tesh, R. B.; Ebihara, H. Comprehensive molecular detection of tick-borne Phleboviruses leads to the retrospective

identification of taxonomically unassigned Bunyaviruses and the discovery of a novel member of the genus Phlebovirus. J Virol 2015, 89, 594–604.

104. Matsuoka, Y.; Ihara, T.; Bishop, D.H.; Compans, R.W. Intracellular accumulation of Punta Toro virus glycoproteins expressed from cloned cDNA. Virology 1988, 167, 251–260.

105. Middeldorp, J.M.; Brink, A.A.; van den Brule, A.J.; Meijer, C.J. Pathogenic roles for Epstein-Barr virus (EBV) gene products in EBV-associated proliferative disorders. Crit Rev Oncol Hematol. 2003, 45:1–36.

106. Miller, B.R. Arboviruses. In: Mahy BWJ, Van Regenmortel MHV (eds) Encyclopedia of virology (Third Edition). Academic Press, Oxford, 2008; pp 170–176.

107. Murphy, F. A.; Harrison, A. K.; Whitfield, S. G. Bunyaviridae: Morphologic and morphogenetic similarities of Bunyamwera supergroup viruses and several other arthropod borne viruses. Intervirology 1973, 1, 297-316.

108. Nichol, S.T.; Beaty, B.J.; Elliott, R.M.; Goldbach, R.; Plyusin, A.; Schmaljohn, C. et al. Family Bunyaviridae. Academic Press, London, Elsevier, 2005; pp.

109. Nicoletti, L.; Verani, P.; Caciolli, S.; Ciufolini, M.G.; Renzi, A.; Bartolozzi, D.; Paci, P.; Leoncini, F.; Padovani, P.; Traini, E. Central nervous system involvement during infection by Phlebovirus toscana of residents in natural foci in central Italy (1977-1988). Am J Trop Med Hyg 1991, 45, 429-434.

110. Nilsson, K.; Klein, G. Phenotypic and cytogenetic characteristics of human B lymphoid cell lines and their relevance for the etiology of Burkitt's lymphoma. Adv. Cancer Res. 1982, 37,319-380.

111. Novoa, R.R.; Calderita, G.; Cabezas, P.; Elliott, R.M.; Risco, C. Key Golgi factors for structural and functional maturation of bunyamwera virus. J. Virol. 2005, 79, 10852–10863.

112. Overby, A. K.; Pettersson, R. F.; Neve, E. P. The glycoprotein cytoplasmic tail of Uukuniemi virus (Bunyaviridae) interacts with ribonucleoproteins and is critical for genome packaging. J Virol 2007, 81, 3198–3205.

113. Overby, A.K.; Popov, V.; Neve, E.P.; Pettersson, R.F. Generation and analysis of infectious virus-like particles of Uukuniemi virus (Bunyaviridae): A useful system for studying bunyaviral packaging and budding. J. Virol. 2006, 80, 10428–10435.
114. Palacios, G.; Savji, N.; Travassos da Rosa, A.; Guzman, H.; Yu, X.; Desai, A.; Rosen, G. E.; Hutchison, S.; W. Ian Lipkin, W. L.; Tesh, R. Characterization of the Uukuniemi virus group (Phlebovirus: Bunyaviridae): evidence for seven distinct species. J Virol. 2013, 87, 3187–95.
115. Park, S.W.; Han, M.G.; Park, C.; Ju, Y.R.; Ahn, B.Y.; Ryou, J. Hantaan virus nucleocapsid protein stimulates MDM2-dependent p53 degradation. J Gen Virol. 2013, 94: 2424–2428.
116. Patterson, J.L.; Holloway, B.; Kolakofsky, D. La Crosse virions contain a primer-stimulated RNA polymerase and a methylated cap-dependent endonuclease. J Virol 1984, 52, 215–222.
117. Pauli, C.; Schwarz, T.F.; Meyer, C.G.; Jäger, G. Neurologische Symptome nach Infektion durch Sandfliegenfieber-Virus [Neurological symptoms after an infection by the sandfly fever virus]. Dtsch Med Wochenschr. 1995, 20, 1468-72.
118. Pelloquin, F.; Lamelin, J.P.; Lenoir, G.M. Human B lymphocyte immortalization by Epstein-Barr virus in the presence of cyclosporin A. In Vitro Cell Devel Biol. 22:689–689.
119. Pifat, D.Y.; Osterling, M.C.; Smith, J.F. Antigenic analysis of Punta Toto virus and identification of protective determinants with monoclonal antibodies. Virology 1988, 167, 442-450.
120. Piper, M.E.; Sorenson, D.R.; Gerrard, S.R. Efficient cellular release of Rift Valley fever virus requires genomic RNA. PLoS ONE 2011, 6, e18070.
121. Portolani, M.; Sabbatini, A.M.; Beretti, F.; Gennari, W.; Tamassia, M.G.; Pecorari, M.; Symptomatic infections by Toscana virus in the Modena province in the triennium 1999–2001. New Microbiol. 2002, 25, 485–488.
122. Powers, A.M. Overview of emerging Arboviruses. Future Virology. 2009, 4, 391-401

123. Price, A.M.; Luftig, M.A. Dynamic Epstein–Barr virus gene expression on the path to B-cell transformation. Adv Virus Res. 2013, 88:279–313.
124. Punda-Polić, V.; Mohar, B.; Duh, D.; Bradarić, N.; Korva, M.; Fajs, L.; et al. Evidence of an autochthonous Toscana virus strain in Croatia. J. Clin. Virol. 2012, 55, 1:4–7.
125. Ranki, M.; Pettersson, R.F. Uukuneimi virus contains an RNA polymerase. J Virol 1975, 16,1420–1425.
126. Reed, L.J.; Muench, H. A simple method of estimating fifty per cent endpoints. Am J Hyg 1938, 27, 493-497
127. Remi, N.; Charrel, Chapter 8 - Toscana Virus Infection, Editor(s): Önder Ergönül, Füsun Can, Lawrence Madoff, Murat Akova, Emerging Infectious Diseases, Academic Press, 2014, Pages 111-119.
128. Ribeiro, D.; Borst, J. W.; Goldbach, R.; Kormelink, R. Tomato spotted wilt virus nucleocapsid protein interacts with both viral glycoproteins Gn and Gc in planta. Virology 2009, 383, 121–130.
129. Rickinson, A.B.; Moss, D.J.; Pope, J.H. Long-term T cell-mediated immunity to Epstein-Barr virus in man. II. Components necessary for regression in virus-infected leukocyte cultures. Int. J. Cancer 1979, 23, 610-617.
130. Rinaldi, R.; Goteri, G.; Biagetti, S.; Cusi, M.G.; Rossini, S. Histological description of the lymphadenopathy related to Toscana virus infection. Report of a case. Pathol. Res. Pract. 2011, 207,197-201.
131. Rizk, R.Z.; Christensen, N.D.; Michael, K.M.; Müller, M.; Sehr, P.; Waterboer, T.; Pawlita, M. Reactivity pattern of 92 monoclonal antibodies with 15 human papillomavirus types. J Gen Virol. 2008, 89, 117-129.
132. Rogers, T. F.; Zhao, F.; Huang, D.; Beutler, N.; Burns, A.; He, W. T.; Limbo, O.; Smith, C.; Song, G.; Woehl, J.; Yang, L.; Abbott, R. K.; Callaghan, S.; Garcia, E.; Hurtado, J.; Parren, M.; Peng, L.; Ramirez, S.; Ricketts, J.; Ricciardi, M. J.; Burton, D.R. Isolation of potent SARS-CoV-2 neutralizing antibodies and protection from disease in a small animal model. Science (New York, N.Y.), 2020, 369,6506, 956–963.

133. Rosenberg, R.; Johansson, M.A.; Powers, A.M.; Miller, B.R. Search strategy has influenced the discovery rate of human viruses. Proc. Natl. Acad. Sci. USA 2013, 110, 13961–13964.
134. Salanueva, I.J.; Novoa, R.R.; Cabezas, P.; Lopez-Iglesias, C.; Carrascosa, J.L.; Elliott, R.M.; Risco, C. Polymorphism and structural maturation of bunyamwera virus in Golgi and post-Golgi compartments. J. Virol. 2003, 77, 1368–1381.
135. Saluzzo, J.F.; Anderson Jr., G.W.; Hodgson, L.A.; Digoutte, J.P.; Smith, J.F. Antigenic and biological properties of Rift Valley fever virus isolated during the 1987 Mauritanian epidemic. Res. Virol. 1989, 140, 155–164.
136. Saluzzo, J.F.; Anderson Jr., G.W.; Smith, J.F.; Fontenille, D.; Coulanges, P. Biological and antigenic relationship between Rift Valley fever virus strains isolated in Egypt and Madagascar.Trans. R. Soc. Trop. Med. Hyg. 1989, 83, 701.
137. Sanbonmatsu Gamez, S.; Perez Ruiz, M.; Collao, X.; Sanchez Seco, M.P.; Morillas Marquez, F.; de la Rosa Fraile, M.; Navarro-Mari, J.M.; Tenorio, A. Toscana virus in Spain. Emerg Infect Dis. 2005,11, 1701–1707.
138. Sanbonmatsu Gàmez, S.; Pèrez Ruiz, M.; Palop Borràs, B.; Navarro Marì, J.M. Unusual Manifestation of Toscana virus Infection, Spain. Emerg infect Dis 2009,15, 347-348.
139. Sanger, F.; Nicklen, S.; Coulson, A.R. DNA sequencing with chain-terminating inhibitors. Proc Natl Acad Sci USA. 1977, 74, 12: 5463-5467.
140. Schmaljohn, C. S.; Hooper, J. W. (2001). Bunyaviridae. In Fields Virology,4th Edition, vol 2, pp: 1293-1309. Edited by D. M. Knipe & P. M. Howley. Philadelphia, PA: Lippincott Williams & Wilkins.
141. Schmaljohn, C. S.; Nichol, S. T. (2006). Bunyaviridae. In Fields Virology, 5th Edition, vol. 2, pp. 1741–1789. Edited by D. M. Knipe & P. M.Howley. Philadelphia, PA: Lippincott Williams & Wilkins.
142. Schmaljohn, C.; Elliott, R.M. Bunyaviridae. In Fields Virology, 6th Edition.; Knipe, D.M., Howley, P.M., Eds.; Lippincott Williams & Wilkins: Philadelphia, PA, USA, 2014; Volume 1, pp. 1244–1282.

143. Schmaljohn, C.S.; Schmaljohn, A.L.; Dalrymple, J.M. Hantaan virus M RNA: Coding strategy, nucleotide sequence, and gene order. Virology 1987, 157, 31–39.
144. Schwarz, T.F.; Gilch, S.; Jäger, G. Aseptic meningitis caused by sandfly fever virus, serotype Toscana. Clin Infect Dis 1995, 21, 669-671.
145. Schwarz, T.F.; Gilch, S.; Pauli, C.; Jager, G. Immunoblot detection of antibodies to Toscana virus J Med Virol 1996, 49, 83-86.
146. Schwarz, T.F.; Jäger, G.; Gilch, S. et al. Travel-related vector-borne virus infections in Germany. Arch Virol Suppl. 1996, 11, 57–65.
147. Schwarz, T.F.; Jäger, S.; Gilch, S.; Pauli, C. Serosurvey and laboratory diagnosis of imported sandfly fever virus, serotype Toscana, infection in Germany. Epidemiol Infect. 1995, 114, 501–510.
148. Serata, D.; Rapinesi, C.; Del Casale, A.; Simonetti, A.; Mazzarini, L.; Ambrosi, E. Kotzalidis, G. D.; Fensore, C.; Girardi, P.; Tatarelli, R. Personality changes after Toscana virus (TOSV) encephalitis in a 49-year-old man: a case report. Int. J. Neurosci. 2011, 121, 165-169.
149. Shi, X.; Brauburger, K.; Elliott, R.M. Role of N-linked glycans on bunyamwera virus glycoproteins in intracellular trafficking, protein folding, and virus infectivity. J. Virol. 2005, 79, 13725–13734.
150. Shi, X.; Kohl, A.; Li, P.; Elliott, R.M. Role of the cytoplasmic tail domains of Bunyamwera orthobunyavirus glycoproteins Gn and Gc in virus assembly and morphogenesis. J Virol 2007, 81, 10151–10160.
151. Smith, J.F.; Pifat, D.Y. Morphogenesis of sandfly viruses (Bunyaviridae family). Virology 1982, 121, 61–81.
152. Snippe, M.; Willem Borst, J.; Goldbach, R.; Kormelink, R. Tomato spotted wilt virus Gc and N proteins interact in vivo. Virology 2007, 357, 115–123.
153. Sonderegger, B.; Hachler, H.; Dobler, G.; Frei, M. Imported aseptic meningitis due to Toscana virus acquired on the island of Elba, Italy, August 2008. Euro Surveill. 2009, 14, 7-8.
154. Spiegel, M.; Plegge, T.; Pöhlmann, S. The role of phlebovirus glycoproteins in viral entry, assembly and release. Viruses. 2016, 8, 1-20.

155. Spiropoulou, C.F. Hantavirus maturation. In Hantaviruses; Schmaljohn, C.S., Nichol, S.T., Eds.; Springer-Verlag: Heidelberg/Berlin, Germany, 2001; pp. 33–46.
156. Steinitz M, editor. Production of human monoclonal antibodies by the Epstein-Barr virus method. Human monoclonal antibodies. London: Springer. 2014, p. 111–122.
157. Steinitz, M.; Klein, G.; Koskimies, S.; Makel, O. EB virus-induced B lymphocyte cell lines producing specific antibody. Nature 1977, 269, 420–422.
158. Sugden, B.; Mark,W. Clonal transformation of adult human leukocytes by Epstein-Barr virus. J. Virol. 1977, 23, 503-508.
159. Sugden, B.; Phelps, M.; Domoradski, J. Epstein-Barr virus DNA is amplified in transformed lymphocytes. J. Virol. 1979, 31, 590-595.
160. Terrosi, C.; Olivieri, R.; Bianco, C.; Cellesi, C.; Cusi, M.G. Age-dependent seroprevalence of Toscana virus in central Italy and correlation with the clinical profile. Clin Vaccine Immunol. 2009, 16, 1251-1252.
161. Tesh, R.B.; Peters, C.J.; Meegan, J.M. Studies on the antigenic relationship among phleboviruses. Am J Trop Med Hyg 1982, 31,149-155
162. Tosato, G.; Pike, S.E.; Koski, I.; Blaese, R.M. Selective inhibition of immunoregulatory cell functions by Cyclosporin A. J. Immunol. 1982, 128,1986-1991.
163. Traggiai, E. editor. Immortalization of human B-cells: Analysis of B-cell repertoire and production of human monoclonal antibodies. Antibody methods and protocols. London: Springer. 2012, p. 161–170.
164. Valassina, M.; Cuppone, A.M.; Bianchi, S.; Santini, L.; Cusi, M.G. Evidence of Toscana virus variants circulating in Tuscany, Italy, during the summers of 1995 to 1997. J Clin Microbiol. 1998, 36, 2103–2104.
165. Valassina, M.; Cusi, M.G.; Valensin, P.E. A Mediterranean arbovirus: The Toscana virus. Journal of Neuro Virology 2003, 9, 577-583.
166. Valassina, M.; Cusi, M.G.; Valensin, P.E. Rapid identification of Toscana virus by nested PCR during an outbreak in the Siena area of Italy. J. Clin. Microbiol. 1996, 34, 2500–2502.

167. Valassina, M.; Meacci, F.; Valensin, P.E.; Cusi, M.G. Detection of neurotropic viruses circulating in Tuscany: the incisive role of Toscana virus. J Med Virol. 2000, 60, 86–90.

168. Valassina, M.; Valentini, M.; Pugliese, A.; Valensin, P.E.; Cusi, M.G. Serological Survey of Toscana Virus Infections in a High-Risk Population in Italy. 2003, 10, 483-484.

169. Valentini, M.; Valassina, M.; Savellini, G.G.; Cusi, M.G. Nucleotide variability of Toscana virus M segment in strains isolated from clinical cases. J.Virus Res 2008, 135, 187-190.

170. Varani, S.; Gelsomino, F.; Bartoletti, M.; Viale, P.; Mastroianni, A.; Briganti, E.; Ortolani, P.; Albertini, F.; Calzetti, C.; Prati, F.; Cenni, P.; Castellani, G.; Morini, S.; Rossini, G.; Landini, M. P.; Sambri, V. Meningitis caused by Toscana Virus is associated with strong Antiviral response in the CNS and Altered Frequency of Blood Antigen- Presenting Cells. 2015, 7, 5831-5843.

171. Venturi, G.; Ciccozzi, M.; Montieri, S.; Bartoloni, A.; Francisci, D.; Nicoletti, L.; Fortuna, C.; Marongiu, L.; Rezza, G.; Ciufolini, M.G. Genetic variability of the M genome segment of clinical and environmental Toscana virus strains. J Gen Virol. 2007, 88, 1288–94.

172. Venturi, G.; Madeddu, G.; Rezza, G.; Ciccozzi, M.; Pettinato, M.L.; Cilliano, M.; Fiorentini, C.; Mura, M.S.; Ciufolini, M.G. Detection of Toscana virus central nervous system infections in Sardinia Island, Italy. J. Clin. Virol. 2007, 40, 90–91.

173. Verani, P.; Ciufolini, M.G.; Caciolli, S.; Renzi, A.; nicoletti, L.; Sabatinelli, G.; Dario Bartolozzi, D.; Volpi, G.; Amaducci, L.; Coluzzi, M.; Paci, P.; Balducci, M. Ecology of viruses isolated from sand flies in Italy and characterized of a new Phlebovirus (Arabia virus). Am J Trop Med Hyg. 1988, 38, 433-439.

174. Verani, P.; Ciufolini, M.G.; Nicoletti, L.; Balducci, M.; Sabatinelli, G.; Coluzzi, M.; Paci, P.; Amaducci, L. Ecological and epidemiological studies of Toscana virus, an arbovirus isolated from Phlebotomus. Ann Ist Super Sanità 1982,18, 397–399.

175. Verani, P.; Nicoletti, L.; Ciufolini, M.G. Antigenic and biological characterization of Toscana virus, a new Phlebotomus fever group virus isolated in Italy. Acta Virol. 1984, 28, 39–47.
176. Vocale, C.; Bartoletti, M.; Rossini, G.; Macini, P.; Pascucci, M.G.; Mori, F.; Tampieri, A.; Lenzi, T.; Pavoni, M.; Giorgi, C.; Gaibani, P.; Cavrini, F.; Pierro, A.; Landini, M.P.; Viale, P.; Sambri, V. Toscana virus infections in northern Italy: laboratory and clinical evaluation. Vector Borne Zoonotic Dis. 2012, 12, 526–529.
177. Walter, C.T.; Barr, J.N. Recent advances in the molecular and cellular biology of bunyaviruses. 2011, 92, 2467-2484.
178. Weaver, S.C.; Reisen, W.K. Present and future arboviral threats. Antiviral Research. 2010, 85, 328-345.
179. Weber, F.; Bridgen, A.; Fazakerley, J.K.; Streitenfeld, H.; Kessler, N.; Randall, R.E.; Elliot, R.M. Bunyamwera bunyavirus nonstructural protein NSs counteracts the induction of alpha/beta interferon. J Virol. 2002,76, 7949–7955.
180. Weber, M.; Weber, F. RIG-I-like receptors and negative-strand RNA viruses: RLRly bird catches some worms. Cytokine Growth Factor Rev. 2014 b, 25, 621–628.
181. Weber, M.; Weber, F. Segmented negative-strand RNA viruses and RIG-I: Divide (your genome) and rule. Curr. Opin. Microbiol. 2014 a, 20, 96–102.
182. Wec, A. Z.; Wrapp, D; Herbert, A. S.; Maurer, D. P.; Haslwanter, D.; Sakharkar, M.; Jangra, R. K.; Dieterle, M. E.; Lilov, A.; Huang, D.; Tse, L. V.; Johnson, N. V.; Hsieh, C. L.; Wang, N.; Nett, J. H.; Champney, E.; Burnina, I.; Brown, M.; Lin, S.; Sinclair, M.; Walker, L. M. Broad neutralization of SARS-related viruses by human monoclonal antibodies. Science (New York, N.Y.), 2020 ,369, 6504, 731–736.
183. Whitehorn, J.; Yacoub, S. Global warming and arboviral infections. Clin Med (Lond). 2019,19,149-152.
184. WHO Fact Sheet: Vector-Borne Diseases. Available online: https://www.who.int/news-room/fact-sheets/detail/vector-borne-diseases (accessed on 22 August 2020).

185. Wichgers Schreur, P.J.; Kormelink, R.; Kortekaas, J. Genome packaging of the Bunyavirales. Curr. Opin. Virol. 2018, 33, 151–155.

186. Won, S.; Ikegami, T.; Peters, C. J.; Makino, S. NSm protein of Rift Valley fever virus suppresses virus-induced apoptosis. J Virol 2007, 81, 13335–13345.

187. Woolhouse, M.E.; Howey, R.; Gaunt, E.; Reilly, L.; Chase-Topping, M.; Savill, N. Temporal trends in the discovery of human viruses. Proc. R. Soc. B Biol. Sci. 2008, 275, 2111–2115.

188. Wu, Y.; Zhu, Y.; Gao, F.; Jiao, Y.; Oladejo, B.O.; Chai, Y.; Bi, Y.; Lu, S.; Dong, M.; Zhang, C.; Huang, G.; Wong, G.; Li, N.; Zhang, Y.; Li, Y.; Feng, W.H.;, Shi, Y.; Liang, M.; Zhang, R.; Qi, J.; Gao, G.F. Structures of phlebovirus glycoprotein Gn and identification of a neutralizing antibody epitope. Proc Natl AcadSci USA. 2017, 114, E7564-E7573.

189. Xu, F.; Chen, H.; Travassos da Rosa, A.P.; Tesh, R.B.; Xiao, S.Y. Phylogenetic relationships among sandfly fever group viruses (Phlebovirus: Bunyaviridae) based on the small genome segment. J Gen Virol. 2007, 88, 2312–2319.

190. Younesi, V.; Shirazi, F.G.; Memarian, A.; Amanzadeh, A.; Jeddi Tehrani, M.; Shokri, F. Assessment of the effect of TLR7/8, TLR9 agonists and CD40 ligand on the transformation efficiency of Epstein-Barr virus in human B-lymphocytes by limiting dilution assay. Cytotechnology, 2014, 66:95–105.

191. Young, L.S.; Rickinson, A.B. Epstein-Barr virus: 40 years on. Nat Rev Cancer. 2004, 4:757–768.

192. Yousefi, M.; Khosravi-Eghbal, R.; Mahmoudi, A.R.; Jeddi.Tehrani, M.; Rabbani, H.; Shokri, F. Comparative in vitro and in vivo assessment of toxin neutralization by anti-tetanus toxin monoclonal antibodies. Hum Vac Immunother. 2013a, 10:16–15.

193. Yousefi, M.; Tahmasebi, F.; Younesi, V.; Razavi, A.; Khoshnoodi, J.; Bayat, A.A.; Abbasi, E..; Rabbani, H.; Jeddi-Tehrani, M.; Shokri, F. Characterization of neutralizing monoclonal antibodies directed against tetanus toxin fragment C. J Immunotoxicol. 2013b, 11:28–34.

194. Yu, X.J.; Liang, M.F.; Zhang, S.Y.; Liu, Y.; Li, J.D.; Sun, Y.L.; Zhang, L.; Zhang, Q.F.; Popov, V.L.; Li, C.; Li, C.; Qu, J.; Li, Q.; Zhang, Y.P.; Hai, R.; Wu, W.; Wang, Q.; Zhan, F.X.; Wang, X.J.; Kan, B.; Wang, S.W.; Wan, K.L.; Jing, H.Q.; Lu, J.X.; Yin, W.W.; Zhou, H.; Guan, X.H.; Liu, J.F.; Bi, Z.Q.; Liu, G.H.; Ren, J.; Wang, H.; Zhao, Z.; Song, J.D.; He, J.R.; Wan, T.; Zhang, J.S.; Fu, X.P.; Sun, L.N.; Dong, X.P.; Feng, Z.J.; Yang, W.Z.; T.H.;Y.Z.; D.H.; Wang, Y.; Li, D.X. Fever with thrombocytopenia associated with a novel bunyavirus in China. N. Engl. J. Med. 2011, 364, 1523–1532.

195. Zhang, Y.Z. Discovery of hantaviruses in bats and insectivores and the evolution of the genus Hantavirus. Virus Res. 2014,17,15-21.

196. Zost, S.J.; Gilchuk, P.; Chen, R.E. Rapid isolation and profiling of a diverse panel of human monoclonal antibodies targeting the SARS-CoV-2 spike protein. Nat Med, 2020, 26, 1422–1427.

CHAPTER 8

ANNEXURE

Activities carried out during PhD course

Trainings and Workshops

I Year

One day workshop on 'Multiplexing Elispot' at Vismederi srl, Siena in collaboration with CTL Europe Gmbh.

II Year

Two days training in 'EBV mediated immortalization of B cells' at Department of Medical Biotechnologies, University of Siena by Prof. Micheal Steinitz (Professor at The Hebrew University, Jerusalem, Israel).

Congress Presentations

I Year

'Ubiquitination of Toscana Virus NSs undermines itd stability and has role in RIG-I degradation': Claudia Gandolfo, Gianni Gori Savellini, Shibily Prathyumnan, Maria Grazia Cusi. Poster presented at the 2018 Negative Strand RNA Virus (NSV2018), Verona, June 17-22, 2018.

II Year

'B cell epitope mapping and selection of Toscana Virus neutralizing epitopes for vaccine design': Gandolfo Claudia, Shibily Prathyumnan, Chiara Terrosi, Gabriele Anichini, Gianni Gori Savellini, Davide Corti, Luisa Bracci, Antonio Lanzavecchia, Maria Grazia Cusi. Poster presented at the 3rd National Congress of the Italian Society for Virology "SIV-ISV", Padua, September 10-12, 2019.

Papers Published

1. Anichini G, Gandolfo C, Terrosi C, Fabrizi S, Miceli GB, Gori Savellini G, Prathyumnan S, Franchi F, Cusi MG. Antibody response to SARS-CoV-2 in infected patients with different clinical outcome. J Med Virol. 2021 93(4):2548-2552. doi: 10.1002/jmv.26789. Epub 2021 Jan 26.

2. Gori Savellini G, Bini L, Gagliardi A, Anichini G, Gandolfo C, Prathyumnan S, Cusi MG. Ubiquitin and Not Only Unfolded Domains Drives Toscana Virus Non-Structural NSs Protein Degradation. Viruses. 2020 Oct 12;12(10):1153. doi: 10.3390/v12101153.

3. Anichini G, Gandolfo C, Fabrizi S, Miceli GB, Terrosi C, Gori Savellini G, Prathyumnan S, Orsi D, Battista G, Cusi MG. Seroprevalence to Measles Virus after Vaccination or Natural Infection in an Adult Population, in Italy. Vaccines (Basel). 2020 Feb 3;8(1):66. doi: 10.3390/vaccines8010066.

4. Gori Savellini G, Anichini G, Gandolfo C, Prathyumnan S, Cusi MG. Toscana virus non-structural protein NSs acts as E3 ubiquitin ligase promoting RIG-I degradation. PLoS Pathog. 2019 Dec 9;15(12):e1008186. doi: 10.1371/journal.ppat.1008186. eCollection 2019 Dec.

PAPERS PUBLISHED

PLOS PATHOGENS

RESEARCH ARTICLE

Toscana virus non-structural protein NSs acts as E3 ubiquitin ligase promoting RIG-I degradation

Gianni Gori Savellini, Gabriele Anichini, Claudia Gandolfo, Shibily Prathyumnan, Maria Grazia Cusi*

Department of Medical Biotechnologies, University of Siena, Siena, Italy

* mariagrazia.cusi@unisi.it

OPEN ACCESS

Citation: Gori Savellini G, Anichini G, Gandolfo C, Prathyumnan S, Cusi MG (2019) Toscana virus non-structural protein NSs acts as E3 ubiquitin ligase promoting RIG-I degradation. PLoS Pathog 15(12): e1008186. https://doi.org/10.1371/journal.ppat.1008186

Editor: Holly Ramage, University of Pennsylvania Perelman School of Medicine, UNITED STATES

Received: May 27, 2019

Accepted: November 4, 2019

Published: December 9, 2019

Data Availability Statement: All relevant data are within the manuscript and its Supporting Information files.

Funding: This study was partially funded by MIUR (PRIN2017.0001336.27-03-2018). The funders had no role in study design, data collection and analysis, decision to publish, or preparation of the manuscript.

Competing interests: The authors have declared that no competing interests exist.

Abstract

It is known that the non-structural protein (NSs) of Toscana virus (TOSV), an emergent sandfly-borne virus causing meningitis or more severe central nervous system injuries in humans, exerts its function triggering RIG-I for degradation in a proteasome-dependent manner, thus breaking off the IFN-β production. The non-structural protein of different members of Bunyavirales has recently appeared as a fundamental protagonist in immunity evasion through ubiquitination-mediated protein degradation targets. We showed that TOSV NSs has an E3 ubiquitin ligase activity, mapping at the carboxy-terminal domain and also involving the amino-terminal of the protein. Indeed, neither the amino- (NSsΔN) nor the carboxy- (NSsΔC) terminal-deleted mutants of TOSV NSs were able to cause ubiquitin-mediated proteasome degradation of RIG-I. Moreover, the addition of the C-terminus of TOSV NSs to the homologous protein of the Sandfly Fever Naples Virus, belonging to the same genus and unable to inhibit IFN-β activity, conferred new properties to this protein, favoring RIG-I ubiquitination and its degradation. NSs lost its antagonistic activity to IFN when one of the terminal residues was missing. Therefore, we showed that NSs could behave as an atypical RING between RING (RBR) E3 ubiquitin ligases. This is the first report which identified the E3 ubiquitin ligase activity in a viral protein among negative strand RNA viruses.

Author summary

Toscana virus is an emergent sandfly-borne virus mainly transmitted to humans by phlebotomine sandflies, which can cause meningitis or more severe central nervous system injuries in some subjects. As many other RNA viruses, it counteracts IFN-β expression by its non-structural protein. Our results expanded our knowledge about the molecular mechanisms by which TOSV exerts its activity as an E3 ubiquitin ligase. This is the first example of a viral protein presenting this activity among negative-strand RNA viruses. Thus, the recognition of this activity and its substrates among viruses are of primary importance to understand how viruses can alter their fitness by the ubiquitin pathway and provide an attractive target for the development of antiviral therapies.

Introduction

Toscana virus (TOSV; *Phenuiviridae* family, Phlebovirus genus) is an emergent sandfly-borne virus mainly transmitted to humans by phlebotomine sandflies [1–3]. A large number of infections is asymptomatic, however, TOSV infection is the leading cause of meningitis or more severe central nervous system (CNS) injuries, such as encephalitis and ischemia during the summer season in southern Europe [4–5]. The viral genome is composed of the large (L), medium (M) and small (S) segments [6]. The L segment encodes an RNA-dependent RNA-polymerase, the M segment encodes the envelope glycoproteins (Gn and Gc) and a non-structural protein (NSm) and the S segment encodes a nucleocapsid (N) protein and a non-structural (NSs) protein [6, 7, 8, 9]. The NSs protein of some members of the *Phenuiviridae* family represents an important virulence factor being a potent antagonist of type I interferons (IFN-α/β), the main protagonists of the host innate immunity against viral infections. The signaling pathway leading to the secretion of IFN-β and the establishment of an antiviral state are achieved by the induction of the cytoplasmic viral sensors RIG-I (Retinoic-acid Inducible Gene I) and MDA-5 (Melanoma Differentiation Associated gene-5) able to recognize dsRNA molecules generated during viral replication [10]. In order to overcome this first-line defense implemented by the host, viruses have evolved protein(s) able to block IFN-β production and its downstream activity at different steps in the signaling cascade. Among Bunyavirales, Toscana virus (TOSV), the Bunyamwera Virus (BUNV), La Crosse Virus (LACV), Sin Nombre (SNV), Tula (TULV) and Puumala (PUUV) Hantaviruses, Rift Valley Fever Virus (RVFV) and Severe Fever with Thrombocytopenia Syndrome Virus (SFTSV), express the NSs protein acting as a suppressor of IFNs [11–21]. Along with this evidence, previous studies have shown that TOSV NSs could exert its function by triggering RIG-I for degradation in a proteasome-dependent manner, thus breaking off the IFN-β production and blocking the establishment of an efficient antiviral state [21, 22]. The proteasomal degradation of proteins by ubiquitination is a process consisting of a covalent attachment of ubiquitin to target proteins. The molecular machinery which leads to the assembly and linkage of poly-Ub chains to the target protein consists of three enzymes defined as ubiquitin-activating enzymes (E1), ubiquitin-conjugating enzymes (E2) and ubiquitin-ligases (E3), which work sequentially in a cascade. In this context, the E3 ubiquitin ligase is the only enzyme which confers specificity to this system by recognizing a selected target protein [23, 24, 25]. E3 ligases are distinguished in RING (Really Interesting New Gene), HECT (Homologous to the E6-AP Carboxy Terminus) and RBR (RING Between RING). A notable distinction in the mechanism among the classes is that RING E3 catalyzes a direct transfer of ubiquitin from E2 to the target protein, whereas a transfer of ubiquitin by HECT E3 involves an intermediate step where the ubiquitin is first transferred from E2 to an active cysteine residue on HECT E3 ligase, then it is conjugated to the target protein [26–35]. RBR combines properties of RING and HECT E3s to conjugate Ub to target proteins. [32]. Based on the linkage generated between ubiquitin moieties, the cognate proteins undergo regulation of their physiological functions, although the role of some chains is still elusive [36–41]. The non-structural protein of different members of Bunyavirales has recently appeared as a fundamental protagonist in virus replication and immunity evasion through ubiquitination-mediated protein degradation [22, 42–45]. To better understand the interaction between the ubiquitin system and TOSV NSs, we investigated whether this viral protein could be responsible for ubiquitin modifications of specific targets. In this study, we showed that TOSV NSs has an E3 ubiquitin ligase activity mapping at the carboxy- and the amino-terminal domains of the protein. Indeed, it appears to promote the transfer of ubiquitin to RIG-I, thus favoring its proteasome-dependent proteolysis. During the course of evolution and adaptation, many of the large DNA viruses have shown to encode their own Ub modifying machinery to facilitate viral

replication through regulating immune responses. Here, we present the first report which identifies the E3 ubiquitin ligase activity in a viral protein among negative-strand RNA viruses, to mediate host–virus interactions.

Results

NSs and RIG-I expression in Toscana virus infected cells

Previous results have shown that TOSV was able to induce a RIG-I-mediated IFN-β expression in infected cells, likely because NSs was expressed at a low level and relatively late during the viral replication cycle [18]. Therefore, only the *in vitro* over-expression of NSs could evidence its properties mediating a decrease of RIG-I, due to the ubiquitination and proteasomal degradation of RIG-I after their interaction [21]. To better characterize the role of NSs during TOSV infection, the IFN-β competent cell line, Lenti-X 293T, was infected and analysed. The immunoblotting evaluating the expression of endogenous RIG-I performed on cell lysates of mock-infected, TOSV infected, or poly(I:C) stimulated cells showed that RIG-I was induced as revealed at 24h and 48h post-infection (p.i.), alongside with the NSs protein. To better address whether the lack of endogenous RIG-I degradation in TOSV infected cells was due to the low amount of the non structural protein in the early phase of replication, an over-expression of NSs was performed by transient transfection in infected cells. The immunoblotting of these cell lysates confirmed that the level of endogenous RIG-I was reduced in the presence of a higher amount of NSs (S1 Fig, S1 Dataset). Therefore, as previously reported [18], we might hypothesize that the fast replication of TOSV was able to trigger an early innate immune response by inducing IFNs, and that the NSs protein could not counteract this effect, as it was produced later during the virus replication cycle. (S1 Fig, S1 Dataset). As expected, stimulation with poly(I:C) strongly induced cellular accumulation of RIG-I in the selected cell line and the over-expression of TOSV NSs was able to contrast poly(I:C) effects (S1 Fig, S1 Dataset).

NSs contains an E3 ubiquitin ligase activity *in vitro*

Previous results [18, 21, 22] have shown that TOSV NSs presented inhibitory properties versus the IFN-β mediated immune response. In particular, RIG-I was targeted for proteasomal-degradation through the action of NSs, and its functional activity was related to the carboxyl-terminus of the protein itself [22], however, assuming that other domains could also be involved. Therefore, we also tested the activity of the amino-terminus (71 aa.) deleted NSs protein (NSsΔN) (S2 Fig) towards RIG-I. Surprisingly, we found a behavior similar to the one observed for the carboxy-terminus deleted NSs (NSsΔC). NSsΔN significantly lost its degrading activity on RIG-I upon co-transfection of cells with the respective plasmids (Fig 1A, S2 Dataset). Moreover, RIG-I-mediated IFN-β promoter activation was not affected by NSsΔN, as shown by the luciferase reporter assay ($p = 0.638$) (Fig 1A, S2 Dataset). Since the treatment with the proteasome inhibitor MG-132 reversed RIG-I degradation by NSs [21], the possibility of a ubiquitin-mediated proteasomal degradation was evaluated. A growing number of viruses was found to weaponize the ubiquitin modification system to suppress IFN [11–21]. Thus, looking for a tool to identify a functional site of the protein, we submitted the NSs protein sequence to the Phyre2 prediction software (www.sbg.bio.ic.ac.uk/phyre2/html/page.cgi) [46], which provided an alignment of 15 residues (aa. 277–292) and a confidence of 30.7% between NSs and RNF31, the E3 ubiquitin-protein ligase. Considering the potentiality of NSs both to act as an E3 ligase and its ability to induce proteasome degradation of RIG-I, we investigated whether TOSV NSs could have this activity *in vitro*. The His-tagged recombinant NSs protein was produced in bacteria, purified and tested for the E3 ubiquitin ligase activity, as described in Materials and Methods. In such reactions, the ability of a protein to promote a ubiquitin-

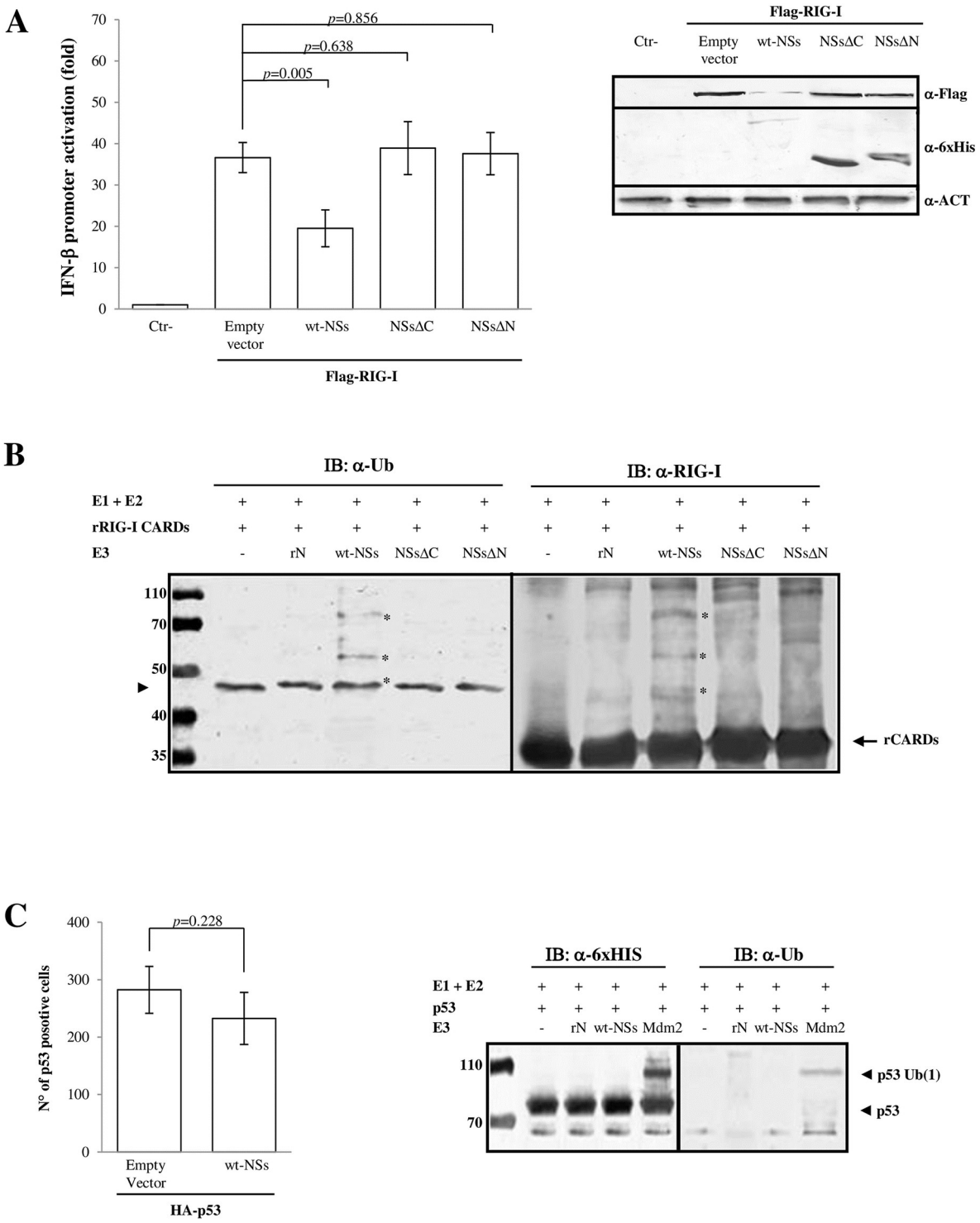

Fig 1. NSs acts as E3 ubiquitin ligase on RIG-I CARDs. Toscana virus NSs inhibits the IFN-β promoter activation through the RIG-I signalling pathway mediating its degradation. Lenti-X 293T cells were transfected (A) with IFN-β promoter-driven FireFly Luciferase (p125-FFLuc) reporter plasmid, expression plasmid encoding FLAG-RIG-I and wild-type (wt-) NSs, as well as deleted NSs expression plasmids, as indicated. In addition, pSV40-RenLuc plasmid was added as internal control. Luciferase activity was analyzed at 48h post-transfection by the Dual-Luciferase Reporter assay as described by the manufacturer (Promega). Relative luciferase activities were measured as fold induction (relative to the basal level of reporter genes in the presence of empty vector after normalization with co-transfected RenLuc activities). Values represent means of triplicate independent experiments ± standard deviations (SD). Representative western blot showing the protein expression levels in the reporter gene assay samples was done on whole cell extracts, resolved by sodium dodecyl sulfate

(SDS)-polyacrylamide gel electrophoresis (PAGE) and analyzed by immunoblotting with the FLAG-RIG-I, 6xHis-NSs and β-Actin specific antibodies and densitometric analysis (Supplement data 2). (B) Recombinant proteins were used in the *in vitro* ubiquitination assay using UbcH5b/c as E2 and wt-rNSs, rNSsΔC or rNSsΔN as source of E3 ubiquitin ligase. The negative controls were represented by rRIG-I CARDs tested with the ubiquitination reagents except for E3 Ub ligase or TOSV nucleoprotein (rN) in place of E3 Ub ligase. The ubiquitinated rRIG-I CARDs were detected with anti-ubiquitin (left panel) or anti-RIG-I (right panel) antibodies. The ubiquitinated forms of rCARDS (indicated by asterisk) are present only in the samples containing wt-rNSs, as demonstrated by mass-spectrometry (S4 Fig). The band indicated by arrowhead (left panel) corresponding to the ubiquitinated-E2 (Ub-E2) intermediate present in all the tested samples, comigrates with the monoubiquitinated-rRIG-I CARDs in presence of rNSs. (C) NSs does not affect p53 expression in cells transfected with HA-p53 and 6xHis-NSs expressing plasmids (left panel). Immunofluorescence was performed with indicated specific antibodies; positive cells were counted. The bars depict the average number of p53 positive cells in the presence or absence of wt-NSs. The mean ± SD of three independent experiments is shown. The specificity of the E3 ubiquitin ligase activity of wt-NSs was evaluated in the *in vitro* ubiquitination assay using UbcH5b/c as E2 and recombinant p53 protein as acceptor target for ubiquitination (right panel). Poly-ubiquitinated forms were detected by anti-6xHis tag and anti-ubiquitin antibodies. Higher molecular weight bands corresponding to ubiquitinated p53 were detected only in the reaction supplemented with Mdm2 E3 ubiquitin ligase, but not in the samples containing wt-rNSs or rN.

https://doi.org/10.1371/journal.ppat.1008186.g001

protein ligation was indicative of an E3 ligase activity. For this purpose, an *in vitro* biochemical assay was performed with E1, E2, rNSs and recombinant full-length RIG-I (FL-rRIG-I). When the wt-NSs was used as a source of E3 Ub ligase in the assay, a shift in RIG-I molecular weight, corresponding to its ubiquitinated form, was revealed by immunoblotting using anti-Ub or anti-RIG-I antibodies (S3 Fig). In subsequent experiments, the recombinant N-terminus of RIG-I containing two tandem-repeated CAspase Recruitment Domains (CARDs), necessary and sufficient to activate RIG-I and induce the recruitment of downstream signaling molecules, were tested. Likewise, when the E3 Ub ligase was substituted by the wt-NSs in the assay, higher molecular weight ubiquitinated bands were revealed by immunoblotting on rRIG-I CARDs, using anti-Ub or anti-RIG-I antibodies (Fig 1B). In order to better evaluate which domain of NSs could have a role in the ubiquitination process, the His-tagged recombinant NSs protein, NSsΔC and NSsΔN deleted proteins were produced in bacteria, purified and tested for the E3 ubiquitin ligase activity. Ubiquitinated rRIG-I CARDs bands were not present when NSsΔC, NSsΔN or TOSV nucleocapsid (N) proteins were added in place of NSs (Fig 1B), indicating that NSs possessed an E3 Ub ligase activity directed to RIG-I. Furthermore, as this activity was not observed in deletion mutants, it was likely located in the amino- and carboxy-terminus regions. In the attempt to investigate the potential substrate specificity of TOSV NSs protein, we tested NSs with the recombinant human p53 protein, known to be ubiquitinated by many different E3 ligases. The co-expression of NSs and p53 plasmids in cells did not reveal any decrease of the p53 protein, in comparison with the control represented by cells transfected with p53 plasmid alone, as evidenced by immunoblotting and immunofluorescence (Fig 1C). Moreover, in biochemical assays, p53 was ubiquitinated by Mdm2 E3 Ub ligase, and not by NSs (Fig 1C), indicating that its activity appeared to be target specific. Finally, ubiquitinated products were not detected in the negative controls, when E3 ubiquitin ligase was omitted or substituted by TOSV N protein in the reaction (Fig 1C).

E3 ubiquitin ligase activity is associated with the C-terminus of NSs

In order to confirm whether NSs E3 ubiquitin ligase activity, required for targeting RIG-I to proteasomal degradation, mapped to the C-terminal sequence of the NSs, we adopted a 'twist' strategy and constructed a TOSV-Sandfly Fever Naples Virus (SFNV) NSs chimeric protein. Toscana virus and Sandfly Fever Naples virus (SFNV) belong to the same viral genus and share a high sequence homology in the non-structural protein (54%) (S4 Fig). However, SFNV NSs lacks the last 78 aa, present in TOSV NSs. Since this domain was proved to be strikingly associated to TOSV NSs degrading activity on RIG-I [22], we generated a chimeric SFNV NSs (cSFNV) protein by fusing the C-terminus of TOSV NSs onto the NSs of the related SFNV. In comparison with TOSV NSs, SFNV NSs was well expressed in transfected cells and did not

show any RIG-I-mediated IFN-β inhibition, since unable to mediate RIG-I degradation ($p = 0.166$) (Fig 2A and 2B). Thus, we supposed that the addition of TOSV C-terminus to SFNV NSs could confer new properties to this protein. Analysing the cSFNV NSs expression by immunofluorescence and immunoblotting, no significant difference was evidenced with the wild-type counterpart ($p = 0.255$) (Fig 2A). On the other hand, the addition of a partial TOSV sequence completely altered the SFNV NSs function. Indeed, an evident decrease of RIG-I was revealed in cSFNV and FLAG-RIG-I plasmids transfected cells, showing few RIG-I positive cells by immunofluorescence ($p = 0.00006$) and a faint band of RIG-I by immunoblotting (Fig 2A, S3 Dataset). Furthermore, the newly acquired IFN-β antagonistic property of cSFNV NSs was confirmed by luciferase reporter assay, demonstrating a strong inhibition of RIG-I-mediated IFN-β promoter activation (Fig 2B) and endorsing the hypothesis of an E3 ubiquitin ligase activity related to the C-terminal domain of TOSV NSs. This data was also supported by the *in vitro* ubiquitination assay of rRIG-I CARDs in the presence of the recombinant cSFNV NSs protein. As shown in Fig 2C, rRIG-I CARDs were ubiquitinated when the chimeric protein was added in the reaction, in place of the E3 Ub ligase. On the contrary, SFNV NSs protein did not have any effect on rRIG-I CARDs (Fig 2C). Moreover, the mass spectrometry, performed on the products of the *in vitro* ubiquitination reactions, identified RIG-I CARDs ubiquitinated at the lysine residues 115 and 172 (S5 Fig). Since Ub-CARDs specific peptides were only identified in the wt-NSs and cSFNV containing samples, the E3 ubiquitin ligase activity of TOSV NSs and the incisive role of its C-terminal domain were further confirmed.

Cysteine $_{27}$ at the N-terminus of NSs is also involved in the ubiquitination process

Since we have demonstrated that NSsΔC and NSsΔN did not have any inhibitory activity to RIG-I mediated IFN-β promoter activation (Fig 1A), we hypothesized that both the C- and N-terminus of NSs might be involved in the ubiquitination of RIG-I. We suspected that NSs could behave such as an RBR E3 Ub ligase, which transfers ubiquitin to a catalytic cysteine on the E3 ligase and then to the substrate. Therefore, a mass spectrometry analysis was performed on the wt-NSs protein, recovered from transfected Lenti-X 293T cells, to see whether a cysteine of NSs was ubiquitinated. The analysis revealed a ubiquitinated cysteine at position 27, in the N-terminal of TOSV protein (S6 Fig). In the recent years, several new modes of ubiquitin chain attachment have emerged and even the thiol groups of cysteine residues could be employed as sites of ubiquitination [47]. However, the potential importance of this 'non-canonical ubiquitination' and its roles still need to be elucidated [48]. Therefore, in order to understand the role of this cysteine in the ubiquitination process, we mutated Cys_{27} to Gly in the wt-NSs and tested the new construct in the *in vitro* ubiquitination assay of rRIG-I CARDs. rNSs-C_{27}G was unable to ubiquitinate rRIG-I CARDs (S7 Fig) and the result was supported by immunofluorescence, immunoblotting (Fig 3A, S4 Dataset) and luciferase assays (Fig 3B), which revealed a behaviour of rNSs-C_{27}G similar to the one observed for NSsΔN and NSsΔC, and indicated the fundamental role elicited by this amino-acid, interfering with cell signaling. Therefore, this result also validated the involvement of the NSs N-terminus in the ubiquitination process.

Discussion

Innate immunity is fundamental to protect host cells against pathogens. In turn, viruses have developed different strategies to counteract host innate immune response [11–21, 42–45]. New mechanisms of viral evasion of host immune response, exploiting the ubiquitin system,

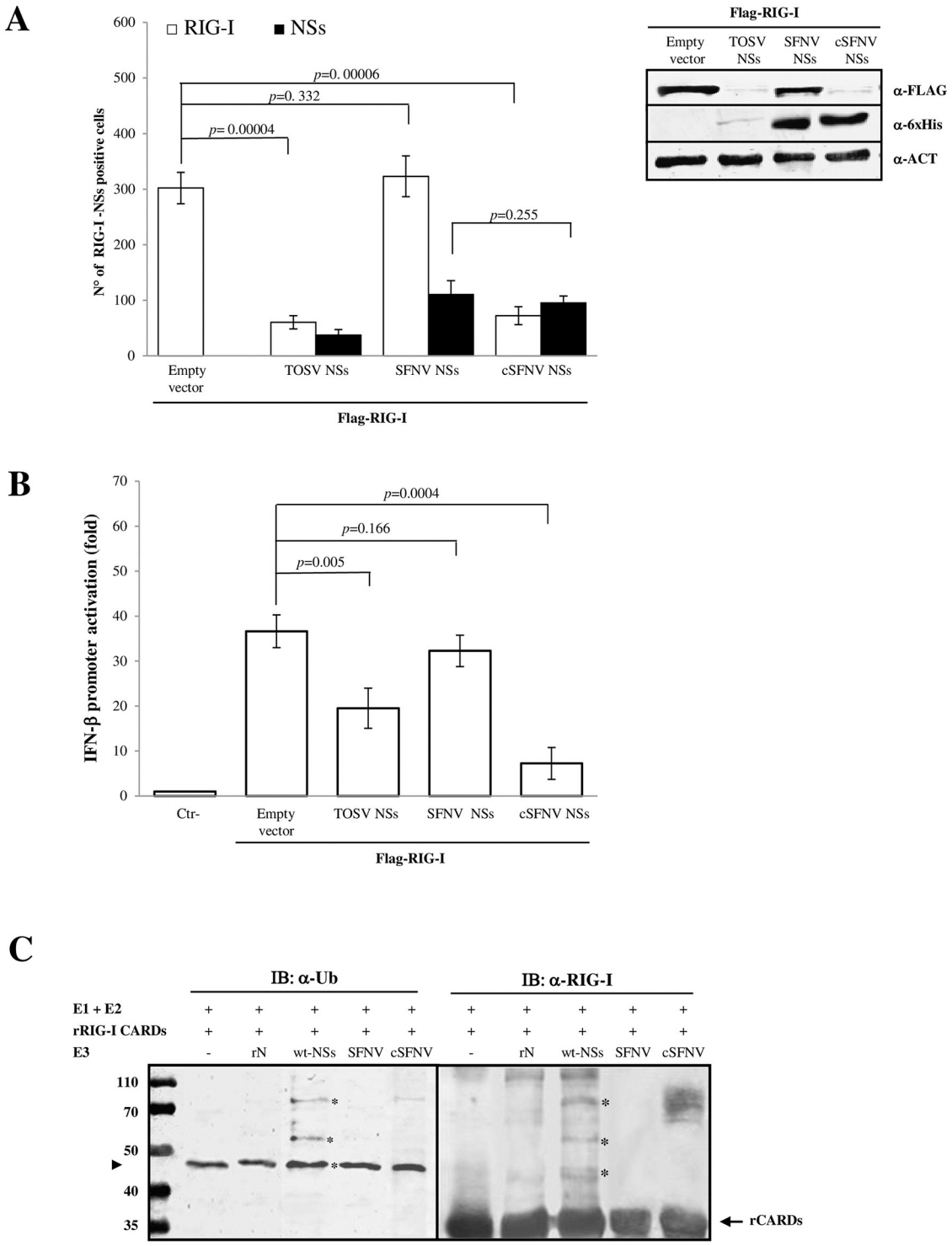

Fig 2. C-terminus of TOSV NSs is linked to E3 ubiquitin ligase activity. The fusion of TOSV NSs C-terminus to Sandfly Fever Naples Virus (SFNV) NSs conferred it a different behaviour. (A, left panel) The chimeric protein cSFNV NSs was tested for its degrading activity on RIG-I co-transfected cells, by immunofluorescence, using specific antibodies [RIG-I (□), NSs (■)]. Graphs are based on the mean values of three independent experiments ± SD. (A, right panel) A more accurate analysis of cellular RIG-I degradation was performed in co-transfected cells by immunoblotting on the whole cell lysates using anti-FLAG or anti-6xHis antibodies. The intensity of the RIG-I band was quantified by densitometry (Supplement data 3). (B) Lenti-X 293T cells were transfected with IFN-β reporter plasmid, FLAG-RIG-I expression plasmid along with TOSV wt-NSs, SFNV wt-NSs or chimeric cSFNV NSs expressing plasmids. Luciferase activities were measured after poly(I:C) treatment. Fold induction was calculated for

each sample with respect to the basal empty plasmid transfected sample, after normalization of the signal with the pSV40-RenLuc internal control. The mean values of at least three sets of experiments ± SD are presented. C) cSFNV NSs showed E3 ubiquitin ligase activity in the biochemical reaction, in association with UbcH5b/c as E2. Poly-ubiquitinated bands of rRIG-I CARDs were detected by immunoblotting using anti-RIG-I or anti-Ub antibodies when cSFNV or TOSV NSs was used in the reaction in place of E3 Ub ligase. No ubiquitination activity was shown when SFNV NSs was used.

https://doi.org/10.1371/journal.ppat.1008186.g002

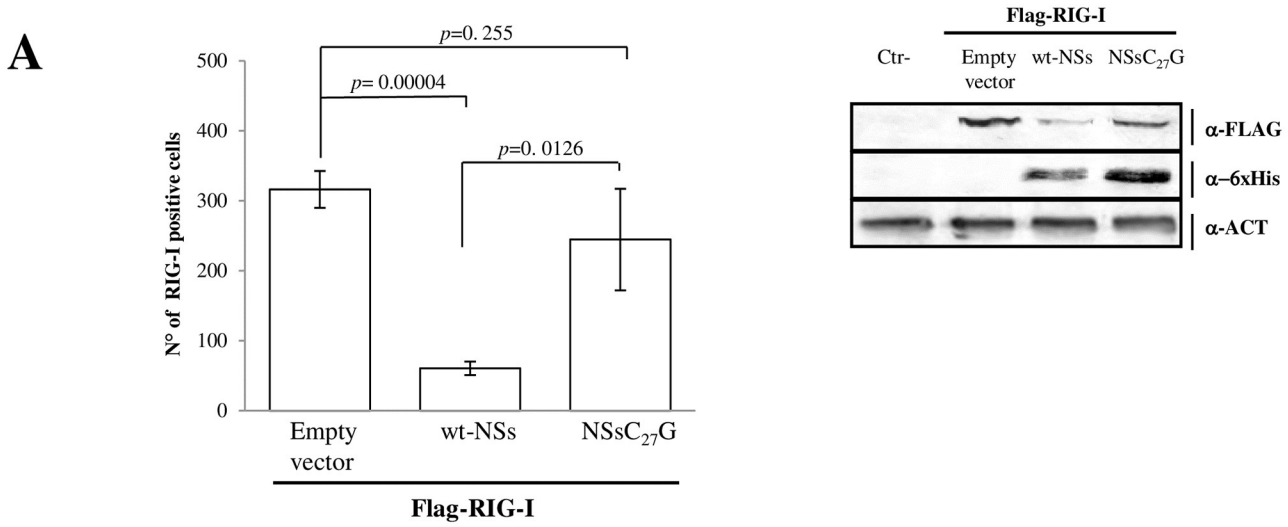

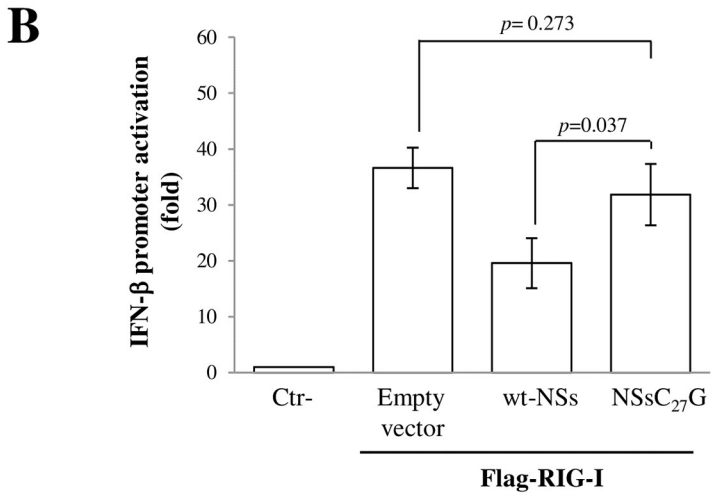

Fig 3. Effects of TOSV NSs N-terminal domain on E3 ubiquitin ligase activity. (A) The involvement of NSs Cystein$_{27}$ in the ubiquitination of RIG-I was evaluated by immunofluorescence on cells co-transfected with RIG-I and NSs plasmids. Cells were stained with anti-FLAG antibody and RIG-I positive cells were counted on different fields. Mean values ± SD of more than three independent experiments were plotted (left panel). Results were validated by immunoblotting (right panel) using total cell lysates of co-transfected cells and semi-quantitative analysis was done by densitometry (supplement data 4). (B) Lenti-X 293T cells were transfected with IFN-β reporter plasmid (p125-FFLuc) along with RIG-I and pSV40-RenLuc plasmids in addition with the wild type-NSs, or C_{27}G-NSs mutant or empty plasmids. After stimulation with poly(I:C), luciferase activity was analyzed. For each sample, luciferase was normalized to the RenLuc reporter activity. Data are representative of three independent experiments and are expressed as mean ± SD of normalized luciferase activity.

https://doi.org/10.1371/journal.ppat.1008186.g003

have recently been described. Indeed, some viruses encode proteins that manipulate the ubiquitin pathway, inhibiting the immune signaling and forwarding the degradation of host proteins [49–53]. Examples are provided by members of the *Herpesviridae* family; Varicella Zoster virus (VZV) encodes ORF61 containing a RING domain, which inhibits the IFN expression, by targeting IRF3 degradation [54]. Similarly, Herpes virus type 1 (HSV-1) has a RING domain in the ICP0 protein that confers E3Ub ligase activity for the degradation of host proteins involved in the innate immunity [55]. Poxviruses behave in a similar way [56]. Thus, ubiquitination has an important role in regulating signal transduction during the immune response [53, 57, 58]. Although viral E3 Ub ligases have been identified in large DNA viruses, some RNA viruses have developed mechanisms to interact with host molecules involved in the ubiquitination pathway. Influenza NS1 protein binds and inactivates the TRIM-25 and Riplet E3 ubiquitin ligase, preventing the downstream activation by K_{63} poly-Ub chain moiety of RIG-I [59, 60, 61]. Likewise, the Paramyxovirus V protein interacts with RIG-I/TRIM-25 regulatory complex by inhibiting RIG-I signaling [62]. Hepatitis C virus NS3-4A protein targets Riplet for degradation [57]; Rotavirus NSP1 triggers the degradation of targets by hijacking a subset of E3 Ub ligases, the cullin-RING ligases [63]. Among *Phenuiviridae* members, Rift Valley fever virus (RVFV) is the most investigated virus for the antagonistic effects of its NSs protein on the innate immune response and recently, the involvement of ubiquitin system, particularly the SCF E3 ubiquitin ligase complex, has been elucidated [44, 58]. Ubiquitin-proteasomal degradation of p62 subunit of the transcription factor TFIIH is a consequence of the interaction between RVFV NSs and the F-box protein FBXO3-SKP1-Cullin1/7 SCF multi-protein complex [43]. Furthermore, RVFV NSs is able to recruit the F-box protein FBXW11 and induce ubiquitination and proteasomal degradation of the antiviral protein PKR [44, 58]. In this study, we have shown how TOSV NSs protein was inducing RIG-I degradation upon their binding [21]. In particular, TOSV NSs revealed an E3 ubiquitin ligase activity related to both the carboxy- and amino-terminal domains of the protein, promoting the transfer of ubiquitin to RIG-I and favoring its proteasome-dependent proteolysis. Indeed, TOSV NSs mutants, such as those deleted at the amino- or carboxy-terminal (NSsΔN, NSsΔC), unlike wt-NSs, were not able to activate IFN induction. This data conferred a new role to the protein terminal sequences and suggested an involvement of these protein regions in the E3 ligase activity. Initially, an E3 ubiquitin ligase activity appeared to be localized at the NSs carboxy-terminal; thus, in order to demonstrate it, the amino-acid stretch 248–316 was fused to the carboxy-terminus of the SFNV NSs, sharing a homology of 54% with TOSV NSs, and lacking this sequence (S4 Fig). SFNV NSs did not show any degrading activity to RIG-I; on the contrary, the obtained chimeric protein acquired the features of TOSV NSs, becoming capable to degrade RIG-I. Then, we demonstrated that neither NSsΔC nor NSsΔN were able to ubiquitinate RIG-I *in vitro*. Thus, it appeared that both the amino-acid ends of TOSV NSs could be involved in an E3 ubiquitin ligase activity. Indeed, NSs, but not NSsΔC or NSsΔN, could transfer ubiquitin to the RIG-I substrate, as shown in the *in vitro* reaction in which ubiquitination process only occurred in the presence of E1, E2 and wt-NSs in place of the E3 Ub ligase. The results were also confirmed by mass spectrometry analysis, which revealed the presence of ubiquitin at positions 115 and 172 of rRIG-I CARDS after the *in vitro* reaction, in the presence of NSs. Moreover, this reaction was specific for RIG-I CARDs, since NSs did not show this activity with a different target, such as the onco-suppressor protein p53. Therefore, it was interesting to understand which type of E3 ubiquitin ligase could be ascribed to TOSV NSs. While some RING or HECT E3 ligases appear to interact directly with the substrate and E2 [25, 26, 29, 31, 64], others require additional components and interact with the substrate only indirectly, as part of a multi-subunit CRL complex [26–35]. Both RING and HECT E3 ligases transfer ubiquitin to a lysine residue on the substrate, RING E3s act as a platform to allow a

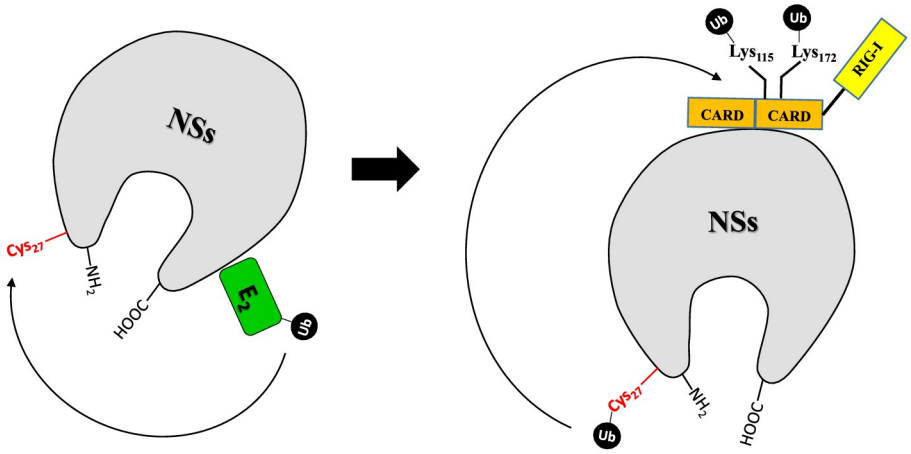

Fig 4. Model for NSs E3 Ub ligase function. Schematic model for TOSV NSs which carries out an unconventional E3 Ub ligase activity (RING between RING; RBR) by a RING-HECT-hybrid mechanism. The model proposes the transfer of ubiquitin from the charged E2 Ub conjugating enzyme, bound to the C-terminal of NSs, to Cysteine $_{27}$ located at the N-terminal of the protein. Then, ubiquitin is transferred to the lysine residues of RIG-I target protein, interacting with the central region of TOSV NSs, and leading to its proteasome-dependent degradation.

https://doi.org/10.1371/journal.ppat.1008186.g004

direct transfer of ubiquitin from the E2 to the substrate [64]. On the other hand, HECT E3s accept ubiquitin from E2 to form a ubiquitin-thioester intermediate with an active cysteine, then transfer ubiquitin to both the ε-amino groups of lysine side chains of the substrate [25, 31]. Thus, cysteine may play a significant role, particularly in the ubiquitin modification for signaling. In our study, the finding of a ubiquitinated cysteine, a non-canonical site [47, 48], at position 27 of TOSV NSs, led us to suppose that this residue could also be involved in the E3 ubiquitin ligase activity, in addition to the C-terminal sequence of the same protein. Indeed, even the $C_{27}G$ mutant of NSs was no more able to degrade RIG-I and could induce an IFN promoter in transfected cells, although at a lower level, in comparison to the NSsΔN. Therefore, we hypothesized that NSs could behave as an atypical RBR that has elements of both HECT and RING ligases: one RING domain binds the charged E2, while the other domain accepts the ubiquitin molecule before transferring it onto the substrate [32]. We hypothesized that ubiquitin-conjugated E2, bound to the carboxyl-terminus of NSs, transferred the ubiquitin to Cys_{27} (thioester intermediate), in the amino-terminal, as demonstrated by mass spectrometry, and, from there, to RIG-I, linked to NSs (Fig 4). This model might explain why NSs was losing its antagonistic activity to IFN, when one of the two amino-acid ends was lost. At present, we do not know why cSFNV NSs showed a ubiquitin E3 ligase activity, despite not having a cysteine at position 27, but it is possible that cysteine at position 39 of SNFV NSs was processed in the same way. Further investigations are ongoing in order to better determine the dynamics of the steps in this ubiquitination process; however, this is the first study showing a viral protein with an E3 ubiquitin ligase activity among negative strand RNA viruses. Although viruses have acquired tactics to minimize host antiviral responses by co-evolving with their hosts, RING E3s, encoded or hijacked by viruses for evading immune responses, are largely undiscovered and can clarify how viruses play this game with their host.

Materials and methods

Cells and viruses

Vero cells (ATCC CCL-81) and human embryonic kidney Lenti-X 293T cells (Clontech, Milan, Italy) were cultured in Dulbecco's modified Eagle's medium (DMEM) (Lonza, Milan,

Italy) supplemented with 100 U/mL penicillin/streptomycin (Hyclone Europe, Milan, Italy) and 10% heat-inactivated foetal calf serum (FCS) (Lonza), respectively, at 37 ˚C. Toscana virus (TOSV) strain 1812 [18] was used for all the experiments described.

Reagents and antibodies

Transient transfections were performed with GeneJuice Transfection reagent (Novagen, Milan, Italy), according to the manufacturer's instruction, or standard calcium phosphate method [65]. Chemicals were all purchased from AppliChem GmbH (Germany). The proteasome inhibitor MG-132 was purchased from Sigma-Aldrich (Milan, Italy). Mouse anti-6xHis tag antibody (GE Healthcare, Milan, Italy), anti-RIG-I (DDX58) polyclonal antibody (OriGene, Rockville, MD, USA), mouse anti-FLAG M2 monoclonal antibody (Agilent Technologies, Milan, Italy), mouse monoclonal anti-HA tag antibody, fluorescein (FITC)-labeled anti-mouse IgG and anti-mouse IgG HRP-conjugated were purchased from Sigma-Aldrich. Anti-rabbit IgG HRP-conjugated was supplied by Santa Cruz Biotechnology Inc. (Heidelberg,Germany) Ni-NTA sepharose was purchased from Novagen (Milan, Italy) and anti-Ub FK2 clone from Enzo Life Sciences (New York, USA).

RIG-I expression in TOSV infected cells

Lenti-X 293T cells were grown in a 24-wells plate ($5x10^5$/ml). After 24h, cell monolayers were infected with TOSV 1812, by using a multiplicity of infection (MOI) of 1. After 1h adsorption at 37 ˚C, viral inoculum was removed and replaced by complete growth medium. Cells were collected at 24h and 48h post-infection (p.i.). Where indicated, infected cells were transfected with 1 μg of NSs expression plasmid or empty plasmid, 5h after infection. Positive control was obtained by stimulating cell with poly(I:C) for 18h. Cell lysates were collected in RIPA buffer; 50 μg of total proteins were resolved by SDS-PAGE and then transferred to nitrocellulose (NC) membrane (Santa Cruz Biotechnology, Heidelberg, Germany). After blocking with 5% non-fat dry milk, filters were incubated O/N at room temperature with anti-RIG-I (1:5000 dilution), anti-NSs (1:200 dilution) or anti-N (1:200 dilution) mouse sera. After being washed with PBS 0.2% Tween-20 (PBS-T), membranes were incubated with anti-mouse HRP-conjugated secondary antibody (1:5000 dilution) and proteins were detected with TMB Enhanced One Component HRP Membrane Substrate (Tebu-bio, Milan, Italy).

Plasmids

Toscana virus full-length, NSsΔC (nt: 1–861) expressing plasmids were cloned in pcDNA4HisMax (Life Technologies, Milan, Italy) as described elsewhere [22]. Similarly, NSsΔN (nt: 217–537) expressing plasmid was generated by PCR with NSsΔN BamHI sense (nt 217–231) 5'-CGCGGATCCCCATGGCTGTACTGGGGCCT-3' and NSs EcoRI antisense (nt 948–931) 5'-CCGGAATTCTAAGGGTGGGTAGTGGGG -3' primers (Sigma-Aldrich). The gene was cloned in pcDNA4HisMax-A plasmid (Invitrogen) at the BamHI-EcoRI unique sites of the polylinker in frame with the 6xHis tag. The $Cysteine_{27}$ mutant was obtained by using QuikChange II Site-Directed Mutagenesis Kit (Agilent Technologies, Milan, Italy), according to the manufacture's instruction. Sandfly Fever Naples Virus (SFNV), strain Sabin (GenBank Accession N˚ EF201829) chimeric NSs gene carrying the TOSV C-terminal domain (cSFNV) was generated by PCR using, as reverse primer, a synthetic DNA fragment (gBlock: Integrated DNA Technologies) consisting of the C-terminus of TOSV NSs gene (nt: 739–951) partially overlapping to the 3'-end of SFNV NSs ORF, and a SFNV-NSs sense primer (primers sequences available upon request). The chimeric gene was cloned in the pcDNA4HisMax plasmid (Life Technologies) by standard procedure. Full-length Toscana virus NSs gene was also

cloned in the bacterial expression plasmid pET15b (Novagen), while ORFs coding for all the NSs mutants and RIG-I RIG-I CARDs were cloned in pRSET plasmid (Life Technologies). All the recombinant plasmids were confirmed by sequencing. The reporter plasmid encoding Firefly Luciferase downstream the complete interferon-beta promoter (p125-Luc) was kindly provided by Takashi Fujita (Tokyo Metropolitan Institute of Medical Science, Tokyo, Japan) [66], while the *Renilla* Luciferase reporter plasmid (pSV40-RL) was purchased from Promega (Promega, Milan, Italy). Plasmids for FLAG-tagged human RIG-I, RIG-I N-terminal RIG-I CARDs domain (RIG-IN), HA- human p53 and the HA-tagged human ubiquitin were kindly provided by A. García-Sastre (Mount Sinai School of Medicine, New York), T. Fujita (Tokyo Metropolitan Institute of Medical Science, Tokyo, Japan), M. Tommasino (International Agency for Research on Cancer, Lyon, France) and D. Arnoult (Inserm, France), respectively.

Recombinant proteins expression and purification

Recombinant proteins production was achieved by induction of transformed BL21(DE3)-pLys (Novagen) cells with 1 mM IPTG for 3h at 37 ˚C. TOSV NSs was recovered from inclusion bodies via solubilisation with 50 mM Tris-HCl [pH 7.5]; 300 mM NaCl; 0.3% w/v N-laurylsarcosine (SRK) and 6xHis tagged fusion proteins were purified by using Ni-NTA sepharose following manufacturer's instruction. 6xHis-RIG-I CARDs were purified from IPTG induced BL21(DE3)-pLys (Novagen) bacterial culture as described above, with SRK omission. Purified protein fractions were analysed by SDS-PAGE and pure protein containing fractions were pooled, diluted ten-folds with 10 mM Tris-HCl [pH 8.0] and dialysed against the same buffer O/N at room temperature. Recovered proteins were concentrated by using ultrafiltration devices, quantified by BCA reagent (Pierce, Milan, Italy) and stored at -80 ˚C in aliquots. TOSV recombinant nucleoprotein N was produced and purified as described elsewhere [67]. Recombinant human full-length RIG-I was purchased by BPS Bioscience Inc. (San Diego, CA, USA).

Immunofluorescence

Lenti-X 293T cells, seeded in 24-wells culture plate, were transfected with 0.5 μg of wt-, deleted- or mutated-NSs expressing plasmids, alone or in combination with 0.05 μg of FLAG-RIG-I or HA-p53 expressing plasmids. Cells were collected and stained with anti-6xHis antibody (1:2000 dilution), anti-HA antibody (1:500 dilution) or with anti-FLAG M2 antibody (1:500 dilution). FITC-labeled anti-mouse IgG (1:320 dilution) was used as secondary antibody. Immunofluorescence was visualized by a Diaplan microscope (Leica Microsystems, Milan, Italy). RIG-I and NSs positive cells were counted in three different fields of the same slide. The mean value of positive cells was calculated with respect to the total number of spotted cells ($3.5x10^5$/well).

Luciferase reporter gene assay

$2x10^5$ Lenti-X 293T cells were seeded in 24-well plates and transfected with indicated plasmids as previously described. Briefly, 0.2 μg of p125-FFLuc, 0.05 μg of RIG-I and, where indicated, 0.5 μg of wt-NSs or NSs mutants expressing plasmids were co-transfected. Empty plasmid was used to normalize total DNA amount. Twenty ng of pSV40-RL were co-transfected as internal control. Thirty-six hours post-transfection, cells were stimulated with 2 μg/ml of poly(I:C). After additional 12h, cells were collected and luciferase activities were measured on lysates by using dual Luciferase reporter assay reagent (Promega), according to the manufacturer's instructions. Cell lysates were stored at -20 ˚C for further analysis by immunoblotting. Results are given as mean values of several experiments ± standard deviations (SD).

Immunoblot analysis

Fifty μg of total cell lysates of co-transfected cells were resolved by SDS-PAGE and then transferred to nitrocellulose membrane. Immunoblotting was performed as described above, by using anti-HA (1:1000 dilution), anti-FLAG (1:2000 dilution) or anti-6xHis (1:1000 dilution). Quantitative comparison among samples was performed by densitometric analysis using the ImageJ software as reported in Supplement data.

In vitro ubiquitination assay

To evaluate TOSV NSs E3 ubiquitin ligase activity, purified recombinant wt-NSs or its mutants were used in the *in vitro* protein Ubiquitination assay (Enzo Life Science). Experimental reactions and controls were added as suggested by the manufacturer. Briefly, 100 nM ubiquitin activating enzyme (E1); 2.5 μM of ubiquitin conjugating enzyme (E2) UbcH5b/c; 1 μM of rNSs protein or its mutants as source of E3 ligase, 2.5 μM of biotinylated ubiquitin and 1 μM of recombinant purified RIG-I, RIG-I CARDs or p53 were incubated at 37 ˚C for 4-6h. Negative control reactions lacking rNSs or containing 1 μM of TOSV rN in place of E3 ubiquitin ligase were included in the experiment set. Reactions were quenched by adding 5X gel loading buffer and analysed by western blotting for ubiquitinated RIG-I CARDs by anti-DDX58 polyclonal antibody (1:500 dilution) or anti-Ub FK2 clone (1:1000 dilution).

Mass spectrometry detection of ubiquitinated protein residues

Lenti-X 293T seeded in T25 flasks were transfected with 3 μg of wt-NSs plasmid in combination with 1 μg of plasmid encoding for HA-tagged ubiquitin. At 36h post-transfection, cells were treated with MG-132 to a final concentration of 1 μM for additional 12h and collected at 48 h post-transfection. Pull-down for NSs was achieved by Immobilized Metal Affinity Chromatography (IMAC) under denaturing conditions. Briefly, cell pellets were lysed in 5 M guanidine-HCl; 10 mM HEPES [pH 8.0] with sonication. His-tagged NSs was bound to Ni-NTA sepharose for 3h at room-temperature. Beads were collected and extensively washed with 10 mM HEPES [pH 8.0], 1 M NaCl, 0.3% w/v SRK, 50 mM imidazole. Bound proteins were eluted with Laemmli denaturing sample buffer, loaded on SDS-PAGE and stained with Bio-safe Coomassie stain (Bio-Rad, Milan, Italy). Protein bands were cut from gel and prepared for mass-spectrometry analysis as carried out by Cogentech Proteomics/MS (Cogentech S.c.a.r.l., Milan, Italy), by using the nLC-ESI-MS/MS QExactive-HF system. Similarly, the rRIG-I CARDs ubiquitination was confirmed by mass-spectrometry performed on the *in vitro* ubiquitination reaction products.

Statistical analysis

The mean differences were statistically analyzed using Stat View statistical software (Abacus Concepts, Berkeley, CA). Immunofluorescence and luciferase reporter gene assay results were expressed as the mean ± SD of determinations made in three different experiments. Probability (p) values were calculated by t-test. A p value of less than 0.05 was considered statistically significant.

Supporting information

S1 Fig. Toscana virus infection leads to RIG-I production. Endogenous RIG-I protein level was observed by western blotting. Lenti-X 293T cells were stimulated with polyI:C transfection for 18h, mock-infected or infected with TOSV (MOI = 1). Where indicated, stimulated or infected cells were either transfected with empty plasmid or plasmid

expressing wt-NSs. Cell lysates were prepared at indicated times post-infections and 50 μg of total proteins were resolved by SDS-PAGE and assessed for RIG-I expression by specific antibody. TOSV NSs expression, along with nucleoprotein N, was determined on the same lysates to confirm viral infection and replication. Band intensity was determined by densitometric analysis performed on at least three independent experiments. Results are given in Supplement data 1.
(TIF)

S2 Fig. TOSV NSs amino-acid sequence. Full-length NSs amino-acidic sequence showing the amino-terminal (NSsΔN) and the carboxy-terminal (NSsΔC) deleted mutants of the protein. The functional active Cysteine residue at position 27 is shown in bold.
(TIF)

S3 Fig. Toscana virus NSs protein retains E3 ubiquitin ligase activity on RIG-I. Recombinant NSs and RIG-I proteins were used in combination with E1 ubiquitin activating enzyme, UbcH5b/c E2 ubiquitin conjugating enzyme and wt-rNSs, as source of E3 ubiquitin ligase, in the ubiquitination assay *in vitro*. Target protein for ubiquitination was represented by the full-length human rRIG-I. Negative controls, including the recombinant TOSV viral nucleoprotein (rN) or the omission of ATP energy source, were included. The presence of poly-ubiquitinated rRIG-I was revealed with anti-ubiquitin or anti-RIG-I antibodies represented by an increase of the specific molecular weight.
(TIF)

S4 Fig. Sequence alignment of TOSV and SFNV NSs proteins. Comparison of the amino acid sequences of Toscana virus (TOSV; strain 1812, GenBank Accession N° ABY19522.1) and Sandfly Fever Naples virus (SFNV; strain Sabin, GenBank Accession N° EF201829) NSs showing the homology (54%) between the two related viral proteins and the lack of TOSV C-terminal domain in SFNV NSs.
(TIF)

S5 Fig. Tracking of RIG-I CARDs ubiquitination by mass spectrometry. Confirmatory results of RIG-I CARDs ubiquitination by TOSV NSs were obtained by the mass spectrometry analysis. The $\geq$ 40 KDa fraction of the biochemical reaction products revealed the presence of ubiquitinated RIG-I peptides only in samples supplemented with wt-rNSs or cSFNV NSs. Moreover, this approach allowed the identification of RIG-I CARDs lysine residues 115 and 172 as target for ubiquitination by the NSs.
(TIF)

S6 Fig. Mass spectrum of Toscana virus NSs protein. A cell line derived from Lenti-X 293T cells stably expressing Toscana virus NSs protein was used for purification under denaturing conditions of the viral protein. The enriched substrate protein was subjected to mass spectrum showing the identification of TOSV NSs peptide containing the ubiquitinated Cysteine residue at position 27 (Cys_{27}).
(TIF)

S7 Fig. C_{27}G-NSs mutant is unable to mediate RIG-I rCARDs ubiquitination. The key role of C_{27} in the N-terminus of TOSV NSs was further investigated by *in vitro* ubiquitination of RIG-I rCARDs. Higher molecular weight bands corresponding to rCARDs ubiquitinated forms were detected by both anti-RIG-I and anti-Ub antibodies only when the wt-NSs was used in the biochemical reaction. On the contrary, C_{27}G-NSs mutant was unable to mediate RIG-I rCARDs ubiquitination, confirming a direct involvement of the C_{27} in the ubiquitination process. Asterisk in the sample containing wt-NSs indicates ubiquitinated rRIG-I CARDs,

as reported by mass spectrometry (S5 Fig). On the contrary, the corresponding immune-reactive bands evidenced in other samples were identified as the E2-Ub intermediate.
(TIF)

S1 Dataset. Evaluation of TOSV effects on endogenous RIG-I expression. Immunoblotting for detection of endogenous RIG-I expression in TOSV infected, poly(I:C) and NSs transfected Lenti-X 293T cells were subjected to densitometric analysis. Raw dataset of RIG-I, TOSV NSs and actin band intensity was reported from three independent experiments. After normalization with respect to relative actin values, a comparison was performed and protein expression levels ± standard deviation (SD) were calculated as fold induction. A *p* value of less than 0.05 was considered statistically significant.
(XLS)

S2 Dataset. Ubiquitination activity of wt NSs and NSs deleted variants. Lenti-X 293T cells were transfected with RIG-I or p53 expressing plasmids, alone or in combination to wt-NSs or its deleted mutants. Quantification of RIG-I or p53 expression levels was performed by densitometric analysis on immunoblotting and raw dataset of RIG-I, p53, NSs and actin band intensity were reported from three independent experiments. After normalization with respect to relative actin values, a comparison was performed and protein expression levels ± standard deviation (SD) were calculated as fold induction. Moreover, specificity of wt-NSs was assessed by immunofluorescence in p53 plasmid co-transfected cells. Both p53 or NSs positive cells were counted and percentage was calculated ± standard deviation (SD). The influence of NSs deleted mutants on RIG-I-mediated IFN-β promoter activation was assessed by Luciferase reporter gene assay. Fold induction of IFN-β promoter activation was reported from three independent experiments ± standard deviation (SD). A *p* value of less than 0.05 was considered statistically significant.
(XLS)

S3 Dataset. C-terminal domain of TOSV NSs is associated to its ubiquitination function. Quantification of RIG-I cellular accumulation was performed by densitometric analysis on immunoblotting from Fig 2. Raw dataset of RIG-I, TOSV or SFNV NSs, chimeric cSFNV NSs and actin band intensity was listed from three independent experiments. After normalization with respect to relative actin values, fold induction/decrease in protein expression levels ± standard deviation (SD) was calculated. Immunofluorescence data referring to RIG-I or NSs positive cells were given and final results were expressed as percentage of positive cells with respect to the total number of spotted cell. A more accurate analysis was performed by Luciferase reporter gene assay by which the effects of different NSs variants on RIG-I-mediated IFN-β promoter activation was evaluated. Fold induction was calculated for each sample with respect to the basal empty plasmid transfected sample, after normalization of the signal with the pSV40-RenLuc internal control. The mean values of at least three sets of experiments ± SD were presented. For all the experimental procedures a *p* value of less than 0.05 was considered statistically significant.
(XLS)

S4 Dataset. C_{27} residue at the TOSV NSs N-terminal domain is critical for its E3 ubiquitin ligase activity. RIG-I expression levels were quantified by densitometric analysis on immunoblotting performed on cell lysates of RIG-I and NSs, wild-type or cystein mutant, co-transfected cells. Raw dataset represented the band intensity for RIG-I, wt-NSs, NSsC_{27}G and actin. Fold induction/decrease in protein expression levels was calculated after actin normalization. Immunofluorescence results performed for RIG-I or NSs immune-staining were given. Positive cells for both RIG-I or NSs were counted; results were expressed as percentage of positive

cells with respect to the total number of tested cells. Reporter gene assay was used to determine the effects of cysteine mutated NSs on RIG-I-mediated IFN-β promoter activation. Luciferase reporter gene assay was performed and fold induction in IFN-β promoter activation was calculated for each sample after normalization of the signal with the pSV40-RenLuc internal control. For all the experimental procedures, results were collected from three independent experiments and expressed as mean values ± standard deviations (SD). A p value of less than 0.05 was considered statistically significant.
(XLS)

Author Contributions

Conceptualization: Gianni Gori Savellini, Maria Grazia Cusi.

Data curation: Gianni Gori Savellini, Maria Grazia Cusi.

Investigation: Gianni Gori Savellini.

Methodology: Gianni Gori Savellini, Gabriele Anichini, Claudia Gandolfo, Shibily Prathyumnan.

Resources: Maria Grazia Cusi.

Supervision: Maria Grazia Cusi.

Writing – original draft: Gianni Gori Savellini, Maria Grazia Cusi.

Writing – review & editing: Maria Grazia Cusi.

References

1. Braito A, Ciufolini MG, Pippi L, Corbisiero R, Fiorentini C, Gistri A, et al. Phlebotomus-transmitted Toscana virus infections of the central nervous system: a seven-year experience in Tuscany. Scand J Infect Dis. 1998; 30: 505–508. https://doi.org/10.1080/00365549850161539 PMID: 10066054
2. Verani P, Ciufolini MG, Nicoletti L, Calducci M, Sabatinelli G, Coluzzi M, Paci P, et al. Ecological and epidemiological studies of Toscana virus, an arbovirus isolated from Phlebotomus. Ann Ist Super Sanità. 1982; 18: 397–399. PMID: 7187828
3. Kuhn J, Bewermeyer H, Hartmann-Klosterkoetter U, Emmerich P, Schilling S, Valassina M. Toscana virus causing severe meningoencephalitis in an elderly traveler. J Neurol Neurosurg Psychatry. 2005; 76: 1605–1606.
4. Bartels S, Heckmann JG. Lethal encephalitis caused by Toscana virus in an elderly patient. J Neurol. 2012; 259: 175–177. https://doi.org/10.1007/s00415-011-6121-y PMID: 21656341
5. Sanbonmatsu-Gámez S, Pérez-Ruiz M, Palop-Borrás B, Navarro-Marí JM. Unusual manifestation of Toscana virus infection, Spain. Emerg Infect Dis. 2009; 15: 347–348 https://doi.org/10.3201/eid1502.081001 PMID: 19193294
6. Bouloy M. Bunyaviridae: genome organization and replication strategies. Adv Virus Res. 1991; 40: 235–75 https://doi.org/10.1016/s0065-3527(08)60281-x PMID: 1957720
7. Di Bonito P, Mochi S, Grò MC, Fortini D, Giorgi C. Organization of the M genomic segment of Toscana phlebovirus. J Gen Virol. 1997; 76: 77–81.
8. Accardi L, Gro MC, Di Bonito P, Giorgi C. Toscana virus genomic L segment: molecular cloning, coding strategy and amino acid sequence in comparison with other negative strand RNA viruses. Virus Res. 1993; 27: 119–131. https://doi.org/10.1016/0168-1702(93)90076-y PMID: 8460526
9. Grò MC, Di Bonito P, Fortini D, Mochi S, Giorgi C. Completion of molecular characterization of Toscana phlebovirus genome: nucleotide sequence, coding strategy of M genomic segment and its amino acid sequence comparison to other phleboviruses. Virus Res. 1997; 51: 81–91. https://doi.org/10.1016/s0168-1702(97)00076-2 PMID: 9381797
10. Reikine S, Nguyen JB, Modis Y. Pattern Recognition and Signaling Mechanisms of RIG-I and MDA5. Front Immunol. 2014; 5: 342. https://doi.org/10.3389/fimmu.2014.00342 PMID: 25101084

11. Weber F, Bridgen A, Fazakerley JK, Streitenfeld H, Kessler N, Randall RE, et al. Bunyamwera bunyavirus nonstructural protein NSs counteracts the induction of alpha/beta interferon. J Virol. 2002; 76: 7949–7955. https://doi.org/10.1128/JVI.76.16.7949-7955.2002 PMID: 12133999
12. Jääskeläinen KM, Kaukinen P, Minskaya ES, Plyusnina A, Vapalahti O, Elliott RM, et al. Tula and Puumala hantavirus NSs ORFs are functional and the products inhibit activation of the interferon-beta promoter. J Med Virol. 2007; 79: 1527–1536. https://doi.org/10.1002/jmv.20948 PMID: 17705180
13. Bridgen AM, Weber F, Fazakerley JK, Elliott RM. Bunyamvera bunyavirus non-structural protein NSs is nonessential gene product that contributes to the viral pathogenesis. Proc Natl Acad Sci. 2001; 98: 664–669. https://doi.org/10.1073/pnas.98.2.664 PMID: 11209062
14. Blakqori G, Delhaye S, Habjan M, Blair CD, Sánchez-Vargas I, Olson KE, et al. La Crosse bunyavirus nonstructural protein NSs serves to suppress the type I interferon system of mammalian hosts. J Virol. 2007; 81: 4991–4999. https://doi.org/10.1128/JVI.01933-06 PMID: 17344298
15. Léonard VH, Kohl A, Hart TJ, Elliott RM. Interaction of Bunyamwera Orthobunyavirus NSs protein with mediator protein MED8: a mechanism for inhibiting the interferon response. J Virol. 2006; 80: 9667–9675. https://doi.org/10.1128/JVI.00822-06 PMID: 16973571
16. Wuerth JD, Weber F. Phleboviruses and the Type I Interferon Response. Viruses. 2016; 8:pii: E174.
17. Brisbarre NM, Plumet S, de Micco P, Leparc-Goffart I, Emonet SF. Toscana virus inhibits the interferon beta response in cell cultures. Virology. 2013; 442: 189–194. https://doi.org/10.1016/j.virol.2013.04.016 PMID: 23684418
18. Gori Savellini G, Weber F, Terrosi C, Habjan M, Martorelli B, Cusi MG. Toscana virus induces interferon although its NSs protein reveals antagonistic activity. J Gen Virol. 2011; 92: 71–79. https://doi.org/10.1099/vir.0.025999-0 PMID: 20861320
19. Chen X, Ye H, Li S, Jiao B, Wu J, Zeng P, et al. Severe fever with thrombocytopenia syndrome virus inhibits exogenous Type I IFN signaling pathway through its NSs in vitro. PLoS One. 2017; 12: e0172744. https://doi.org/10.1371/journal.pone.0172744 PMID: 28234991
20. Zhang S, Zheng B, Wang T, Li A, Wan J, Qu J, et al. NSs protein of severe fever with thrombocytopenia syndrome virus suppresses interferon production through different mechanism than Rift Valley fever virus. Acta Virol. 2017; 61: 289–298. https://doi.org/10.4149/av_2017_307 PMID: 28854793
21. Gori Savellini G, Valentini M, Cusi MG. Toscana virus NSs protein inhibits the induction of type I interferon by interacting with RIG-I. J Virol. 2013; 87: 6660–6667. https://doi.org/10.1128/JVI.03129-12 PMID: 23552410
22. Gori Savellini G, Gandolfo C, Cusi MG. Truncation of the C-terminal region of Toscana Virus NSs protein is critical for interferon-β antagonism and protein stability. Virology. 2015; 486: 255–262. https://doi.org/10.1016/j.virol.2015.09.021 PMID: 26474372
23. Pickart CM. Mechanisms underlying ubiquitination. Annu Rev Biochem. 2001; 70: 503–533. https://doi.org/10.1146/annurev.biochem.70.1.503 PMID: 11395416
24. Scheffner M, Nuber U, Huibregtse JM. Protein ubiquitination involving an E1-E2-E3 enzyme ubiquitin thioester cascade. Nature. 1995; 373: 81–83. https://doi.org/10.1038/373081a0 PMID: 7800044
25. Ardley HC, Robinson PA. E3 ubiquitin ligases. Essays Biochem. 2005; 41: 15–30. PMID: 16250895
26. Bernassola F, Karin M, Ciechanover A, Melino G. The HECT family of E3 ubiquitin ligases: multiple players in cancer development. Cancer Cell. 2008; 14: 10–21. https://doi.org/10.1016/j.ccr.2008.06.001 PMID: 18598940
27. Bosu DR, Kipreos ET. Cullin-RING ubiquitin ligases: global regulation and activation cycles. Cell Div. 2008; 3: 7. https://doi.org/10.1186/1747-1028-3-7 PMID: 18282298
28. Zheng N, Shabek N. Ubiquitin Ligases: Structure, Function, and Regulation. Annu Rev Biochem. 2017; 86: 129–157. https://doi.org/10.1146/annurev-biochem-060815-014922 PMID: 28375744
29. Jackson PK, Eldridge AG, Freed E, Furstenthal L, Hsu JY, Kaiser BK, et al. The lore of the RINGs: substrate recognition and catalysis by ubiquitin ligases. Trends Cell Biol. 2000; 10: 429–439. https://doi.org/10.1016/s0962-8924(00)01834-1 PMID: 10998601
30. Weber J, Polo S, Maspero E. HECT E3 Ligases: A Tale With Multiple Facets. Front Physiol. 2019; 10: 370. https://doi.org/10.3389/fphys.2019.00370 PMID: 31001145
31. Rotin D, Kumar S. Physiological functions of the HECT family of ubiquitin ligases. Nat Rev Mol Cell Biol. 2009; 10: 398–409. https://doi.org/10.1038/nrm2690 PMID: 19436320
32. Spratt DE, Walden H, Shaw GS. RBR E3 ubiquitin ligases: new structures, new insights, new questions. Biochem J. 2014; 458: 421–437. https://doi.org/10.1042/BJ20140006 PMID: 24576094
33. Sluimer J, Distel B. Regulating the human HECT E3 ligases. Cell Mol Life Sci. 2018; 75: 3121–3141. https://doi.org/10.1007/s00018-018-2848-2 PMID: 29858610

34. Metzger MB, Pruneda JN, Klevit RE, Weissman AM. RING-type E3 ligases: master manipulators of E2 ubiquitin-conjugating enzymes and ubiquitination. Biochim Biophys Acta. 2013; 1843: 47–60. https://doi.org/10.1016/j.bbamcr.2013.05.026 PMID: 23747565

35. Deshaies RJ, Joazeiro CA. RING domain E3 ubiquitin ligases. Annu Rev Biochem. 2009; 78: 399–434. https://doi.org/10.1146/annurev.biochem.78.101807.093809 PMID: 19489725

36. Finley D. Recognition and processing of ubiquitin-protein conjugates by the proteasome. Annu Rev Biochem. 2009; 78: 477–513. https://doi.org/10.1146/annurev.biochem.78.081507.101607 PMID: 19489727

37. Thrower JS, Hoffman L, Rechsteiner M, Pickart CM. Recognition of the polyubiquitin proteolytic signal. EMBO J. 2000; 19: 94–102. https://doi.org/10.1093/emboj/19.1.94 PMID: 10619848

38. Akutsu M, Dikic I, Bremm A. Ubiquitin chain diversity at a glance. J Cell Sci. 2016; 129: 875–880. https://doi.org/10.1242/jcs.183954 PMID: 26906419

39. Komander D. The emerging complexity of protein ubiquitination. Biochem Soc Trans. 2009; 37: 937–953. https://doi.org/10.1042/BST0370937 PMID: 19754430

40. Chen ZJ, Sun LJ. Nonproteolytic functions of ubiquitin in cell signaling. Mol Cell. 2009; 33: 275–286. https://doi.org/10.1016/j.molcel.2009.01.014 PMID: 19217402

41. Kawadler H, Yang X. Lys63-linked polyubiquitin chains: linking more than just ubiquitin. Cancer Biol Ther. 2006; 5: 1273–1274. https://doi.org/10.4161/cbt.5.10.3289 PMID: 16969079

42. Park SW, Han MG, Park C, Ju YR, Ahn BY, Ryou J. Hantaan virus nucleocapsid protein stimulates MDM2-dependent p53 degradation. J Gen Virol. 2013; 94: 2424–2428. https://doi.org/10.1099/vir.0.054312-0 PMID: 23994832

43. Kainulainen M, Habjan M, Hubel P, Busch L, Lau S, Colinge J, et al. Virulence factor NSs of rift valley fever virus recruits the F-box protein FBXO3 to degrade subunit p62 of general transcription factor TFIIH. J Virol. 2014; 88: 3464–3473. https://doi.org/10.1128/JVI.02914-13 PMID: 24403578

44. Kainulainen M, Lau S, Samuel CE, Hornung V, Weber F. NSs Virulence Factor of Rift Valley Fever Virus Engages the F-Box Proteins FBXW11 and β-TRCP1 To Degrade the Antiviral Protein Kinase PKR. J Virol. 2016; 90: 6140–6147. https://doi.org/10.1128/JVI.00016-16 PMID: 27122577

45. van Knippenberg I, Carlton-Smith C, Elliott RM. The N-terminus of Bunyamwera orthobunyavirus NSs protein is essential for interferon antagonism. J Gen Virol. 2010; 91: 2002–2006. https://doi.org/10.1099/vir.0.021774-0 PMID: 20427562

46. Kelley LA, Mezulis S, Yates CM, Wass MN, Sternberg MJ. The Phyre2 web portal for protein modeling, prediction and analysis. Nat Protoc. 2015; 10: 845–858. https://doi.org/10.1038/nprot.2015.053 PMID: 25950237

47. Vosper JM, McDowel GS, Hindley CJ, Fiore-Heriche CS,Kucerova R, Horan I, Philpott A. Ubiquitylation on canonical and non-canonical sites targets the transcription factor neurogenin for ubiquitin-mediated proteolysis. J Biol Chem. 2009; 284: 15458–15468 https://doi.org/10.1074/jbc.M809366200 PMID: 19336407

48. Kravtsova-Ivantsiv Y, Ciechanover A. Non-canonical ubiquitin-based signals for proteasomal degradation. J Cell Sci. 2012; 125: 539–548 https://doi.org/10.1242/jcs.093567 PMID: 22389393

49. Viswanathan K, Früh K, DeFilippis V. Viral hijacking of the host ubiquitin system to evade interferon responses. Curr Opin Microbiol. 2010; 13: 517–523. https://doi.org/10.1016/j.mib.2010.05.012 PMID: 20699190

50. Rahman MM, McFadden G. Modulation of NF-κB signalling by microbial pathogens. Nat Rev Microbiol. 2011; 9: 291–306. https://doi.org/10.1038/nrmicro2539 PMID: 21383764

51. Lindner HA. Deubiquitination in virus infection. Virology. 2007; 362: 245–256. https://doi.org/10.1016/j.virol.2006.12.035 PMID: 17291557

52. Maelfait J, Beyaert R. Emerging role of ubiquitination in antiviral RIG-I signaling. Microbiol Mol Biol Rev. 2012; 76: 33–45. https://doi.org/10.1128/MMBR.05012-11 PMID: 22390971

53. Heaton SM, Borg NA, Dixit VM. Ubiquitin in the activation and attenuation of innate antiviral immunity. J Exp Med. 2016; 213: 1–13. https://doi.org/10.1084/jem.20151531 PMID: 26712804

54. Zhu H, Zheng C, Xing J, Wang S, Li S, Lin R, et al. Varicella-zoster virus immediate-early protein ORF61 abrogates the IRF3-mediated innate immune response through degradation of activated IRF3. J Virol. 2011; 85: 11079–11089. https://doi.org/10.1128/JVI.05098-11 PMID: 21835786

55. Lanfranca MP, Mostafa HH, Davido DJ. HSV-1 ICP0: An E3 Ubiquitin Ligase That Counteracts Host Intrinsic and Innate Immunity. Cells. 2014; 3: 438–454. https://doi.org/10.3390/cells3020438 PMID: 24852129

56. Zhang L, Villa NY, McFadden G. Interplay between poxviruses and the cellular ubiquitin/ubiquitin-like pathways. FEBS Lett. 2009; 583: 607–614. https://doi.org/10.1016/j.febslet.2009.01.023 PMID: 19174161

57. Oshiumi H, Miyashita M, Matsumoto M, Seya T. A distinct role of Riplet-mediated K63-Linked polyubiquitination of the RIG-I repressor domain in human antiviral innate immune responses. PLoS Pathog. 2013; 9: e1003533. https://doi.org/10.1371/journal.ppat.1003533 PMID: 23950712

58. Mudhasani R, Tran JP, Retterer C, Kota KP, Whitehouse CA, Bavari S. Protein Kinase R Degradation Is Essential for Rift Valley Fever Virus Infection and Is Regulated by SKP1-CUL1-F-box (SCF) FBXW11-NSs E3 Ligase. PLoS Pathog. 2016; 12: e1005437. https://doi.org/10.1371/journal.ppat.1005437 PMID: 26837067

59. Koliopoulos MG, Lethier M, van der Veen AG, et al. Molecular mechanism of influenza A NS1-mediated TRIM25 recognition and inhibition. Nat Commun. 2018; 9: 1820. https://doi.org/10.1038/s41467-018-04214-8 PMID: 29739942

60. Rajsbaum R, Albrecht RA, Wang MK, Maharaj NP, Versteeg GA, Nistal-Villán E, et al. Species-specific inhibition of RIG-I ubiquitination and IFN induction by the influenza A virus NS1 protein. PLoS Pathog. 2012; 8: e1003059. https://doi.org/10.1371/journal.ppat.1003059 PMID: 23209422

61. Gack MU, Albrecht RA, Urano T, Inn KS, Huang IC, Carnero E, et al. Influenza A virus NS1 targets the ubiquitin ligase TRIM25 to evade recognition by the host viral RNA sensor RIG-I. Cell Host Microbe. 2006; 5: 439–449.

62. Sánchez-Aparicio MT, Feinman LJ, García-Sastre A, Shaw ML. Paramyxovirus V Proteins Interact with the RIG-I/TRIM25 Regulatory Complex and Inhibit RIG-I Signaling. J Virol. 2018; 92: e01960–17. https://doi.org/10.1128/JVI.01960-17 PMID: 29321315

63. Ding S, Mooney N, Li B, et al. Comparative Proteomics Reveals Strain-Specific β-TrCP Degradation via Rotavirus NSP1 Hijacking a Host Cullin-3-Rbx1 Complex. PLoS Pathog. 2016; 12: e1005929. https://doi.org/10.1371/journal.ppat.1005929 PMID: 27706223

64. Riley BE, Lougheed JC, Callaway K, Velasquez M, Brecht E, Nguyen L, et al. Structure and function of Parkin E3 ubiquitin ligase reveals aspects of RING and HECT ligases. Nat Commun. 2013; 4: 1982. https://doi.org/10.1038/ncomms2982 PMID: 23770887

65. Kingstone RE, Chen CA, Rose JK. Calcium phosphate transfection. In: Ausubel F, Brent R, Kingston R, Moore D, Seidman J, Smith J, Struhl K, editors. Curr Protoc Mol Biol. New York: 63; 2003. 1–9.

66. Yoneyama M, Suhara W, Fukuhara Y, Sato M, Ozato K, Fujita T. Autocrine amplification of type I interferon gene expression mediated by interferon stimulated gene factor 3 (ISGF3). J Biochem. 1996; 120: 160–169. https://doi.org/10.1093/oxfordjournals.jbchem.a021379 PMID: 8864859

67. Valassina M, Soldateschi D, dal Maso GM, Santini L, Bianchi S, Valensin PE, Cusi MG. Diagnostic Potential of Toscana Virus N Protein Expressed in Escherichia coli. J Clin Microbiol. 1999; 37: 1237.

viruses

MDPI

Article

Ubiquitin and Not Only Unfolded Domains Drives Toscana Virus Non-Structural NSs Protein Degradation

Gianni Gori Savellini [1,*], Luca Bini [2], Assunta Gagliardi [3], Gabriele Anichini [1], Claudia Gandolfo [1,4], Shibily Prathyumnan [1] and Maria Grazia Cusi [1,4]

1 Department of Medical Biotechnologies, University of Siena, 53100 Siena, Italy; gabriele.anichini@student.unisi.it (G.A.); claudia.gandolfo@unisi.it (C.G.); shibilyps@gmail.com (S.P.); mariagrazia.cusi@unisi.it (M.G.C.)
2 Department of Life Sciences, University of Siena, 53100 Siena, Italy; luca.bini@unisi.it
3 Department of Cellular, Computational and Integrative Biology (CIBIO), University of Trento, Laboratory of Synthetic and Structural Vaccinology, 38122 Trento, Italy; assunta.gagliardi@unitn.it
4 S. Maria delle Scotte Hospital, V.le Bracci, 1, 53100 Siena, Italy
* Correspondence: gianni.gori@unisi.it; Tel.: +39-0577-233864

Received: 11 September 2020; Accepted: 9 October 2020; Published: 12 October 2020

Abstract: The non-structural protein NSs of the *Phenuiviridae* family members appears to have a role in the host immunity escape. The stability of Toscana virus (TOSV) NSs protein was tested by a cycloheximide (CHX) chase approach on cells transfected with NSs deleted versions fused to a reporter gene. The presence of intrinsically disordered regions (IDRs) both at the C- and N-terminus appeared to affect the protein stability. Indeed, the NSsΔC and NSsΔN proteins were more stable than the wild-type NSs counterpart. Since TOSV NSs exerts its inhibitory function by triggering RIG-I for proteasomal degradation, the interaction of the ubiquitin system and TOSV NSs was further examined. Chase experiments with CHX and the proteasome inhibitor MG-132 demonstrated the involvement of the ubiquitin-proteasome system in controlling NSs protein amount expressed in the cells. The analysis of TOSV NSs by mass spectrometry allowed the direct identification of K_{104}, K_{109}, K_{154}, K_{180}, K_{244}, K_{294}, and K_{298} residues targeted for ubiquitination. Analysis of NSs K-mutants confirmed the presence and the important role of lysine residues located in the central and the C-terminal parts of the protein in controlling the NSs cellular level. Therefore, we directly demonstrated a new cellular pathway involved in controlling TOSV NSs fate and activity, and this opens the way to new investigations among more pathogenic viruses of the *Phenuiviridae* family.

Keywords: ubiquitin-proteasome system; NSs protein; protein stability

1. Introduction

Toscana virus (TOSV) is a member of the *Phenuiviridae* family (*Phlebovirus genus*) classified as an emergent sandfly-borne virus. It is mainly transmitted to humans by *Phlebotomus perfiliewi*, *P. perniciosus*, and *P. papatasi* sandfly species [1–3]. Although pauci-symptomatic infections are described in endemic countries [4], TOSV infection is mostly associated to meningitis or more severe central nervous system (CNS) injuries, such as encephalitis and cerebral ischemia [4–6]. Nowadays, TOSV is widely present in the Mediterranean basin [7–11] and represents a significant public health threat.

The non-structural protein (NSs) of the *Phenuiviridae* and *Bunyaviridae* family members represents an important virulence factor, inhibiting the host innate immunity to viral infections, mainly mediated by type I interferons (IFN-α/β) [12–21]. In order to overcome this first-line defense implemented by

the host, viruses evolved protein(s) able to block the IFN-β production and its downstream activity at different steps in the signaling cascade.

However, TOSV is the first Phlebovirus described to date, whose behavior is different from that observed among the *Bunyaviridae* or *Phenuiviridae* members, since interferons are not inhibited during viral infection and replication, despite its NSs protein. TOSV NSs protein is rapidly degraded by the ubiquitin-proteasome system, as previously demonstrated [19–21]. Therefore, during TOSV infection in humans, the ubiquitination and degradation of the NSs protein occur very early in virus replication to prevent IFN-β inhibition in the host.

The proteasomal degradation of proteins is triggered by ubiquitination, a process consisting of covalent attachment of poly-ubiquitin (poly-Ub) chains at lysine residues on the target protein. The assembly of poly-Ub chains to the target protein is accomplished by the cooperation of ubiquitin-activating enzymes (E1), ubiquitin-conjugating enzymes (E2), and ubiquitin-ligases (E3), which work in a sequential cascade [22–34]. A well-characterized cellular complex, which mediates ubiquitination of target proteins, is represented by the Skp, Cullin, and F-box (SCF)-containing complex. Cullin activity is regulated by their NEDdylation, which is the covalent attachment of the small ubiquitin-like protein NEDD8 (neural precursor cell expressed developmentally downregulated 8) to the cullin subunit via the NEDD8 activating enzyme (NAE) [25,26]. In this context, the E3 ubiquitin ligase is the only enzyme that confers specificity to this system by recognizing selected target proteins [24–26].

The structure of the poly-Ub chain assembled by the E3 ligase is crucial for target protein fate and function [22,33]. Covalent bonding between ubiquitin monomers occurs at one of the seven lysine residues in the previously attached ubiquitin molecule, resulting in the formation of ubiquitin chains containing distinctive linkages between the ubiquitin moieties, thus creating a different structure. Based on the linkage generated between ubiquitin moieties, the cognate proteins undergo regulation of their physiological functions, although the role of some chains is still elusive [34–38]. Notably, Lys_{48} (K_{48}) ubiquitin linkage has been reported to be involved in targeting proteins for degradation by the 26S proteasome, while the Lys_{63} (K_{63}) linkage has been proved to regulate protein functions, especially those involved in signal transduction, cell cycle, and gene expression [23,28,31]. So far, the involvement of the ubiquitin system in virus replication, latency, oncogenic properties, and immunity escape has been widely demonstrated [39–59].

Among *Phenuiviridae* members, Rift Valley fever virus (RVFV) is the most investigated virus in terms of antagonistic effects of its NSs protein. The involvement of the ubiquitin system, and in particular of the SCF E3 ubiquitin ligase complex, has been recently elucidated [59–61]. However, despite the involvement of RVFV NSs in the ubiquitin-proteasome control of cellular components, no direct evidence of its ubiquitination and fate/function regulation has been shown.

Regarding TOSV, the involvement of the ubiquitin system in controlling its NSs activity was further demonstrated by a recent work, where an E3 ubiquitin ligase activity has been attributed to the viral protein. Similarly to RVFV, this E3 ligase activity was necessary to mediate RIG-I ubiquitination and proteasomal degradation and, consequently, impede IFN-β production [57]. The only evidence that Bunyaviridae NSs protein could be subjected to ubiquitination has been investigated in the Bunyamwera virus [62,63]. Indeed, analysis of recombinant virus carrying lysine knockdown NSs variant highlighted the increased stability of the mutated protein.

However, no significant advantage in virus growth and virulence in mice were reported, suggesting that NSs ubiquitination is not essential for the virus life cycle [62].

Here, we reported the first evidence of TOSV NSs ubiquitination. Mass spectrometry analysis allowed the identification of lysine residues 104, 109, 154, 180, 244, 294, and 298 on the NSs targeted for ubiquitination. The influence of these sites on protein stability was deeply investigated to evidence their role in protein function and stability, along with the effects of disordered regions located at the C- and N-terminus of the protein.

2. Materials and Methods

2.1. Cells and Viruses

Human embryonic kidney Lenti-X 293T cells (Clontech, Milan, Italy) were cultured in Dulbecco's modified Eagle's medium (DMEM) (Lonza, Milan, Italy) supplemented with 100 U/mL penicillin/streptomycin (Hyclone Europe, Milan, Italy) and 10% heat-inactivated fetal calf serum (FCS) (Lonza), at 37 °C. Toscana virus (TOSV) strain 1812 [64] was used as a template source for NSs cloning described where the N-terminal deleted (NSsΔN) NSs protein variant was generated.

2.2. Reagents and Antibodies

Transient transfections were performed with GeneJuice® Transfection reagent (Novagen, Milan, Italy), according to the manufacturer's instructions, or standard calcium phosphate method. The proteasome inhibitor MG-132 and cycloheximide (CHX) were purchased from Sigma-Aldrich (Milan, Italy). Mouse anti-6×His tag antibody (GE Healthcare, Milan, Italy), mouse monoclonal anti-HA tag antibody, and HRP-conjugated anti-mouse IgG were purchased from Sigma-Aldrich. Ni-NTA sepharose was from Novagen (Milan, Italy).

2.3. Plasmids

Six His-tagged full-length TOSV NSs expression vector was described elsewhere [58]. Amino-terminal-deleted (NSsΔN) and carboxy-terminal-deleted (NSsΔC) NSs protein variants were generated by cloning the nt: 217–948 and nt: 1–537 sequences on TOSV 1812 strain (GenBank: EU327772.1) in-frame into the pcDNA4HisMax (Life Technologies, Milan, Italy) expression plasmid. Having arginine instead of lysine 104, 108, 109, 150, 154, and 179, NSs mutant (NSs-6KR) was generated by using QuikChange II Site-Directed Mutagenesis Kit (Agilent Technologies, Milan, Italy) according to the manufacturer's instructions. NSs variants with lysine residues at the N-terminus (9, 17, 36, 57, 59, and 69) mutated to arginine (NSs-NKR and NSs-6KR-NKR) were generated substituting the N-terminal part with a mutated synthetic fragment (gBlocks, IDT Integrated DNA technologies, Leuven, Belgium). To measure NSs mutant proteins' stability, FireFly Luciferase (FFLuc) fused proteins were generated. FFLuc-NSs and FFLuc-NSsΔC were already described elsewhere [58]. A similar approach was used to obtain the FFLuc-NSs new variants. Briefly, the NSs recombinant plasmids were linearized with BamHI and the FFLuc coding gene was inserted upstream and in frame with the NSs gene by the InFusion system (Clontech, Milan, Italy) following the manufacturer's instructions. All the recombinant plasmids were verified by sequencing. The *Renilla* Luciferase reporter plasmid (pSV40-RL) was purchased by Promega (Promega, Milan, Italy). HA-tagged ubiquitin expressing plasmid was a kind gift of D. Arnoult (Inserm, France) while K48-only and K63-only ubiquitin plasmids were purchased from Addgene (Teddington, UK).

2.4. Cycloheximide Chase Analysis and NSs Protein Stability

Lenti-X 293T cells were seeded in 6-well plates and, after 24 h, transfected with the FFLuc-fused wt-; deleted or mutated NSs expressing plasmids along with 200 ng of pRL-SV40 (Promega) for normalization. Twenty-four hours later, transfected cells were split in a 24-well plate, in triplicate and, after additional 12 h, cells were treated with 25 μM MG-132 for 30 min or untreated. After the inhibitor treatment, in order to start protein expression quantification (T0), cell samples were collected, while the remaining samples were exposed to 100 μg/mL of CHX, or 25 μM MG-132 or 25 μM MG-132 along with 100 μg/mL of CHX. Samples were collected 1.5 and 3 h later for time course quantification. FFLuc-fusion protein amount, detected after translation inhibition by CHX, was quantified by measuring FFLuc activities. Lysates and assay set-up were prepared according to Dual-Luciferase reporter assay (Promega). Relative FFLuc values were normalized with respect to the corresponding RL activities (FFLuc/RL), then fold changes of each sample were calculated with regard to the corresponding T0,

mock-treated, sample. The deduced half-life of each protein was calculated with tools available on the web (https://www.calculator.net/half-life-calculator.html).

2.5. Pull-Down and Immunoblot Analysis

Lenti-X 293T cells, seeded in T25 flasks, were transfected with 4 µg of NSs expressing plasmid and, where indicated, with HA-tagged ubiquitin mutants by using standard calcium phosphate precipitation protocol [65]. Thirty-six hours later, cells were treated with 1 µM MG-132 for additional 12 h and collected 48 h post-transfection. Enrichment of the NSs protein was achieved by Immobilized Metal Affinity Chromatography (IMAC) under denaturing conditions [66]. Briefly, cell pellets were lysed in 5 M guanidine-HCl; 10 mM HEPES (pH 8.0) with sonication to share genomic DNA. His-tagged NSs was bound to Ni-NTA sepharose overnight (o/n) at 4 °C. Beads were collected and washed three times with 10 volumes of 10 mM HEPES (pH 8.0), 1 M NaCl, 0.3% w/v N-lauroylsarcosine (SRK), 20 mM imidazole. Bound proteins were eluted by washing buffer supplemented with 500 mM imidazole. An aliquot of eluted sample was loaded on SDS-PAGE, transferred to nitrocellulose membrane (Santa Cruz Biotechnology, Heidelberg, Germany) and processed for immunoblotting. Briefly, membrane blocking was accomplished with 5% non-fat dry milk, then filters were incubated o/n at 4 °C with anti-NSs (1:200 dilution) or mouse anti-HA monoclonal antibody (1:1000 dilution) (Sigma-Aldrich). After being washed with PBS 0.2% Tween-20 (PBS-T), membranes were incubated with a selected secondary antibody (1:5000 dilution). Immunocomplexes were detected with TMB Enhanced One Component HRP Membrane Substrate (Tebu-bio, Milan, Italy). Ubiquitin modification of the NSs was evidenced by a shift in its MW (10 kDa for mono-ubiquitination, 20 kDa for di-ubiquitination, 10.5 multiples for poly-ubiquitination).

2.6. Mass Spectrometry Detection of NSs Ubiquitination

NSs protein was enriched from Lenti-X 293T-transfected cells. Proteins were separated by SDS-PAGE and stained with Bio-safe Coomassie stain (Bio-Rad, Milan, Italy). Protein bands corresponding to potentially ubiquitinated NSs isoforms were manually cut from gel and prepared for mass-spectrometry analysis. Each band was first destained with 2.5 mM ammonium bicarbonate and 50% acetonitrile, and dehydrated in 100% acetonitrile. A reduction and alkylation procedure was then applied, using 10 mM DTE in 25 mM ammonium bicarbonate for 1 h at 56 °C, followed by incubation in 55 mM iodoacetamide and 25 mM ammonium bicarbonate at room temperature for 45 min, in dark room. Protein bands were rinsed for 10 min with 50 mM ammonium bicarbonate and dehydrated, again, with 100% acetonitrile. Dried gels were rehydrated in trypsin solution (Sigma Aldrich, Italy) and in-gel protein digestion was performed overnight at 37 °C. Protein identification was carried out by Peptide Mass Fingerprinting (PMF) on an ultrafleXtreme™ MALDI-TOF/TOF mass spectrometer (Brucker Corporation, Billerica, MA, USA). In total, 0.75 µL of each digested protein supernatant were spotted onto the MALDI target and allowed to dry. Then, 0.75 µL of matrix solution (5 mg/mL alpha-ciano 4-hydroxycynnamic acid in 50% *v*/*v* acetonitrile and 0.5% *v*/*v* trifluoroacetic acid) were added to the dried sample and air-dried again. A PMF search was performed in NCBInr databases using MASCOT search engine available on-line (Matrix Science Ltd., London, UK, http://www.matrixscience.com). The following parameters were used: taxonomy was limited to viruses, mass tolerance was 100 ppm, the acceptable number of missed cleavage sites was set to two, alkylation of cysteine by carbamidomethylation was assumed as a fixed modification, and oxidation of methionine was considered as a possible modification. The criteria used to accept identifications included the extent of sequence coverage (>15%), the number of matched peptides (>4), and the MASCOT algorithm assigned probabilistic score (>60 or $p < 0.001$). Confirmatory results were also obtained by analysis of the same samples, carried out by Cogentech Proteomics/MS (Cogentech S.c.a.r.l., Milan, Italy) and the mass spectrometry facility at the Toscana Life Sciences (TLS, Siena, Italy) by using the nLC-ESI-MS/MS QExactive-HF system.

3. Results

3.1. NSs Stability Is Influenced by Disordered Regions

Putative intrinsically disordered regions (IDRs) were identified in TOSV NSs by on-line tools (http://prdos.hgc.jp). Based on a predictive algorithm, two IDRs were mapped at aa 1–17 of the N-terminus and aa 295–316 of the C-terminus of the protein. Previous results already showed the important role of the C-terminus, since its deletion influenced protein stability [58]. Next, we assessed the role of the N-terminus on the NSs protein stability by deleting the first 72 aa (Figure 1).

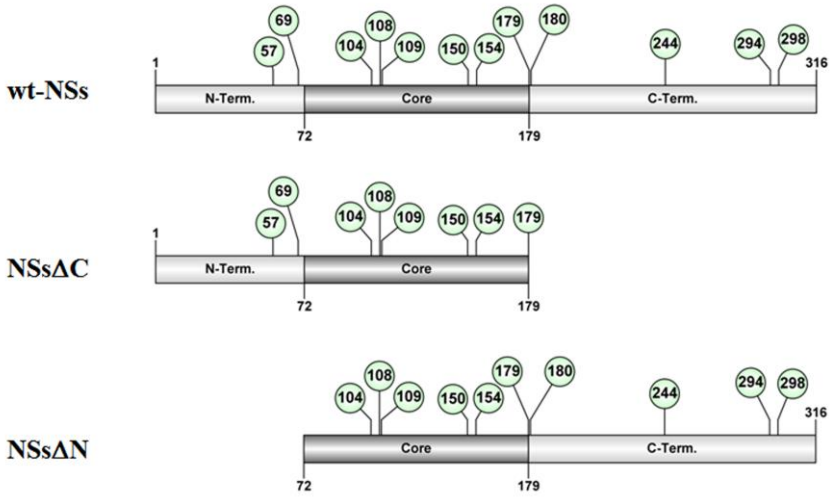

Figure 1. Schematic representation of the of TOSV NSs full-length (wt-NSs) sequence, N-(NSsΔN), or C-terminus deleted (NSsΔC) variants. Green dots indicate the lysine residues with a high predictive score for ubiquitination.

Immunoblotting and densitometric analysis of lysates of Lenti-X 293T cells transfected with NSs expressing plasmid showed a 9-fold increase of NSsΔN protein accumulation compared to the wt-NSs protein ($p \leq 0.0005$) (Figure 2A), confirming the presence of a disordered instable region at the N-terminus.

To better address the involvement of N-terminus IDR on the NSs stability, Firefly Luciferase (FFLuc) fusion proteins were generated. Afterwards, cycloheximide (CHX) chase experiments were performed to compare protein stability among the NSsΔN, NSsΔC, and wt-NSs. Luciferase activities were measured in transfected CHX-treated cells. After normalization with respect to the constitutively expressed *Renilla* luciferase (pSV40-RenLuc), a considerable reduction of the Luciferase activities, consistent with NSs degradation, was reported in wt-NSs lysates just 1.5 h after CHX treatment in comparison with the mock-treated sample. On the contrary, the detection of a higher Luciferase signal for NSsΔN and NSsΔC demonstrated a significant increased protein stability at both 1.5 and 3 h after CHX treatment (Figure 2B). Moreover, based on the CHX chase experiment datasets, the deduced half-lives of NSsΔN ($t_{1/2}$ 8.7 h) and NSsΔC ($t_{1/2}$ 4.8 h) were significantly longer ($p < 0.0001$) than those observed for wt-NSs ($t_{1/2}$ 1.6 h) (Data not shown). These data support the prediction of intrinsic disordered sequences located at the terminal ends of the NSs, thus the deleted variants of the protein acquired greater stability and cytoplasmic accumulation in transfected cells.

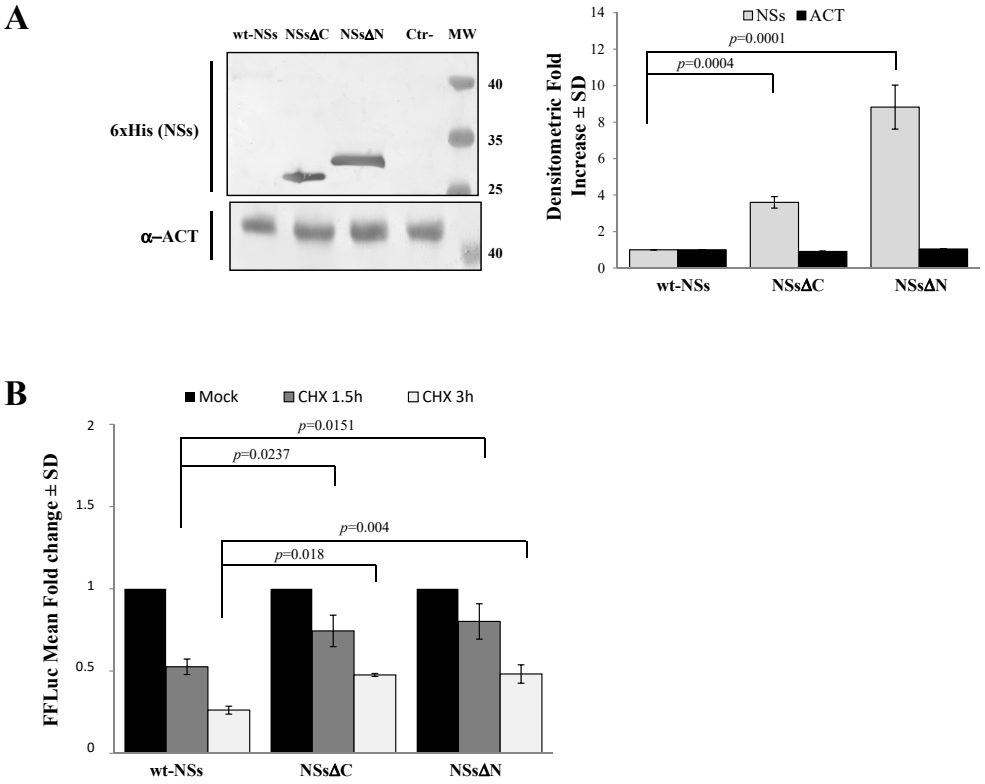

Figure 2. Domains affecting TOSV NSs stability. (**A**) The involvement of TOSV NSs C- and N-terminal regions on protein stability was demonstrated by generating deleted NSs proteins (NSsΔC and NSsΔN). The behavior of the deleted NSs variants was tested by immunoblotting on the whole-cell lysates (50 µg) of Lenti-X 293T-transfected cells. Specific proteins were detected by using anti-6×His (NSs) monoclonal antibody (left figure). Loading control was represented by actin (α-ACT) detection (left figure). Quantitative assessment of deleted NSs variants was determined by densitometric analysis (right figure). (**B**) Lenti-X 293T cells were transfected with FFLuc NSsΔN and NSsΔC fusion constructs and *Renilla* Luciferase as an internal control. Transfected cells were mock-treated or treated with cycloheximide (CHX) and collected at 1.5 and 3 h. Fold induction was obtained by luciferase activity normalization with respect to *Renilla* luciferase values and comparison to the relative mock-treated sample. Results were expressed as mean fold change values collected in at least three independent experiments ± standard deviation.

3.2. Ubiquitin-Dependent NSs Proteasomal Degradation

Previous results have shown that TOSV NSs retains antagonistic function on host innate immunity to viral infection [20,21,58] exhibiting an E3 ubiquitin ligase activity on RIG-I [57]. Therefore, we also investigated the effect of ubiquitination on the fate and function of the viral protein. Similarly to Bunyamwera virus, TOSV NSs protein stability was also evaluated analyzing its possible ubiquitination, since its accumulation into the cell cytoplasm was strongly enhanced by the exposure to the proteasome inhibitor MG-132 [20,21]. Indeed, a significant increase of protein stability ($p < 0.05$) was noticed when the inhibitor MG-132 was included during the CHX chase experiments, with a fold increase of protein accumulation at 3 h treatment of 2.3 for the wt-NSs, 6.1 for NSsΔC, and 3.9 for NSsΔN (Figure 3). Moreover, the immunoblotting confirmed the enhanced protein accumulation in the cell cytoplasm when the transfected cells were exposed only to MG-132 (Figure 3).

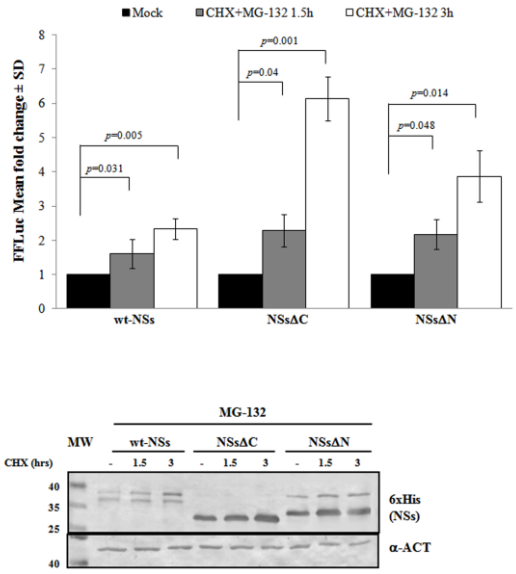

Figure 3. Effects of the proteasome inhibitor MG-132 on NSs deleted mutants were evaluated. (**Upper panel**) wt-NSs, NSsΔN, and NSsΔC expressing cells were treated with 25 μM of the inhibitors along with 100 μg/mL of CHX and collected at 1.5 and 3 h. Cell lysates were subjected to a dual-luciferase assay in order to estimate the stability of NSs protein variants. A significant increase of protein stability over time was noticed for wt-NSs, NSsΔC, and NSsΔN. (**Lower panel**) The immunoblotting with anti-6×His antibody or anti-ACT performed on MG-132 and CHX treated cells confirmed the stabilizing properties of the MG-132 on the NSs proteins tested. The error bars represent the standard deviation from the mean values obtained in independent experiments.

Furthermore, the positive effects of the proteasome inhibitor were evidenced by the deduced half-life of NSsΔC ($t_{1/2}$ 22 h) and NSsΔN ($t_{1/2}$ 26.4 h), which was significantly higher ($p < 0.05$) with respect to the untreated counterparts. This evidence confirmed the ubiquitinated status of TOSV NSs, suggesting that the stability of TOSV NSs was also controlled by ubiquitination and proteasomal degradation and that lysine residues target for ubiquitination were at least located in the central region of the protein, common to the three constructs.

3.3. Evidence of TOSV NSs Ubiquitination

To understand whether TOSV NSs was directly ubiquitinated, the presence of polyubiquitin chains linked to the viral protein was investigated. The denaturant pull-down assay performed on NSs and HA-Ub co-transfected cells allowed the efficient inactivation of de-ubiquitinating enzymes (DUBs), preserving NSs ubiquitinated forms [60]. The ubiquitination status of the affinity purified NSs was detected by immunoblotting using anti-6×His and anti-HA antibodies, demonstrating that NSs protein underwent a robust ubiquitination. Indeed, high-molecular-weight migrating bands with a constant increase were detected with anti-HA monoclonal antibody, corresponding to mono-, multi-, or poly-ubiquitinated forms of NSs (Figure 4A). Unfortunately, the anti-6×His monoclonal weakly detected these bands due to a lower sensitivity of the antibody.

As shown in Figure 4A, both the N- and C-terminal-truncated proteins underwent ubiquitination at a similar extent to that observed for the wt-NSs. On the basis on these results, it appears that lysine residues target for ubiquitination are located in the central region of the protein. We further investigated the ubiquitin-linkage type present on the NSs protein, particularly the K_{48}- or K_{63}-chain. These experiments demonstrated that both K_{48}- and K_{63}-ubiquitination moiety occurs in both wt- and the deleted NSs variants (Figure 4B). Indeed, anti-HA reactive bands corresponding to mono-, multi-, or poly-ubiquitinated forms of the NSs were detected in all the samples tested. These data supported

the idea that both K_{63} and K_{48} ubiquitin linkages take place, thus this type of post-translational modification does not only influence NSs stability, but it could also affect NSs protein activity.

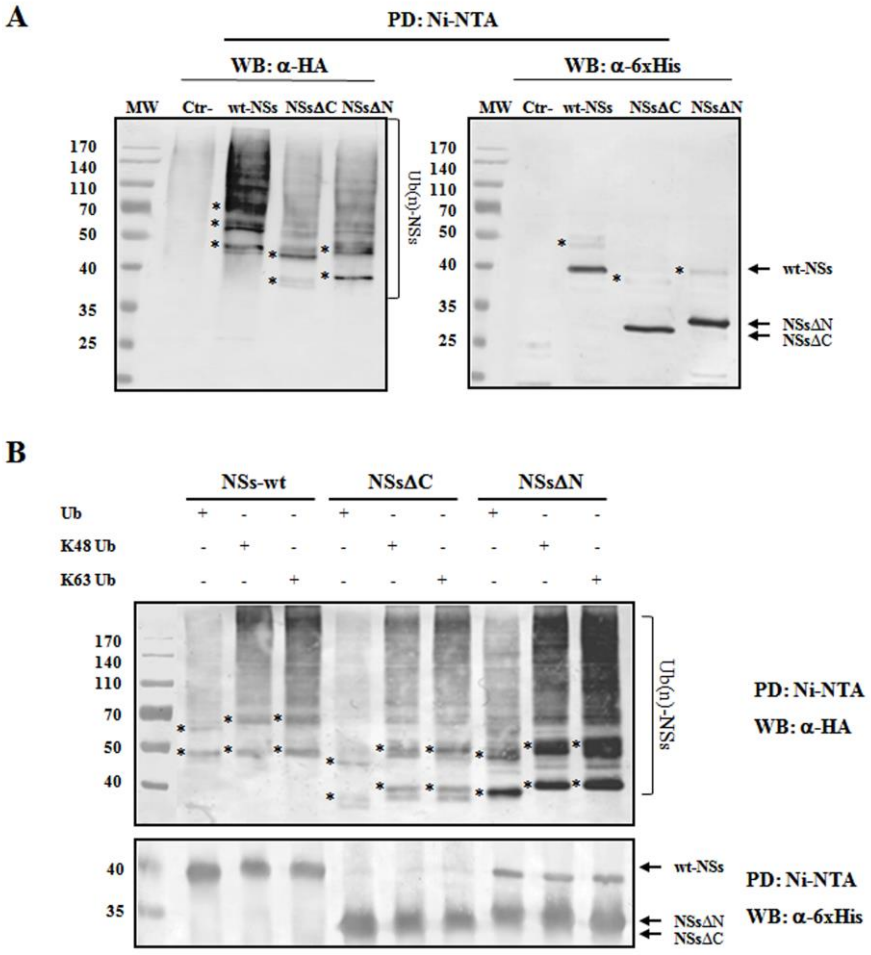

Figure 4. TOSV NSs undergoes ubiquitination. NSs ubiquitination was evaluated by immunoblotting. (**A**) Lenti-X 293T cells were transfected with wt-, ΔC-, or ΔN-expressing plasmids, along with the plasmid expressing HA-tagged wild-type ubiquitin (Ub). Cells treated with the proteasome inhibitor MG-132 were collected at 48 h post-transfection and NSs protein enrichment was performed on cell lysates by pull-down (PD) experiments using Ni-NTA agarose beads. 6×His-NSs-enriched samples were subjected to immunoblotting for Ub (α-HA) or NSs (α-6×His) detection. The ubiquitinated status of the three NSs forms was evaluated as a modification of the targeted substrate, causing a shift in MW of ~10 kDa (mono-ubiquitination) or multiples. Asterisk represents ubiquitinated NSs forms. (**B**) The rate on K_{48}-and K_{63}-moiety ubiquitination was assessed by PD assay and immunoblotting. Lenti-X 293T cells were transfected with wt-, ΔC, or ΔN NSs expressing plasmids, along with the plasmid expressing HA-tagged K_{48}-only or K_{63}-only ubiquitin mutants. Twenty-four hours later, cells were treated with MG-132 and collected after additional 24 h. Lysates were prepared and PD with Ni-NTA agarose beads. Isolated proteins were separated by SDS-PAGE and probed by immunoblotting for NSs (α-6×His) and Ub-K_{48} and Ub-K_{63} (α-HA) detection. Asterisk indicates ubiquitinated forms of the NSs proteins.

3.4. Specific NSs Lysine Residues Undergo Ubiquitination

The identification of specific NSs lysine residues targeted for ubiquitination was mapped by mass spectrometry analysis. NSs protein was enriched from transfected Lenti-X 293T cells under denaturing conditions. The recovered protein was resolved by SDS-PAGE and Coomassie staining. The gel portion of interest was processed for mass spectrometry analysis. NSs peptides generated by trypsin digestion

were subjected to mass spectrometry analysis. Some lysines carrying the Gly-Gly signature di-peptide were detected and assigned as being bound to ubiquitin [67]. Three lysine residues at position 104, 109, and 154, located in the central part of the NSs, were recognized as a target for ubiquitin on the recovered protein (Figure 5).

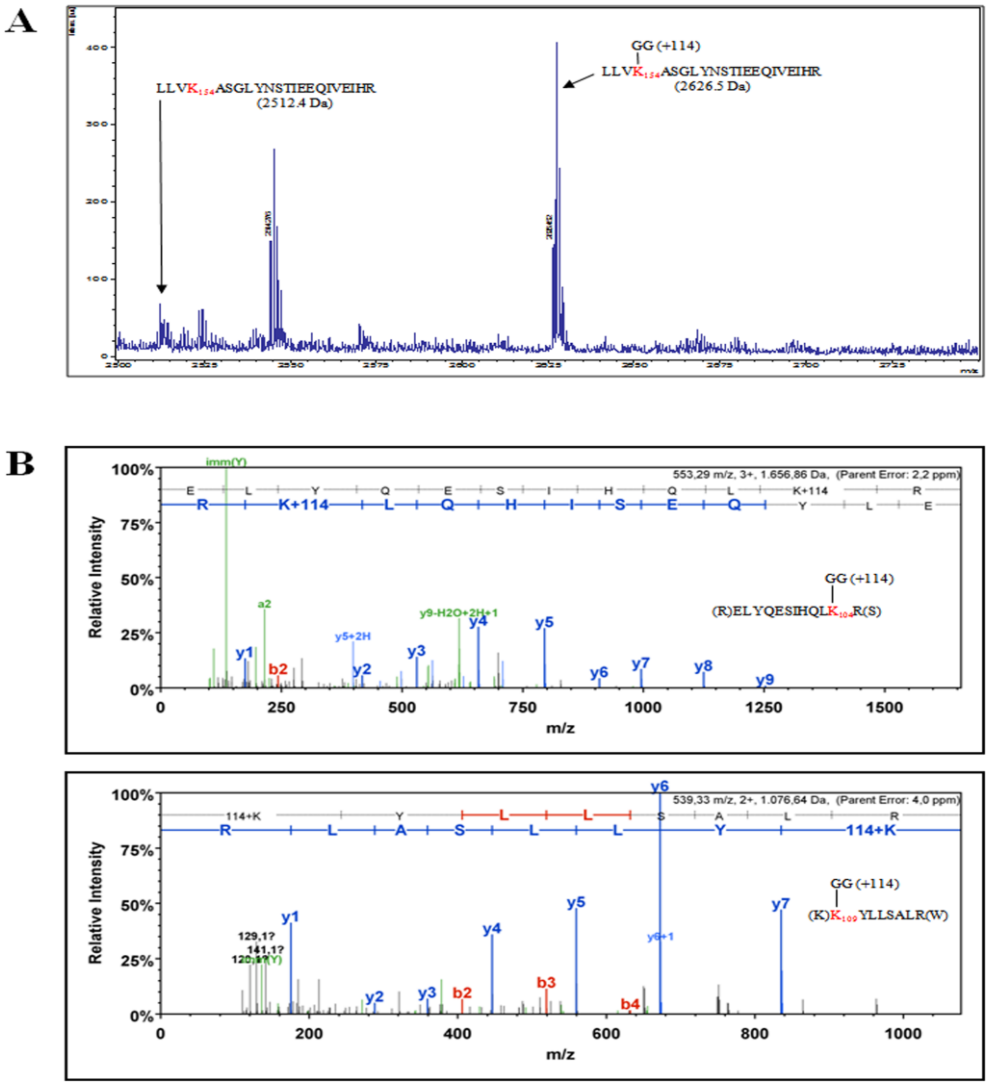

Figure 5. The NSs protein, enriched from cell lysate of transfected cells, was analyzed by mass spectrometry in an attempt to identify lysine residues targeted for specific ubiquitination. (**A**) MS1 mass spectrum (Department of Life Sciences, University of Siena, Siena) showing the identification of TOSV NSs peptide containing the ubiquitinated lysine residue at position 154 and (**B**) MS2 mass spectrum (Cogentech S.c.a.r.l., Milan, Italy) showing TOSV NSs peptides ubiquitinated on lysines at positions 109 and 104.

However, we could not exclude that other lysine residues subjected to ubiquitination were located in other regions of the NSs protein. Therefore, we expressed and tested the NSs-6KR protein variant, consisting of a full-length NSs protein with mutated lysine in the core region (K_{104}; K_{108}; K_{109}; K_{150}; K_{154}; and K_{179}), for the protein degradation rate. As evidenced by CHX chase, the 6KR mutant protein was highly stable compared to wt-NSs ($p = 0.003$), suggesting that lysine residues targeted for ubiquitination were located in the core region of the protein (Figure 6A).

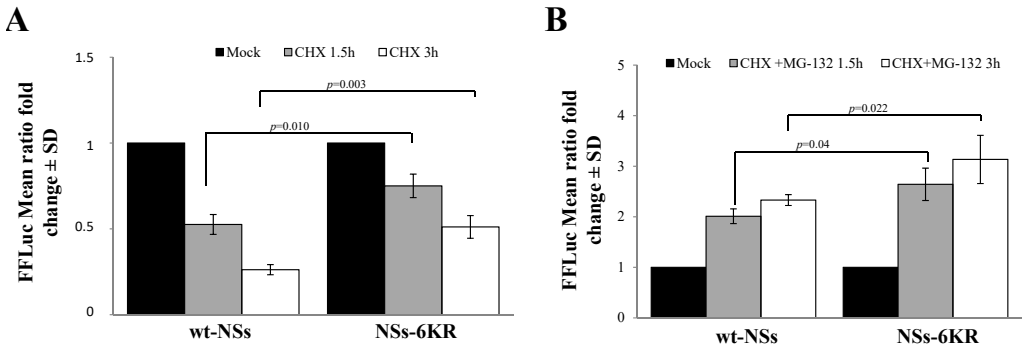

Figure 6. Effects of lysine residues in the core region on protein stability. (**A**) A new NSs mutant (NSs-6KR), consisting of arginine substitution at lysine 104, 108, 109, 150, 154, and 179 position, was generated and tested for protein stability. CHX chase experiments evidenced a significantly increased stability for the NSs mutant with respect to the wt-NSs protein. (**B**) The NSs-6KR mutant still responded to MG-132, as shown by the chase experiments. Transfected cells were treated with CHX in combination with 25 μM of MG-132 and then residual luciferase activities were measured. Graphs represent mean values ± standard deviations (SD) of three independent experiments.

Moreover, the estimated half-life of the NSs-6KR was double (p = 0.0069) than that of wt-NSs ($t_{1/2}$ 3.7 h vs. $t_{1/2}$ 1.6 h). Notwithstanding, MG-132 still affected NSs-6KR protein degradation by increasing its accumulation into the cells, leading to the conclusion that lysine residues other than those in the core region could undergo ubiquitination (Figure 6B).

We then evaluated the presence of specific lysines, which might undergo ubiquitination in the N- or C-terminal part of the NSs protein. Two NSs variants were generated, mutating the lysine residues 9, 17, 36, 57, 59, and 69 at the amino-terminus of the wt protein (NSs-NKR) or of the NSs-6KR mutant (NSs-6KR-NKR). The CHX chase assessed to determine variations in protein stability showed that lysine residues located at the N-terminus did not significantly influence the turnover of the protein. Indeed, compared to the relative counterpart NSsΔN (Figure 2B) and NSs-6KR (Figure 6), the new NSs proteins did not exhibit a remarkable increase ($p > 0.05$) of protein accumulation after exposure to CHX (Figure 7A), suggesting that those sites were not critical in determining the NSs protein fate.

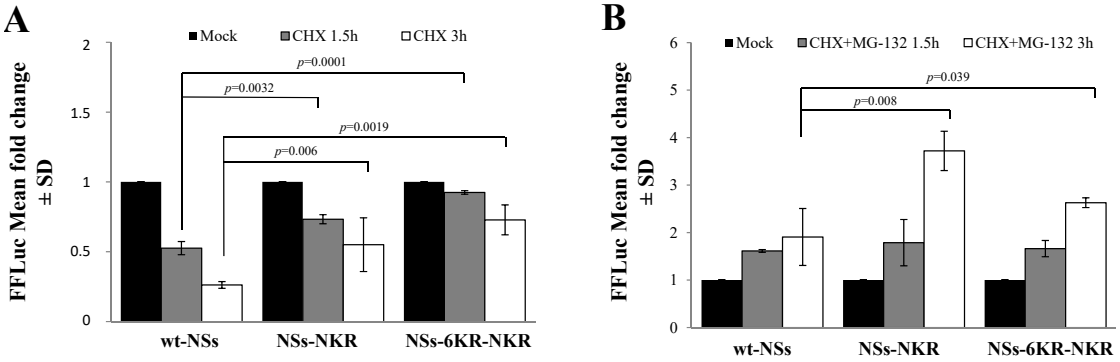

Figure 7. Effects of amino-terminal lysine residues on protein stability. (**A**) Lysates of NSs-NKR and NSs-6KR-NKR-transfected cells were collected at different time points after CHX exposure and subjected to the dual-luciferase assay in order to estimate the stability of NSs protein variants by measuring the FFLuc residual activities. (**B**) Cells expressing new NSs mutants, treated with 25 μM of MG-132, along with 100 μg/mL of CHX, evidenced the activity of the inhibitor on both NSs-NKR and NSs-6KR-NKR. Cells were collected at 1.5 and 3 h post-treatment and lysates were subjected to a dual-luciferase assay in order to estimate the stability of NSs protein variants. The error bars represent the standard deviation from the mean values obtained in independent experiments ± standard deviations (SD).

As expected, the chase experiments conducted in the presence of the proteasome inhibitor MG-132 and CHX evidenced that the NSs-NKR responded to inhibitor (p = 0.008), as lysines in the core region were maintained. However, even the NSs-6KR-NKR variant responded to the drug (p = 0.039) (Figure 7B), indicating that some lysine residues targeted for ubiquitination were still present in the protein besides these sequences. Furthermore, supporting the previous data, the inhibitor substantially (p = 0.036) augmented NSs-6KR-NKR protein mean half-life ($t_{1/2}$ 19.6 h) compared to the relative mock-treated sample ($t_{1/2}$ 9.8 h). A further investigation by mass-spectrometry revealed the presence of four more lysine residues, located in the C-terminal of the protein, which underwent ubiquitination. In particular, we found ubiquitinated lysines at the 180, 244, 294, and 298 position (Table 1).

Table 1. The enriched NSs protein was analyzed by mass spectrometry in an attempt to identify lysine residues targeted for specific ubiquitination. MS2 mass spectrometry results (TLS, Siena, Italy) are reported, showing the identification of TOSV NSs peptide containing the ubiquitinated lysine residues at position 180, 244, 294, and 298.

Lysine Position	Percentage Sequence Coverage	Peptide Sequence	Peptide Identification Probability	Mascot Ion Score	Mascot Identity Score	Mascot Delta Ion Score	Variable Modifications Identified by Spectrum
180	7.21%	VLIEGK*k*HGLTAFDLPGNDILGDICVVQAAR	99.70%	58.6	60.3	36.67597403	K7:GlyGly (+114.04)
180	7.21%	VLIEGK*k*HGLTAFDLPGNDILGDICVVQAAR	99.70%	45.9	33.3	32.14675325	K7:GlyGly (+114.04)
180	6.94%	*k*HGLTAFDLPGNDILGDICVVQAAR	99.70%	63.2	48.6	55.33246753	K1:GlyGly (+114.04)
244	3.80%	KED*k*	99.70%	55.4	60	21.31764706	K4:GlyGly (+114.04)
244	6.33%	KED*k*RAKAKGLmSmCAAR	99.70%	51.2	43.7	31.05	K4:GlyGly (+114.04)
244	6.33%	ED*k*RAKAKGLMSMCAAR	99.70%	48.7	50.4	30.65454545	K3:GlyGly (+114.04)
294–298	6.59%	TDLGFRETALSTFWAKDWPTPQETILSD*k*RcL*k*EDMR	99.70%	48.6	36	34.75324675	K29:GlyGly (+114.04) K33:GlyGly (+114.04)
294–298	6.33%	DWPTLQETILSD*k*RcL*k*EDmRVTK	99.70%	52.6	38	43.26406926	K13:GlyGly (+114.04) K17:GlyGly (+114.04)
294	6.33%	ETALSTFWAKDWPTPQETILSD*k*	99.70%	60.9	65.5	23.27176471	K23:GlyGly (+114.04)
298	6.33%	CL*k*EDMRVTKWLPSPPHYPPL	99.70%	45.8	38.3	27.21315789	K4:GlyGly (+114.04)
298	6.33%	CL*K*EDMRVTKWLPSPPHYPPL	99.70%	44.2	45.9	27.91753247	K23:GlyGly (+114.04)

4. Discussion

The non-structural NSs protein of many *Bunyaviridae* and *Phenuiviridae* family members has been shown to be an important virulence factor, able to counteract host innate immunity to viral infections [13–21,57,58].

An important factor affecting protein behavior resides in its stability and turnover. Indeed, a tight control of cell proteins' half-life is required in order to support an efficient cellular homeostasis, death/survival, and replication. Most of the viral proteins exert their activity by interfering in critical cellular processes, such as signal transduction and cell-cycle progression. Thus, their function is tightly controlled through several viral and cellular mechanisms.

One aspect that determines protein fate is the presence of unfolded domains, which confer a reduced stability and a rapid degradation via lysosome or proteasome systems [68–70]. The intrinsically disordered region (IDR) with an unfolded structure described for Bunyamwera virus (BUNV) NSs was associated with the reduced viral protein stability in infected cells [62,63].

Previously, we demonstrated that the C-terminus of TOSV NSs could retain an IDR with a negative effect on protein turnover [58]. In the present work, a deeper investigation of TOSV NSs protein properties was pursued. New data suggest that TOSV NSs shares similarities with BUNV NSs, since its stability is strongly influenced by IDR located at the N-terminus (NSsΔN), along with that at the C-terminal (NSsΔC) part of the protein. The increased stability of NSsΔN and NSsΔC, demonstrated by semi-quantitative immunoblotting, suggested that these domains are important in order to maintain protein stability. Indeed, the cycloheximide (CHX) chase assay allowed us to confirm that external NSs IDRs are strikingly related to protein half-life, and NSsΔN exhibited a longer half-life. Therefore, the unfolded NSs N-terminus drastically compromised protein stability, along with the C-terminus, which, in turn, had a minor effect.

Nevertheless, apart from protein IDRs, other mechanisms involved in protein stability were proposed. Based on Bunyamwera virus (BUNV) studies where the involvement of the ubiquitin-proteasome system in controlling NSs fate was described [62], post-translational modifications (PTMs) in TOSV NSs were considered. Contrary to RVFV and BUNV, TOSV NSs presented many lysine residues that could undergo ubiquitination.

Under specific experimental conditions, we provided direct evidence of TOSV NSs ubiquitination both by immunoblotting and mass spectrometry (MS). We identified the ubiquitin linkage at lysine residue 104, 109, and 154, as they were modified by the signature peptide 'Gly-Gly' derived from ubiquitin by MS. Surprisingly, identified PTM sites were located in the core region of the protein, suggesting an incisive role of this region in the protein fate.

However, TOSV NSs ubiquitination on other sites of the protein could be neither demonstrated nor excluded. Despite being more stable, the NSs mutant, lacking all the core lysine residues (NSs-6KR), was still susceptible to MG-132 treatment. This suggested the presence of additional lysine residues, located outside the core region, subjected to ubiquitination. In an attempt to better characterize the NSs post-translational modification by ubiquitination, a deeper investigation was conducted. The mutation of lysine residues located at the amino-terminal part of the protein (NSs-NKR) excluded the presence of ubiquitination targets in this region, since the mutation did not affect the protein degradation rate or half-life, as demonstrated by the CHX chase (Figure 7A).

Further experiments using the NSs-6KR-NKR, lacking all the lysines at the N-terminus and core regions, evidenced the presence of additional ubiquitination sites in the C-terminal part. The CHX chase in the presence of the proteasome inhibitor MG-132 revealed that the NSs-6KR-NKR mutant still responded to the inhibitor, thus ubiquitination still occurred on the protein. More comprehensive analysis by MS identified the ubiquitin-derived 'Gly-Gly' signature peptide linked at lysine residues 180, 244, 292, and 298, as they were modified by ubiquitin.

These data open the way to new cellular mechanisms responsible for TOSV NSs functions and to its role in TOSV pathogenicity. Indeed, during the first phases of viral replication, the rapid degradation of the NSs protein by the proteasome could be a regulatory mechanism of cell defense, thus inhibiting RIG-I degradation and allowing the expression of IFN-β in the infected host (Figure 8).

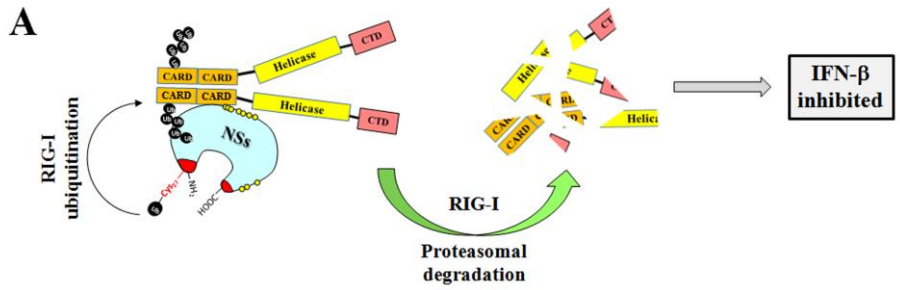

Figure 8. *Cont.*

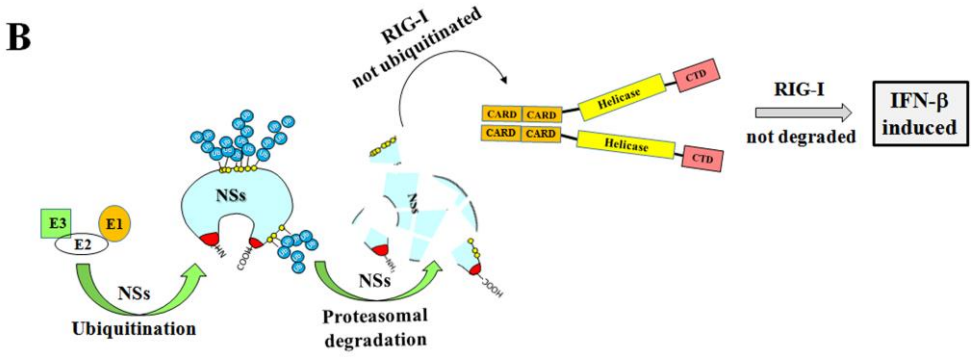

Figure 8. Cartoon representation of the putative function of the TOSV NSs on RIG-I-mediated interferon beta production and the influence of ubiquitination on the viral protein function. (**A**) The TOSV NSs protein accumulated in the cell cytoplasm efficiently interacts with RIG-I and mediates its ubiquitination and subsequent degradation, counteracting IFN-β production. On the contrary (**B**), the high ubiquitination rate of the NSs negatively affects its stability, targeting the protein for proteasomal degradation. Consequently, RIG-I is not depleted and the physiological secretion of IFN-β occurs.

Author Contributions: Conceptualization, G.G.S., L.B. and M.G.C.; methodology, G.G.S., G.A. and A.G.; formal analysis, G.G.S. and A.G.; investigation, G.G.S., G.A., A.G., C.G. and S.P.; data curation, G.G.S.; writing—original draft preparation, G.G.S.; writing—review and editing, G.G.S and M.G.C.; supervision, M.G.C. and L.B.; funding acquisition, M.G.C. All authors have read and agreed to the published version of the manuscript.

Funding: This research was funded by the Italian Ministry of Education, Universities and Research (MIUR), grant number 2017KM79NN.

Conflicts of Interest: The funders had no role in the design of the study; in the collection, analyses, or interpretation of data; in the writing of the manuscript, or in the decision to publish the results.

References

1. Braito, A.; Ciufolini, M.G.; Pippi, L.; Corbisiero, R.; Fiorentini, C.; Gistri, A.; Toscano, L. Phlebotomus-transmitted toscana virus infections of the central nervous system: A seven-year experience in Tuscany. *Scand. J. Infect. Dis.* **1998**, *30*, 505–508. [PubMed]
2. Verani, P.; Ciufolini, M.G.; Nicoletti, L.; Calducci, M.; Sabatinelli, G.; Coluzzi, M.; Paci, P.; Amaducci, L. Ecological and epidemiological studies of Toscana virus, an arbovirus isolated from Phlebotomus. *Ann. Ist. Super. Sanita* **1982**, *18*, 397–399. [PubMed]
3. Verani, P.; Lopes, M.C.; Nicoletti, L.; Balducci, M. Studies on Phlebotomus transmitted viruses in Italy: I. Isolation and characterization of a Sandfly fever Naples-like virus. Arboviruses in the Mediterranean Countries. *Zbl. Bakt. Suppl.* **1980**, *9*, 195–201.
4. Sanbonmatsu-Gámez, S.; Pérez-Ruiz, M.; Palop-Borrás, B.; Navarro-Marí, J.M. Unusual manifestation of Toscana virus infection, Spain. *Emerg. Infect. Dis.* **2009**, *15*, 347–348. [CrossRef]
5. Kuhn, J.; Bewermeyer, H.; Hartmann-Klosterkoetter, U.; Emmerich, P.; Schilling, S.; Valassina, M. Toscana virus causing severe meningoencephalitis in an elderly traveler. *J. Neurol. Neurosurg. Psychatry* **2005**, *76*, 1605–1606. [CrossRef]
6. Bartels, S. Lethal encephalitis caused by Toscana virus in an elderly patient. *J. Neurol.* **2012**, *259*, 175–177. [CrossRef]
7. Sonderegger, B.; Hachler, H.; Dobler, G.; Frei, M. Imported aseptic meningitis due to Toscana virus acquired on the island of Elba, Italy, August 2008. *Euro Surveill.* **2009**, *14*, 19079.
8. Epelboin, L.; Hausfater, P.; Schuffenecker, I.; Riou, B.; Zeller, H.; Bricaire, F.; Bossi, P. Meningoencephalitis due to Toscana virus in a French traveler returning from central Italy. *J. Travel. Med.* **2008**, *15*, 361–363. [CrossRef]
9. Tschumi, F.; Schmutz, S.; Kufner, V.; Heider, M.; Pigny, F.; Schreiner, B.; Capaul, R.; Achermann, Y.; Huber, M. Meningitis and epididymitis caused by Toscana virus infection imported to Switzerland diagnosed by metagenomic sequencing: A case report. *BMC Infect. Dis.* **2019**, *19*, 591. [CrossRef]

10. Howell, B.A.; Azar, M.M.; Landry, M.L.; Shaw, A.C. Toscana virus encephalitis in a traveler returning to the United States. *J. Clin. Microbiol.* **2015**, *53*, 1445–1447. [CrossRef]
11. Dominati, A.; Sap, L.; Vora, S. Fever in a returning traveler from Tuscany. *Rev. Med. Suisse* **2018**, *14*, 294–296. [PubMed]
12. Sato, M.; Suemori, H.; Hata, N.; Asagiri, M.; Ogasawera, K.; Nakao, K.; Nakaya, T.; Katsuki, M.; Noguchi, S.; Tanaka, N.; et al. Distinct and essential roles of transcription factors IRF-3 and IRF-7 in response to viruses for IFN-alpha/beta gene induction. *Immunity* **2000**, *13*, 539–548. [CrossRef]
13. Weber, F.; Bridgen, A.; Fazakerley, J.K.; Streitenfeld, H.; Kessler, N.; Randall, R.E.; Elliott, R.M. Bunyamwera bunyavirus nonstructural protein NSs counteracts the induction of alpha/beta interferon. *J. Virol.* **2002**, *76*, 7949–7955. [CrossRef] [PubMed]
14. Jääskeläinen, K.M.; Kaukinen, P.; Minskaya, E.S.; Plyusnina, A.; Vapalahti, O.; Elliott, R.M.; Weber, F.; Vaheri, A.; Plyusnin, A. Tula and Puumala hantavirus NSs ORFs are functional and the products inhibit activation of the interferon-beta promoter. *J. Med. Virol.* **2007**, *79*, 1527–1536. [CrossRef] [PubMed]
15. Bridgen, A.M.; Weber, F.; Fazakerley, J.K.; Elliott, R.M. Bunyamvera bunyavirus non-structural protein NSs is nonessential gene product that contributes to the viral pathogenesis. *Proc. Natl. Acad. Sci. USA* **2001**, *98*, 664–669. [CrossRef]
16. Blakqori, G.; Delhaye, S.; Habjan, M.; Blair, C.D.; Sánchez-Vargas, I.; Olson, K.E.; Attarzadeh-Yazdi, G.; Fragkoudis, R.; Kohl, A.; Kalinke, U.; et al. La Crosse bunyavirus nonstructural protein NSs serves to suppress the type I interferon system of mammalian hosts. *J. Virol.* **2007**, *81*, 4991–4999. [CrossRef]
17. Léonard, V.H.; Kohl, A.; Hart, T.J.; Elliott, R.M. Interaction of Bunyamwera Orthobunyavirus NSs protein with mediator protein MED8: A mechanism for inhibiting the interferon response. *J. Virol.* **2006**, *80*, 9667–9675. [CrossRef]
18. Wuerth, J.D.; Weber, F. Phleboviruses and the Type I Interferon Response. *Viruses* **2016**, *8*, 174. [CrossRef]
19. Brisbarre, N.M.; Plumet, S.; de Micco, P.; Leparc-Goffart, I.; Emonet, S.F. Toscana virus inhibits the interferon beta response in cell cultures. *Virology* **2013**, *442*, 189–194. [CrossRef]
20. Savellini, G.G.; Weber, F.; Terrosi, C.; Habjan, M.; Martorelli, B.; Cusi, M.G. Toscana virus induces interferon although its NSs protein reveals antagonistic activity. *J. Gen. Virol.* **2011**, *92*, 71–79. [CrossRef]
21. Savellini, G.G.; Valentini, M.; Cusi, M.G. Toscana virus NSs protein inhibits the induction of type I interferon by interacting with RIG-I. *J. Virol.* **2013**, *87*, 6660–6667. [CrossRef] [PubMed]
22. Pickart, C.M. Mechanisms underlying ubiquitination. *Annu. Rev. Biochem.* **2001**, *70*, 503–533. [CrossRef] [PubMed]
23. Bernassola, F.; Karin, M.; Ciechanover, A.; Melino, G. The HECT family of E3 ubiquitin ligases: Multiple players in cancer development. *Cancer Cell* **2008**, *14*, 10–21. [CrossRef] [PubMed]
24. Jackson, P.K.; Eldridge, A.G.; Freed, E.; Furstenthal, L.; Hsu, J.Y.; Kaiser, B.K.; Reimann, J.D. The lore of the RINGs: Substrate recognition and catalysis by ubiquitin ligases. *Trends Cell. Biol.* **2000**, *10*, 429–439. [CrossRef]
25. Skaar, J.R.; Pagan, J.K.; Pagano, M. Mechanisms and function of substrate recruitment by F-box proteins. *Nat. Rev. Mol. Cell. Biol.* **2013**, *14*, 369–381. [CrossRef]
26. Bosu, D.R.; Kipreos, E.T. Cullin-RING ubiquitin ligases: Global regulation and activation cycles. *Cell Div.* **2008**, *3*, 7. [CrossRef]
27. Furukawa, M.; Andrews, P.S.; Xiong, Y. Assays for RING family ubiquitin ligases. *Methods Mol. Biol.* **2005**, *301*, 37–46.
28. Lee, E.K.; Diehl, J.A. SCFs in the new millennium. *Oncogene* **2014**, *33*, 2011–2018. [CrossRef]
29. Hatakeyama, S.; Nakayama, K.I. U-box proteins as a new family of ubiquitin ligases. *Biochem. Biophys. Res. Commun.* **2003**, *302*, 635–645. [CrossRef]
30. Scheffner, M.; Nuber, U.; Huibregtse, J.M. Protein ubiquitination involving an E1-E2-E3 enzyme ubiquitin thioester cascade. *Nature* **1995**, *373*, 81–83. [CrossRef]
31. Rotin, D.; Kumar, S. Physiological functions of the HECT family of ubiquitin ligases. *Nat. Rev. Mol. Cell. Biol.* **2009**, *10*, 398–409. [CrossRef] [PubMed]
32. Ardley, H.C.; Robinson, P.A. E3 ubiquitin ligases. *Essays Biochem.* **2005**, *41*, 15–30. [CrossRef] [PubMed]
33. Komander, D. The emerging complexity of protein ubiquitination. *Biochem. Soc. Trans.* **2009**, *37*, 937–953. [CrossRef] [PubMed]

34. Finley, D. Recognition and processing of ubiquitin-protein conjugates by the proteasome. *Annu. Rev. Biochem.* **2009**, *78*, 477–513. [CrossRef] [PubMed]
35. Akutsu, M.; Dikic, I.; Bremm, A. Ubiquitin chain diversity at a glance. *J. Cell. Sci.* **2016**, *129*, 875–880. [CrossRef]
36. Thrower, J.S.; Hoffman, L.; Rechsteiner, M.; Pickart, C.M. Recognition of the polyubiquitin proteolytic signal. *EMBO J.* **2000**, *19*, 94–102. [CrossRef]
37. Kawadler, H.; Yang, X. Lys63-linked polyubiquitin chains: Linking more than just ubiquitin. *Cancer Biol. Ther.* **2006**, *5*, 1273–1274. [CrossRef]
38. Chen, Z.J.; Sun, L.J. Nonproteolytic functions of ubiquitin in cell signaling. *Mol. Cell* **2009**, *33*, 275–286. [CrossRef]
39. Delboy, M.G.; Roller, D.G.; Nicola, A.V. Cellular proteasome activity facilitates Herpes simplex virus entry at a postpenetration step. *J. Virol.* **2008**, *82*, 3381–3390. [CrossRef]
40. Delboy, M.G.; Nicola, A.V. A pre-immediate-early role for tegument ICP0 in the proteasome-dependent entry of Herpes simplex virus. *J. Virol.* **2011**, *85*, 5910–5918. [CrossRef]
41. Greene, W.; Zhang, W.; He, M.; Witt, C.; Ye, F.; Gao, S.J. The ubiquitin/proteasome system mediates entry and endosomal trafficking of Kaposi's Sarcoma-associated herpesvirus in endothelial cells. *PLoS Pathog.* **2012**, *8*, e1002703. [CrossRef] [PubMed]
42. Chen, C.; Zhuang, X. Epsin 1 is a cargo-specific adaptor for the clathrin-mediated endocytosis of the influenza virus. *Proc. Natl. Acad. Sci. USA* **2008**, *105*, 11790–11795. [CrossRef] [PubMed]
43. Widjaja, I.; de Vries, E.; Tscherne, D.M.; García-Sastre, A.; Rottier, P.J.; de Haan, C.A. Inhibition of the ubiquitin-proteasome system affects influenza A virus infection at a postfusion step. *J. Virol.* **2010**, *84*, 9625–9631. [CrossRef] [PubMed]
44. Wodrich, H.; Henaff, D.; Jammar, B.; Segura-Morales, C.; Seelmeir, S.; Coux, O.; Ruzsics, Z.; Wiethoff, C.M.; Kremer, E.J. A capsid-encoded PPXY-motif facilitates adenovirus entry. *PLoS Pathog.* **2010**, *6*, e1000808. [CrossRef]
45. Nomaguchi, M.; Fujita, M.; Adachi, A. Role of HIV-1 Vpu protein for virus spread and pathogenesis. *Microbes Infect.* **2008**, *10*, 960–967. [CrossRef]
46. Ikeda, M.; Ikeda, A.; Longan, L.C.; Longnecker, R. The Epstein-Barr virus latent membrane protein 2A PY motif recruits WW domain-containing ubiquitin-protein ligases. *Virology* **2000**, *268*, 178–191. [CrossRef]
47. Ning, S.; Pagano, J.S. The A20 deubiquitinase activity negatively regulates LMP1 activation of IRF7. *J. Virol.* **2010**, *84*, 6130–6138. [CrossRef]
48. Beaudenon, S.; Huibregtse, J.M. HPV E6, E6AP and cervical cancer. *BMC Biochem.* **2008**, *9* (Suppl. 1), S4. [CrossRef]
49. Mammas, I.N.; Sourvinos, G.; Giannoudis, A.; Spandidos, D.A. Human papilloma virus (HPV) and host cellular interactions. *Pathol. Oncol. Res.* **2008**, *14*, 345–354. [CrossRef]
50. Huh, K.; Zhou, X.; Hayakawa, H.; Cho, J.Y.; Libermann, T.A.; Jin, J.; Harper, J.W.; Munger, K. Human papillomavirus type 16 E7 oncoprotein associates with the cullin 2 ubiquitin ligase complex, which contributes to degradation of the retinoblastoma tumor suppressor. *J. Virol.* **2007**, *81*, 9737–9747. [CrossRef]
51. Park, S.W.; Han, M.G.; Park, C.; Ju, Y.R.; Ahn, B.Y.; Ryou, J. Hantaan virus nucleocapsid protein stimulates MDM2-dependent p53 degradation. *J. Gen. Virol.* **2013**, *94*, 2424–2428. [CrossRef] [PubMed]
52. Garrus, J.E.; von Schwedler, U.K.; Pornillos, O.W.; Morham, S.G.; Zavitz, K.H.; Wang, H.E.; Wettstein, D.A.; Stray, K.M.; Côté, M.; Rich, R.L.; et al. Tsg101 and the vacuolar protein sorting pathway are essential for HIV-1 budding. *Cell* **2001**, *107*, 55–65. [CrossRef]
53. Demirov, D.G.; Ono, A.; Orenstein, J.M.; Freed, E.O. Overexpression of the N-terminal domain of TSG101 inhibits HIV-1 budding by blocking late domain function. *Proc. Natl. Acad. Sci. USA* **2002**, *99*, 955–960. [CrossRef] [PubMed]
54. Gack, M.U.; Albrecht, R.A.; Urano, T.; Inn, K.S.; Huang, I.C.; Carnero, E.; Farzan, M.; Inoue, S.; Jung, J.U.; García-Sastre, A. Influenza A virus NS1 targets the ubiquitin ligase TRIM25 to evade recognition by the host viral RNA sensor RIG-I. *Cell Host Microbe* **2009**, *5*, 439–449. [CrossRef]
55. Rajsbaum, R.; Albrecht, R.A.; Wang, M.K.; Maharaj, N.P.; Versteeg, G.A.; Nistal-Villán, E.; García-Sastre, A.; Gack, M.U. Species-specific inhibition of RIG-I ubiquitination and IFN induction by the influenza A virus NS1 protein. *PLoS Pathog.* **2012**, *8*, e1003059. [CrossRef]

56. Oshiumi, H.; Miyashita, M.; Matsumoto, M.; Seya, T. A distinct role of Riplet-mediated K63-Linked polyubiquitination of the RIG-I repressor domain in human antiviral innate immune responses. *PLoS Pathog.* **2013**, *9*, e1003533. [CrossRef]
57. Savellini, G.G.; Anichini, G.; Gandolfo, C.; Prathyumnan, S.; Cusi, M.G. Toscana virus non-structural protein NSs acts as E3 ubiquitin ligase promoting RIG-I degradation. *PLoS Pathog.* **2019**, *15*, e1008186. [CrossRef]
58. Savellini, G.G.; Gandolfo, C.; Cusi, M.G. Truncation of the C-terminal region of Toscana Virus NSs protein is critical for interferon-β antagonism and protein stability. *Virology* **2015**, *486*, 255–262. [CrossRef]
59. Kainulainen, M.; Lau, S.; Samuel, C.E.; Hornung, V.; Weber, F. NSs Virulence Factor of Rift Valley Fever Virus Engages the F-Box Proteins FBXW11 and β-TRCP1 To Degrade the Antiviral Protein Kinase PKR. *J. Virol.* **2016**, *90*, 6140–6147. [CrossRef]
60. Mudhasani, R.; Tran, J.P.; Retterer, C.; Kota, K.P.; Whitehouse, C.A.; Bavari, S. Protein Kinase R Degradation Is Essential for Rift Valley Fever Virus Infection and Is Regulated by SKP1-CUL1-F-box (SCF)FBXW11-NSs E3 Ligase. *PLoS Pathog.* **2016**, *12*, e1005437. [CrossRef]
61. Kainulainen, M.; Habjan, M.; Hubel, P.; Busch, L.; Lau, S.; Colinge, J.; Superti-Furga, G.; Pichlmair, A.; Weber, F. Virulence factor NSs of rift valley fever virus recruits the F-box protein FBXO3 to degrade subunit p62 of general transcription factor TFIIH. *J. Virol.* **2014**, *88*, 3464–3473. [CrossRef] [PubMed]
62. van Knippenberg, I.; Fragkoudis, R.; Elliott, R.M. The transient nature of Bunyamwera orthobunyavirus NSs protein expression: Effects of increased stability of NSs protein on virus replication. *PLoS ONE* **2013**, *8*, e64137. [CrossRef] [PubMed]
63. van Knippenberg, I.; Carlton-Smith, C.; Elliott, R.M. The N-terminus of Bunyamwera orthobunyavirus NSs protein is essential for interferon antagonism. *J. Gen. Virol.* **2010**, *91*, 2002–2006. [CrossRef] [PubMed]
64. Cusi, M.G.; Savellini, G.G.; Terrosi, C.; Di Genova, G.; Valassina, M.; Valentini, M.; Bartolommei, S.; Miracco, C. Development of a mouse model for the study of Toscana virus pathogenesis. *Virology* **2005**, *333*, 66–73. [CrossRef] [PubMed]
65. Kingstone, R.E.; Chen, C.A.; Rose, J.K. Calcium phosphate transfection. *Curr. Protoc. Mol. Biol.* **2003**, *63*, 9.1.1–9.1.11. [CrossRef] [PubMed]
66. Taylor, R.T.; Best, S.M. Assessing ubiquitination of viral proteins: Lessons from flavivirus NS5. *Methods* **2011**, *55*, 166–171. [CrossRef]
67. Xu, P.; Duong, D.M.; Seyfried, N.T.; Cheng, D.; Xie, Y.; Robert, J.; Rush, J.; Hochstrasser, M.; Finley, D.; Peng, J. Quantitative proteomics reveals the function of unconventional ubiquitin chains in proteasomal degradation. *Cell* **2009**, *137*, 133–145. [CrossRef]
68. van der Lee, R.; Lang, B.; Kruse, K.; Gsponer, J.; de Groot, N.S.; Huynen, M.A.; Matouschek, A.; Fuxreiter, M.; Babu, M.M. Intrinsically disordered segments affect protein half-life in the cell and during evolution. *Cell Rep.* **2014**, *8*, 1832–1844. [CrossRef]
69. Tompa, P.; Prilusky, J.; Silman, I.; Sussman, J.L. Structural disorder serves as a weak signal for intracellular protein degradation. *Proteins* **2008**, *71*, 903–909. [CrossRef]
70. Dice, J.F. Molecular determinants of protein half-lives in eukaryotic cells. *FASEB J.* **1987**, *1*, 349–357. [CrossRef]

vaccines

MDPI

Article

Seroprevalence to Measles Virus after Vaccination or Natural Infection in an Adult Population, in Italy

Gabriele Anichini [1], Claudia Gandolfo [1], Simonetta Fabrizi [2], Giovan Battista Miceli [2], Chiara Terrosi [1], Gianni Gori Savellini [1], Shibily Prathyumnan [1], Daniela Orsi [2], Giuseppe Battista [2] and Maria Grazia Cusi [2,*]

1 Department of Medical Biotechnologies, University of Siena, Santa Maria delle Scotte Hospital, V.le Bracci, 1 53100 Siena, Italy; gabriele.anichini@student.unisi.it (G.A.); claudia.gandolfo@unisi.it (C.G.); chiara.terrosi@unisi.it (C.T.); gianni.gori@unisi.it (G.G.S.); shibilyps@gmail.com (S.P.)

2 Preventive Medicine and Health Surveillance Unit, Santa Maria delle Scotte Hospital, V.le Bracci, 1 53100 Siena, Italy; s.fabrizi@ao-siena.toscana.it (S.F.); giovanni.miceli@ao-siena.toscana.it (G.B.M.); daniela.orsi@unisi.it (D.O.); giuseppe.battista@unisi.it (G.B.)

* Correspondence: mariagrazia.cusi@unisi.it; Tel.: +39-0577-233871

Received: 23 December 2019; Accepted: 31 January 2020; Published: 3 February 2020

Abstract: An increase in measles cases worldwide, with outbreaks, has been registered in the last few years, despite the availability of a safe and highly efficacious vaccine. In addition to an inadequate vaccination coverage, even in high-income European countries studies proved that some vaccinated people were also found seronegative years after vaccination, thus increasing the number of people susceptible to measles infection. In this study, we evaluated the immunization status and the seroprevalence of measles antibodies among 1092 healthy adults, either vaccinated or naturally infected, in order to investigate the persistence of anti-measles IgG. Among subjects who received two doses of measles vaccine, the neutralizing antibody titer tended to decline over time. In addition, data collected from a neutralization assay performed on 110 healthy vaccinated subjects suggested an inverse correlation between neutralizing antibody titers and the time elapsed between the two vaccinations, with a significant decline in the neutralizing titer when the interval between the two doses was ≥11 years. On the basis of these results, monitoring the serological status of the population 10–12 years after vaccination could be important both to limit the number of people who are potentially susceptible to measles, despite the high efficacy of MMR vaccine, and to recommend a booster vaccine for the seronegatives.

Keywords: measles virus; vaccine; neutralizing antibodies; seroprevalence

1. Introduction

Measles virus (MV) is a negative single-stranded RNA virus belonging to the Morbillivirus genus, *Paramixoviridae* family [1]. It is the causative agent of a highly contagious acute infectious disease, typical of infancy, characterized by fever, skin rash, cough, coryza, conjunctivitis and a generalized immune suppression [1]. The virus is transmitted by large respiratory droplets, it spreads in the respiratory route and in regional lymph nodes, thus resulting in lymphatic and hematic dissemination with appearance of first clinical signs after 9–19 days [2]. Recovery is followed by lifelong immunity to measles. In rare cases, severe measles-associated central nervous system (CNS) complications may develop [3]. MV infection is also responsible for a transient immune suppression that may last longer than two years after infection and it leads to opportunistic infections [4] and to life-threatening complications, such as pneumonia and/or gastrointestinal disease [5,6]. Nevertheless, this disease is associated with the induction of a strong and specific life-long immune response to the virus [7].

There is no specific antiviral treatment against measles, thus the prophylactic vaccine is considered the best strategy to prevent this virus infection [8]. Furthermore, the monotypic nature of the virus and the lack of an animal reservoir make measles a considerable candidate for eradication [9]. In Italy, a single-antigen measles vaccine became commercially available in 1976 and its administration has been recommended by the Ministry of Health since 1979, with one dose for children aged 15 months. In the early 1990s, the trivalent measles-mumps-rubella (MMR) vaccine containing a live attenuated Edmonston B strain was recommended for administration at 12 months of age. Since 2003, the national vaccination schedule has recommended two doses of MMR vaccine in all Italian regions: The first at 12–15 months and the second at six years or older, only for those who had already received one dose and were older than six years at that date [10,11]. Subsequently, due to the lower MMR vaccination coverage (<90%) in Italy, especially among infants and adolescents [12], and the occurrence of a large measles outbreak in January 2017, a new law was passed and adopted in July 2017. This law extended the number of mandatory vaccines from four to ten, including MMR, administered at 13–15 months and six years [13]. Since then, the attenuated varicella strain has been included in the formulation of the vaccine. This can be administered at the same session as trivalent anti-measles-mumps-rubella plus the monovalent anti-varicella vaccine or as quadrivalent MMRV combined vaccine [14].

In spite of this, according to the latest update on measles circulation by ECDC, 29 EU/EEA Member States reported 13,331 cases of measles, from October 2018 to September 2019, 10,541 (79%) of which were laboratory-confirmed. No countries reported zero cases during the 12-month period. The highest number of cases were reported by France (2699), Italy (1845), Poland (1811), and Romania (1485), accounting for 20%, 14%, 12%, and 11% of all cases, respectively [15]. Measles outbreaks mostly occurred in unvaccinated individuals, thus a high vaccination coverage is the most important goal to prevent the disease. Epidemiologic studies have shown that the level of functional neutralizing antibodies at the time of exposure to the wild-type (WT) virus during a measles outbreak is a good correlate of protection from infection, with higher titers needed to prevent infection rather than to prevent the disease [16]. According to literature, levels of anti-measles antibodies tend to decline over the life course, as demonstrated by measuring the level of measles neutralizing antibodies in the subjects' sera at different times after vaccination [17–20]. Moreover, this phenomenon appears to occur faster following vaccination rather than after naturally acquired infection [21,22]. Thus, it is important to better understand vaccine-induced antibody persistence and how persistence patterns may influence the risk of vaccine failure. In this study, we report data concerning the seroprevalence of a healthy population sample, analyzing 1092 sera among healthy adults, the immunogenicity of the vaccine and the protective antibody levels to measles virus after vaccination or natural exposure to the virus.

2. Materials and Methods

2.1. Study Population

The participants in this observational study were students, postgraduates, medical doctorsand health care workers subjected to routine analysis for the biological risk assessment at the Center of Preventive Medicine and Health Surveillance of the University Hospital 'Santa Maria alle Scotte' in Siena between January 2018 and May 2019. Among the participants, some subjects presented their history of vaccination against measles, some had never been vaccinated and others had a history of measles infection. This research was carried out according to the principles of Helsinki declaration. Ethical approval was obtained from the local Ethical Committee for clinical trials (approval n° 11466_2017) (Comitato Etico Regione Toscana-Area Vasta Sud Est) in terms of General Data Protection and Regulation (GDPR) upon written informed consent signed by all subjects prior to participating in this study [23,24]. A total of 1092 subjects, 361 males and 731 females, (mean age 27.1 years; CI 95% 26.6–27.6) were screened for anti-measles IgG. All subjects born before 1977 declared to have contracted measles infection; the others, born later, were distinguished into three groups, according to their vaccination records: vaccinated with one or two doses and nonvaccinated (Figure 1). Lastly, among

those born after 1977, 110 sera of subjects (mean age 24.9 years; CI 95% 24.1–25.7) vaccinated with two doses of measles vaccine, either monovalent (Moraten, Istituto sieroterapico e vaccinogeno svizzero, Berna, Switzerland) or trivalent (measles, mumps and rubella (MMR) Priorix (GlaxoSmithKline, Verona, Italy) were analyzed for the titer of specific neutralizing antibodies. These titers were compared with 100 samples of subjects (mean age 48.6 years; CI 95% 46.2–51.1), who had been exposed to natural infection.

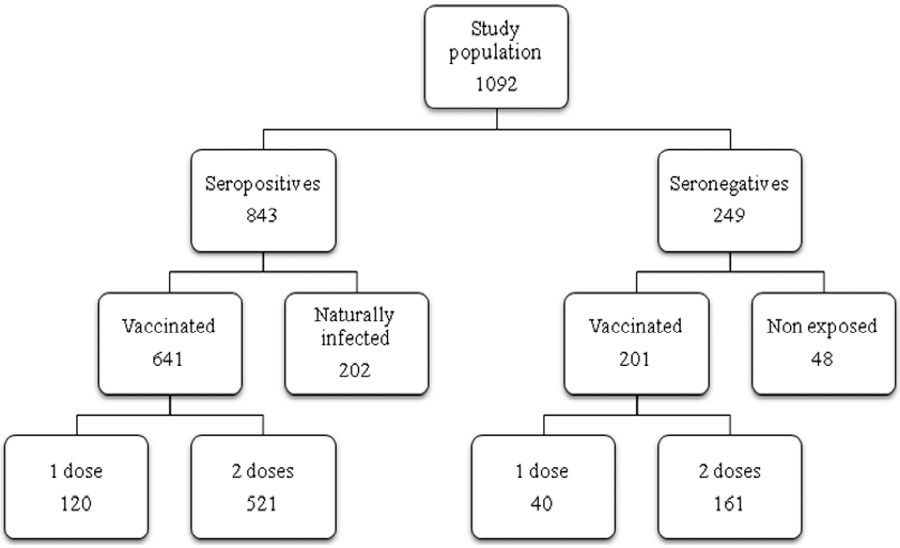

Figure 1. Flow diagram of the study population. Schematic representation of the study population enrolled in the study with the relative number of subjects in each group.

2.2. Cells and Viruses

Vero cells (ATCC CCL-81) were grown as a monolayer in Dulbecco's modified Eagle's medium (DMEM) (Euroclone, Milan, Italy) supplemented with 100 U/mL penicillin/streptomycin (Euroclone) and 5% heat-inactivated fetal calf serum (FCS) (Euroclone) at 37 °C in a humidified 5% CO2 atmosphere. Measles virus Edmonston B strain (ATCC VR-24) was propagated on Vero cells until a cytopathic effect (CPE) appeared. Viral stocks were prepared, titrated on Vero cells, and stored at −80 °C for long term.

2.3. Measles IgM/IgG Antibody Detection

Sera obtained from subjects were analyzed for the presence of measles specific IgM/IgG antibodies to the recombinant MV nucleoprotein, by LIAISON XL (Liaison Measles IgG/IgM, DiaSorin, Saluggia, Italy), a chemiluminescence analyzer using paramagnetic solid phase microparticles. Threshold IgG values regarded as positive immune status were >16.5 AU (Arbitrary Unit)/mL, with detection limit of 13.5 AU/mL; while IgM threshold for the presence of measles infection was >1.1 AU/mL, with detection limit at 0.9 AU/mL.

2.4. Measles Microneutralization Test

The measles virus neutralization assay was carried out on Vero cells in a 96-well microplate. Twenty-five microliters of 2-fold serial dilutions (1:8 to 1:1024) of vaccinated or naturally infected people sera were added to an equal volume of the Edmonston B strain MV containing 250 $TCID_{50}$ and incubated for 90 min at 37 °C. Finally, 50 µL of Vero cells suspension (2×10^5 cells/mL) prepared in a complete DMEM (Euroclone) medium were added to each well. Five days after incubation at 37 °C, the cultures were microscopically examined for the presence of CPE. The 50% end point titer of the serum neutralizing titer was calculated using the Reed and Muench method [25]. Serum samples with neutralizing titers of less than eight were considered negative [26]. A positive and negative control serum (Liaison Measles IgG Ctr) were included in each assay.

2.5. Statistical Analysis

Seroprevalence was calculated as the ratio between the number of positive test results and the number of performed tests. Geometric mean titers (GMTs), obtained by the neutralization assay, were calculated as log-transformed reciprocal titers and reported as back-transformed for each subclass. Differences between vaccination status, sex, time elapsed between dose one and two of the vaccine and time elapsed since the second dose of vaccine, and the last serological measles investigation, were evaluated. Furthermore, statistical significances were assessed with the two-tailed chi-squared test. Results were considered statistically significant at $p < 0.05$. Spearman's rank correlation coefficient was used to assess correlations of log-transformed continuous variables by the group.

3. Results

3.1. Study Group

We enrolled 1092 subjects, who were screened for specific anti-measles IgG. Out of 1092 subjects, 843 (77.2%) were seropositive and 249 (22.8%) seronegative to the measles virus (Figure 1). The mean age of vaccinated subjects was 24.9 years (CI 95% CI 24.1–25.7). Among the nonvaccinated subjects, seropositives (naturally infected) and seronegatives (never exposed to the virus) had, respectively, a mean age of 39.0 years (95% CI 37.1–40.9) and 26.1 years (95% CI 24.6–27.4) ($p < 0.00001$). Vaccination coverage with one or two doses of vaccine of this population sample was estimated 77.1% (842/1092), lower than the 90%–95% threshold required for achieving herd immunity. The enrolled people were lately divided according to their vaccination history (one or two doses) or nonvaccinated (naturally infected or nonexposed to the virus) (Figure 1). Surprisingly, among those who received two doses of vaccine (as recommended by the Italian Ministry of Health since 2003), 161 out of 682 subjects (23.6%) were seronegative after vaccination. Except for one subject, who had not responded to the trivalent vaccine, the others were seropositive to mumps and rubella viruses, indicating that these individuals had responded to the vaccine. Surprisingly, this percentage was similar to that observed for vaccines with only one dose (40/160, 25%) (Figure 1). No significant differences in the seroprevalence rates were found in all the groups with respect to gender ($p > 0.05$).

3.2. Age-Specific IgG prevalence

In order to analyze the IgG prevalence trend, the enrolled subjects have also been divided into groups according to their age, regardless of their vaccination status. There was no significant difference in the percentage of seronegatives ($p > 0.05$) among the groups aged 19–42 (Figure 2). On the contrary, a consistent increase of seropositives, up to almost 100%, was observed in subjects over 43 years old, therefore born before the introduction of measles vaccine in Italy. As far as seronegativity rates are concerned, some differences among the age groups are also worthy of being mentioned. All negative subjects in the 37–42 age group had never been exposed to the virus; most of the subjects aged 31–36 had been vaccinated with just one dose, while the majority of the 19–24 age group had been vaccinated with two doses. Regarding the group aged 25–30, the percentage of seronegatives was equally distributed between those vaccinated with one or two doses of vaccine.

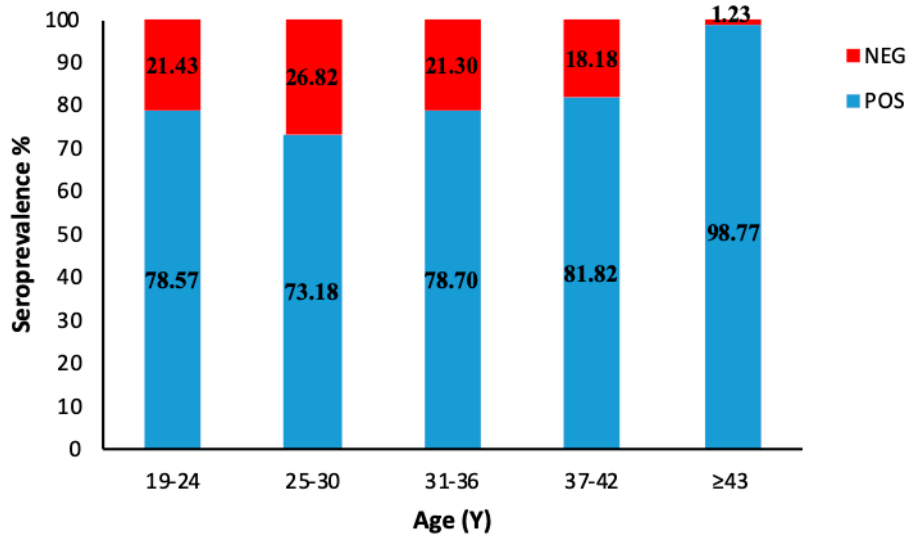

Figure 2. Age-specific measles IgG prevalence categorized into different age groups. Subjects over 43 years old were included into the same group.

3.3. Decline of Humoral Response to Measles after Vaccination

Figure 3 reports the seroprevalence analyzed during the period of 8–18 years after two doses of vaccination in 562 subjects within the same range of age (mean age 24.4 years; CI 95% 24.2–24.6). Although the number of tested subjects decreased over time, it was evident that an increasing number of vaccinees became seronegative in parallel with the increase of time post-vaccination. We noticed a higher percentage of seronegative subjects between 13 and 16 years after vaccination, suggesting that the decrease of the humoral response could be due to a measles-specific antibody titer after vaccination lower than after natural infection. However, this hypothesis could not be endorsed since the antibody titers after vaccine administration were not available. Extending the monitoring time, the trend was similar, although the serological profile appeared variable, probably due to the limited number of tested samples. No specific IgM were detected in any tested sample.

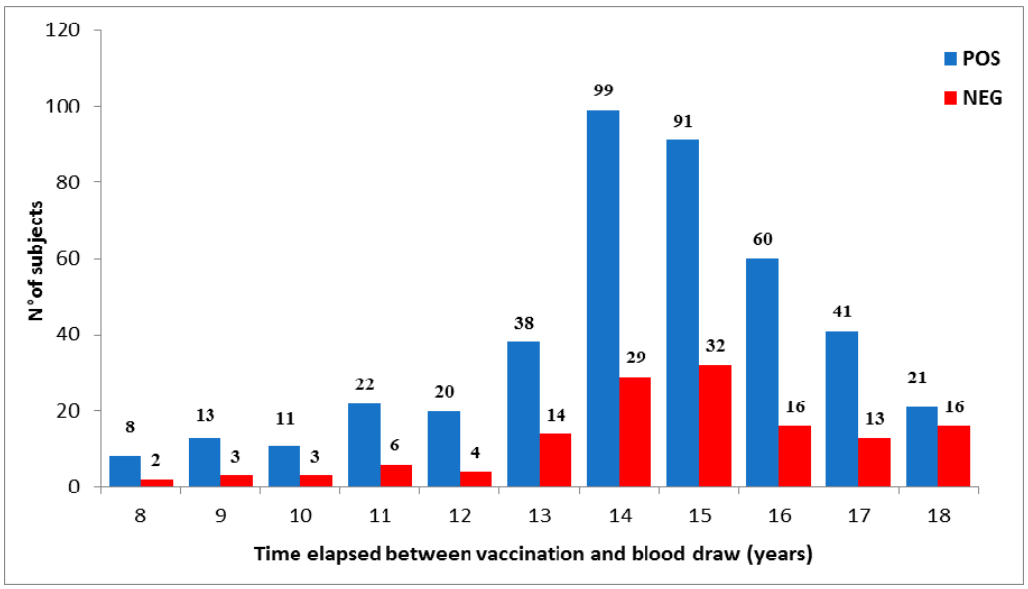

Figure 3. Seroprevalence of measles antibodies after vaccination over-time. Antibody response in vaccinees was analyzed 8–18 years after complete vaccination. The number of seropositive and seronegative subjects was plotted.

3.4. Evaluation of Neutralizing Ab Titers

One hundred and ten sera of seropositive subjects who had received two doses of the measles vaccine and 100 sera of randomly selected subjects who had contracted a natural infection were tested for the presence of neutralizing antibodies against the virus. With regard to naturally infected subjects, the GMT of the tested samples was 570.6 and no substantial differences were found between males and females ($p = 0.46$). Among those vaccinated with two doses of measles vaccine, the GMT was 172.1, which was considerably lower than that recorded in naturally infected subjects ($p < 0.00001$). Moreover, no gender related significant differences in GMT were found during this analysis ($p = 0.38$) (Figure 4).

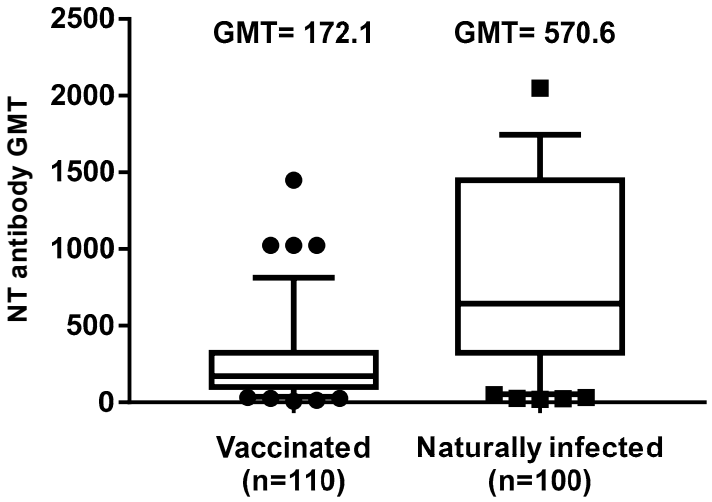

Figure 4. Differences in neutralizing antibody titers between subjects vaccinated with two doses of measles vaccine and naturally infected subjects are shown. The whiskers represent the values from the 5th to the 95th percentiles; the median, the 25th and 75th percentiles are depicted by the horizontal lines in the boxes. Individual data points are shown; outlier values are shown as black circles or squares. GMTs are shown above the population columns. *p*-value of the GMT between the two groups is ≤0.00001.

3.5. Decline of Neutralizing Ab Titers

Since previous studies reported that the measles protective antibody titer was decreasing over time after the administration of the second dose of MMR vaccine [17–21], our aim was to evaluate this phenomenon in our cohort. The vaccinated subjects (110) were divided into three groups, on the basis of the time elapsed since the administration of the second dose of vaccine: eleven years (35 subjects), 12–14 years (39 subjects) and ≥15 years (36 subjects). Results showed a significant decrease in GMT between the groups tested at 1–11 and 12–14 years after vaccination (232.4 vs. 147.4; $p < 0.05$) (Figure 5), thus confirming a possible decline of the protective antibody response against measles during their lifetime. No further difference was evidenced after ≥15 years since vaccination.

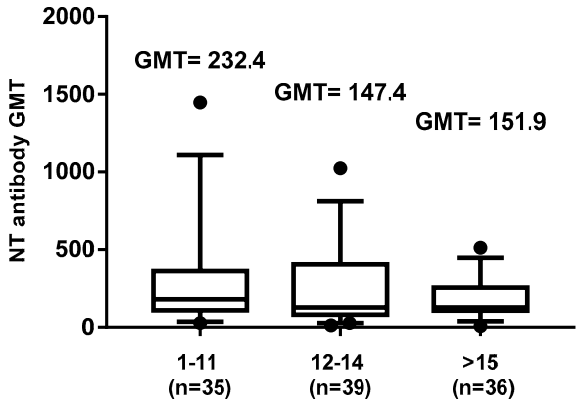

Figure 5. Time elapsed between the second dose of vaccine and the serological test (years). Effects of negative correlation based on the time elapsed between the second dose of measles vaccine and the last measles investigation test on neutralizing antibody response. The whiskers represent the values from the 5th to the 95th percentiles; the median, the 25th and 75th percentiles are depicted by the horizontal lines in the boxes. Individual data points are shown; outlier values are shown as black circles. GMTs are shown above the population columns. *P*-value of the GMT between the first (1–11) and second (12–14) group is <0.05.

Subjects vaccinated with two doses were further studied on the basis of the time elapsed between the first and second dose of vaccine: 1–6 y (49 subjects), 7–10 y (34 subjects), and ≥11y (27 subjects). Spearman's rank correlation analysis showed a statistically significant ($p = 0.004$) inverse correlation ($r = -0.270$), between neutralization titers of subject sera and time elapsed between the two-dose vaccination. Indeed, the GMT comparison among the three groups evidenced a decrease of neutralizing GMTs, 215.5 in the 1–6 y, 165.6 in the 7–10 y, and 120.1 in the ≥11 y groups ($p < 0.05$) (Figure 6), particularly relevant in subjects receiving the second dose of vaccine over 10–11 years since the first vaccination ($p < 0.05$). No significant differences related to the gender were found in this analysis either.

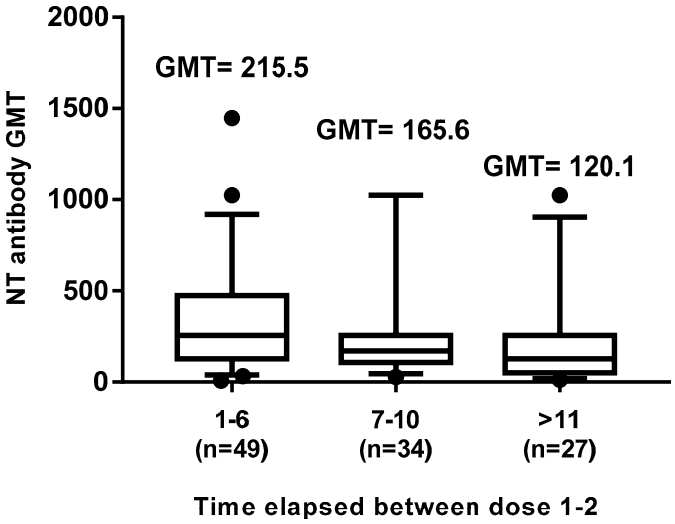

Figure 6. Effect of time elapsed between the two doses of measles vaccine on the neutralizing antibody response. The whiskers represent the values from the 5th to the 95th percentiles; the median, the 25th and 75th percentiles are depicted by the horizontal lines in the boxes. Individual data points are shown; outlier values are shown as black circles or squares. GMTs are shown above the population columns. The difference in GMTs between the first (1–6) and the third (≥11) group is statistically significant ($p \leq 0.05$).

3.6. Neutralizing Antibody GMT in Natural Infected Subjects

No GMT differences were found in serum samples of naturally infected subjects during their childhood, either in those born before (GMT 571.7; mean age 54.8) or after (GMT 552.9; mean age 31.0) the introduction of measles vaccine (Figure 7). These data confirmed a more pronounced tendency of the protective immune response to wane in vaccinated people than in naturally infected people.

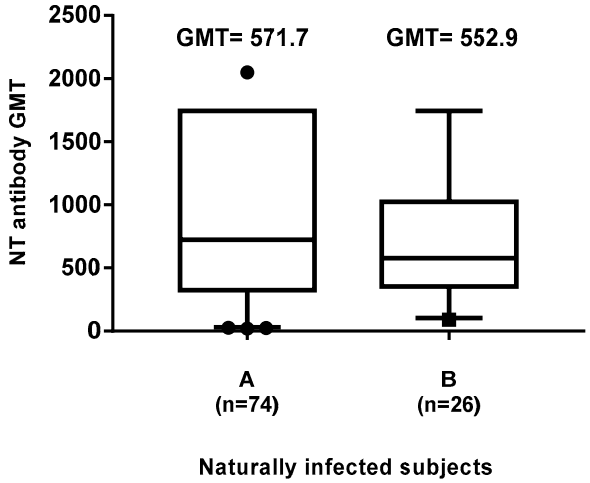

Figure 7. Differences in neutralizing antibody titers in naturally infected subjects born before (A) and after (B) 1977 (one year after the introduction of measles vaccine in Italy). The whiskers represent the values from the 5th to the 95th percentiles; the median, the 25th and 75th percentiles are depicted by the horizontal lines in the boxes. Individual data points are shown; outlier values are shown as black circles or squares. GMTs are shown above the population columns. Difference in GMT between the two groups is not significant ($p > 0.05$).

4. Discussion

Measles morbidity and mortality have been reduced since the implementation of enhanced vaccination strategies [27], and in several countries the interruption of indigenous transmission of measles disease has been reported [28]. Unfortunately, the measles disease continues to be difficult to eradicate, especially in European countries where recurrent outbreaks have been described [29]. In Italy, although a significant reduction of measles infection has been obtained since the introduction of the measles vaccine in 1976, the goal of measles eradication fixed by WHO Europe has still not been met. A new law, adopted in Italy in July 2017 [13], extended the number of mandatory vaccines from four to 10 vaccines for those aged 0–16. This law allowed the vaccine coverage for MMR vaccine to increase up to 94.1% (range 82.2–97.5) but still with geographical variations throughout the country [30]. This program aimed at preventing widespread measles transmission [31], by inducing a specific humoral response in the community, which is a good indicator of protection from infection.

In this study, we evaluated the immunization status and the seroprevalence of measles antibodies among a healthy adult population after vaccination or natural infection. In particular, the aim of this study was to investigate the persistence of anti-measles IgG among vaccinated and naturally infected people. Collected data showed that, out of the 1092 enrolled subjects, 682 (62.45%) had received two doses of measles vaccine (monovalent and/or MMR) and among these, only 24 subjects received as first dose the monovalent vaccine, since this was replaced in the early 1990s by the combined measles–mumps–rubella (MMR). We noted that 23% of the subjects who received two doses of measles vaccine did not show IgG response, similarly to those receiving only one dose of vaccine (25%) (Figure 1). This percentage appeared higher than that reported by other authors [17,20,32,33], thus, it is advisable to monitor the immune status of vaccines 10–15 years since vaccination, in order to evaluate the immune protection against measles and, eventually, implement a possible prophylactic

measure. On the other hand, a long-term high rate of seropositivity persisted after natural infection; indeed, subjects enrolled in this study who reported measles infection history were all seropositive. Therefore, we evaluated the presence of the neutralizing antibody response to the virus in naturally infected subjects and in those vaccinated with two doses. The geometric mean titer to measles was high (GMT 552.9) in naturally infected people, versus a GMT of 172.1 in vaccines of the same age cohort, indicating that the antibody titer decline was more evident in the vaccinated people, probably because the starting antibody titer after vaccination was lower than that induced after natural infection [34]. This finding is also supported by the observation that a measles virus antibody titer decrease has been revealed in source plasma donors after the introduction of measles vaccination in the United States [35], resulting in a high level of immunity and limited spread of the virus, but lower antibody level in the population. Indeed, in this study, the neutralizing antibody titer inversely correlated with the time elapsed between the second dose of vaccine and the blood drawn. This trend was confirmed ($r = -0.11$) by a gradual decrease of GMT titers (Figure 4), concomitant with the increase of years spent since vaccination, particularly over 12–14 years (GMT 232.4 vs. 147.4). Finally, a new interesting factor considered in this analysis was that most of the subjects had been vaccinated at different lifetimes with two doses, because of the change of the national vaccination schedule in 2003. Therefore, this parameter was analyzed to understand whether the interval of time elapsed between the two doses of vaccine could influence the immune response. It is known that schedules which have longer intervals between vaccine doses usually lead to higher immune responses [36–38]. On the contrary, our results, obtained by the neutralization assay on serum samples of subjects vaccinated with two doses (Figure 5), showed a different picture. An inverse correlation between neutralizing titer and time elapsed between the two vaccinations was evidenced ($r = -0.27$) with a significant decline of the GMT when the interval was ≥11 years in comparison to that observed within the 1–6 years interval ($p = 0.02$). The result could be very useful for the formulation of the vaccination schedule, because this finding is not valid for all vaccinations and represents a further variable factor to be considered when new vaccinations are requested. We did not find the gender factor as a variable for the immune response to measles vaccination, since no significant difference was recorded. Nowadays, measles can be easily prevented through a two-dose vaccination; however, the estimated rate of antibody decline along the time upon vaccination might represent a factor to be taken into account to limit the number of people susceptible to measles infection in the future. In this work, we only based our study on the humoral response to measles, without considering the role of cell-mediated immunity for the induction of protective immunity [39], which might be present and re-stimulated in a subject who does not apparently reveal a specific antibody response. The above discussed data suggest that there is still a small nonimmunized portion of adults, thus it is necessary to continue the monitoring of the level of protection in the population in order to limit the endemic circulation and outbreaks of measles. Finally, it is interesting to examine the immune response in depth and in its entirety and evaluate the possibility of a booster vaccination, reassessing the multiple factors that can affect and improve the immunogenicity and efficacy of the vaccine.

5. Conclusions

Although MMR vaccine is very efficacious to induce a protective response against measles, considering that a physiological decline of the humoral response has been revealed in some studies [35], it could be important to monitor the population 10–15 years after vaccination, in order to revaccinate the seronegatives. However, since booster revaccination might not induce a sustainable increase of MV antibodies [40], it could be advisable to implement the prophylaxis with alternative vaccines that could obviate this possibility.

Author Contributions: Conceptualization, M.G.C. and G.B.; methodology, C.T. and S.P.; software, D.O.; validation, G.B.M., G.G.S., and C.G.; formal analysis, G.A.; investigation, C.G. and S.F.; data curation, G.A.; writing—original draft preparation, G.A.; writing—review and editing, G.A. and M.G.C.; supervision, M.G.C. All authors have read and agreed to the published version of the manuscript.

Funding: This research received no external funding.

Conflicts of Interest: The authors declare no conflict of interest.

References

1. Griffin, D.E. Measles virus. In *Fields Virology*; Knipe, D.M., Howley, P.M., Eds.; Wolters Kluwer | Lippincott Williams & Wilkins: Philadelphia, PA, USA, 2013; Volume 6, pp. 1042–1069.
2. de Vries, R.D.; Duprex, W.P.; de Swart, R.L. Morbillivirus infections: An introduction. *Viruses* **2015**, *7*, 699–706. [CrossRef] [PubMed]
3. Buchanan, R.; Bonthius, D.J. Measles virus and associated central nervous system sequelae. *Semin. Pediatr. Neurol.* **2012**, *19*, 107–114. [CrossRef] [PubMed]
4. Mina, M.J.; Metcalf, C.J.; de Swart, R.L.; Osterhaus, A.D.; Grenfell, B.T. Long-term measles-induced immunomodulation increases overall childhood infectious disease mortality. *Science* **2015**, *348*, 694–699. [CrossRef] [PubMed]
5. de Vries, R.D.; McQuaid, S.; van Amerongen, G.; Yüksel, S.; Verburgh, R.J.; Osterhaus, A.D.; Duprex, W.P.; de Swart, R.L. Measles Immune Suppression: Lessons from the Macaque Model. *PLoS Pathog.* **2012**, *8*. [CrossRef] [PubMed]
6. de Vries, R.D.; de Swart, R.L.; Lamouille, B.; Astier, A.; Rabourdin-Combe, C. Measles Immune Suppression: Functional Impairment or Numbers Game? *PLoS Pathog.* **2014**, *10*, e1004482. [CrossRef] [PubMed]
7. Laksono, B.M.; de Vries, R.D.; McQuaid, S.; Duprex, W.P.; de Swart, R.L. Measles Virus Host Invasion and Pathogenesis. *Viruses* **2016**, *8*. [CrossRef] [PubMed]
8. Uzicanin, A.; Zimmerman, L. Field effectiveness of live attenuated measles-containing vaccines: A review of published literature. *J. Infect. Dis.* **2011**, *204*, 133–148. [CrossRef]
9. Rota, P.A.; Moss, W.J.; Takeda, M.; de Swart, R.L.; Thompson, K.M.; Goodson, J.L. Measles. *Nat. Rev. Dis. Primers* **2016**, *2*. [CrossRef]
10. Italian Ministry of Health. Circolare n.12 del 13 luglio 1999. Controllo ed eliminazione di morbillo, rosolia e parotite attraverso la vaccinazione. Available online: http://www.salute.gov.it/imgs/C_17_normativa_86_allegato.pdf (accessed on 13 July 1999).
11. Italian Ministry of Health. Piano nazionale per l'eliminazione del morbillo e della rosolia congenita. 2003. Available online: http://www.salute.gov.it/imgs/C_17_pubblicazioni_730_allegato.pdf (accessed on 13 November 2003).
12. Andrianou, X.D.; Del Manso, M.; Bella, A.; Vescio, M.F.; Baggieri, M.; Rota, M.C.; Pezzotti, P.; Filia, A. Spatiotemporal distribution and determinants of measles incidence during a large outbreak, Italy, September 2016 to July 2018. *Euro. Surveill.* **2019**, *24*. [CrossRef]
13. Italian Ministry of Health. Decree Law 7 June 2017, n. 73, Urgent Provisions on Vaccination Prevention, as Amended by the Conversion Law. Available online: http://www.trovanorme.salute.gov.it/norme/dettaglioAtto?id=60201 (accessed on 31 July 2017).
14. Cocchio, S.; Zanoni, G.; Opri, R.; Russo, F.; Baldo, V.; Collaborative group. A postmarket safety comparison of 2 vaccination strategies for measles, mumps, rubella and varicella in Italy. *Hum. Vaccin. Immunother.* **2016**, *12*, 651–654. [CrossRef]
15. European Centre for Disease Prevention and Control. *Monthly Measles and Rubella Monitoring Report*; ECDC: Stockholm, Sweden, 2019; Available online: https://www.ecdc.europa.eu/en/publications-data/monthly-measles-and-rubella-monitoring-report-september-2019 (accessed on 13 September 2019).
16. Yeung, L.F.; Lurie, P.; Dayan, G.; Eduardo, E.; Britz, P.H.; Redd, S.B.; Papania, M.J.; Seward, J.F. A limited measles outbreak in a highly vaccinated US boarding school. *Pediatrics* **2005**, *116*, 1287–1291. [CrossRef] [PubMed]
17. Kennedy, R.B.; Ovsyannikova, I.G.; Thomas, A.; Larrabee, B.R.; Rubin, S.; Poland, G.A. Differential durability of immune responses to measles and mumps following MMR vaccination. *Vaccine* **2019**, *37*, 1775–1784. [CrossRef] [PubMed]
18. Carryn, S.; Feyssaguet, M.; Povey, M.; Di Paolo, E. Long-term immunogenicity of measles, mumps and rubella-containing vaccines in healthy young children: A 10-year follow-up. *Vaccine* **2019**, *37*, 5323–5331. [CrossRef] [PubMed]

19. Davidkin, I.; Jokinen, S.; Broman, M.; Leinikki, P.; Peltola, H. Persistence of measles, mumps, and rubella antibodies in an MMR-vaccinated cohort: A 20-year follow-up. *J. Infect. Dis.* **2008**, *197*, 950–956. [CrossRef] [PubMed]
20. Seagle, E.E.; Bednarczyk, R.A.; Hill, T.; Fiebelkorn, A.P.; Hickman, C.J.; Icenogle, J.P.; Belongia, E.A.; McLean, H.Q. Measles, mumps, and rubella antibody patterns of persistence and rate of decline following the second dose of the MMR vaccine. *Vaccine* **2018**, *36*, 818–826. [CrossRef] [PubMed]
21. Gonçalves, G.; Frade, J.; Nunes, C.; Mesquita, J.R.; Nascimento, M.S. Persistence of measles antibodies, following changes in the recommended age for the second dose of MMR-vaccine in Portugal. *Vaccine* **2015**, *33*, 5057–5063. [CrossRef]
22. LeBaron, C.W.; Beeler, J.; Sullivan, B.J.; Forghani, B.; Bi, D.; Beck, C.; Audet, S.; Gargiullo, P. Persistence of measles antibodies after 2 doses of measles vaccine in a post-elimination environment. *Arch. Pediatr. Adolesc. Med.* **2007**, *161*, 294–301. [CrossRef]
23. Authorisation no. 9/2014—General Authorisation to Process Personal Data for Scientific Research Purposes. Available online: https://www.gazzettaufficiale.it/atto/serie_generale/caricaDettaglioAtto/originario?atto.dataPbblicazioneGazzetta=2014-12-30&atto.codiceRedazionale=14A09916&elenco30giorni=true (accessed on 30 December 2014).
24. Law Decree 22 December 2017, No. 219, published in the Official Gazette No. 12 of 16 January 2018. Available online: https://www.gazzettaufficiale.it/eli/gu/2018/01/16/12/sg/pdf (accessed on 16 January 2016).
25. Reed, L.J.; Muench, H. A simple method of estimating fifty per cent endpoints. *Am. J. Hyg.* **1938**, *27*, 493–497.
26. Pacenti, M.; Maione, N.; Lavezzo, E.; Franchin, E.; Dal Bello, F.; Gottardello, L.; Barzon, L. Measles Virus Infection and Immunity in a Suboptimal Vaccination Coverage Setting. *Vaccines* **2019**, *7*, 199. [CrossRef]
27. Patel, M.K.; Dumolard, L.; Nedelec, Y.; Sodha, S.V.; Steulet, C.; Gacic-Dobo, M.; Kretsinger, K.; McFarland, J.; Rota, P.A.; Goodson, J.L. Progress Toward Regional Measles Elimination—Worldwide, 2000–2018. *MMWR Morb. Mortal. Wkly. Rep.* **2019**, *68*, 1105–1111. [CrossRef]
28. World Health Organization. Measles Cases Hit Record High in the European Region. 2018. Available online: http://www.euro.who.int/en/media-centre/sections/press-releases/2018/measles-cases-hit-record-high-in-the-european-region (accessed on 20 August 2018).
29. World Health Organization. 8th Meeting of the European Regional Verification Commission for Measles and Rubella Elimination (RVC). Available online: http://www.euro.who.int/en/health-topics/communicable-diseases/measles-and-rubella/publications/2019/8th-meeting-of-the-european-regional-verification-commission-for-measles-and-rubella-elimination-rvc-2019 (accessed on 12 June 2019).
30. D'Ancona, F.; D'Amario, C.; Maraglino, F.; Rezza, G.; Iannazzo, S. The law on compulsory vaccination in Italy: An update 2 years after the introduction. *Euro. Surveill.* **2019**, *24*. [CrossRef] [PubMed]
31. McLean, H.Q.; Fiebelkorn, A.P.; Temte, J.L.; Wallace, G.S. Centers for Disease Control and Prevention. Prevention of measles, rubella, congenital rubella syndrome, and mumps, 2013: Summary recommendations of the Advisory Committee on Immunization Practices (ACIP). *MMWR Recomm. Rep.* **2013**, *62*, 1–34. [PubMed]
32. Bianchi, F.P.; Stefanizzi, P.; De Nitto, S.; Larocca, A.M.V.; Germinario, C.; Tafuri, S. Long-term immunogenicity of Measles vaccine: An Italian retrospective cohort study. *J. Infect. Dis.* **2019**. [CrossRef] [PubMed]
33. Smetana, J.; Chlibek, R.; Hanovcova, I.; Sosovickova, R.; Smetanova, L.; Gal, P.; Dite, P. Decreasing Seroprevalence of Measles Antibodies after Vaccination—Possible Gap in Measles Protection in Adults in the Czech Republic. *PLoS ONE* **2017**, *12*, e0170257. [CrossRef]
34. Christenson, B.; Böttiger, M. Measles antibody: Comparison of long-term vaccination titres, early vaccination titres and naturally acquired immunity to and booster effects on the measles virus. *Vaccine* **1994**, *12*, 129–133. [CrossRef]
35. Modrof, J.; Tille, B.; Farcet, M.R.; McVey, J.; Schreiner, J.A.; Borders, C.M.; Gudino, M.; Fitzgerald, P.; Simon, T.L.; Kreil, T.R. Measles Virus Neutralizing Antibodies in Intravenous Immunoglobulins: Is an Increase by Revaccination of Plasma Donors Possible? *J. Infect. Dis.* **2017**, *216*, 977–980. [CrossRef]
36. Rümke, H.C.; Loch, H.P.; Hoppenbrouwers, K.; Vandermeulen, C.; Malfroot, A.; Helm, K.; Douha, M.; Willems, P. Immunogenicity and safety of a measles-mumps-rubella-varicella vaccine following a 4-week or a 12-month interval between two doses. *Vaccine* **2011**, *29*, 3842–3849. [CrossRef]

37. Middleman, A.B.; Kozinetz, C.A.; Robertson, L.M.; DuRant, R.H.; Emans, S.J. The effect of late doses on the achievement of seroprotection and antibody titer levels with hepatitis b immunization among adolescents. *Pediatrics* **2001**, *107*, 1065–1069. [CrossRef]
38. Sabidó, M.; Gavaldà, L.; Olona, N.; Ramon, J.M. Timing of hepatitis B vaccination: Its effect on vaccine response in health care workers. *Vaccine* **2007**, *25*, 7568–7572. [CrossRef]
39. Griffin, D.E. The Immune Response in Measles: Virus Control, Clearance and Protective Immunity. *Viruses* **2016**, *8*, 282. [CrossRef]
40. Fiebelkorn, A.P.; Coleman, L.A.; Belongia, E.A.; Freeman, S.K.; York, D.; Bi, D.; Kulkarni, A.; Audet, S.; Mercader, S.; McGrew, M.; et al. Measles Virus Neutralizing Antibody Response, Cell-Mediated Immunity, and Immunoglobulin G Antibody Avidity Before and After Receipt of a Third Dose of Measles, Mumps, and Rubella Vaccine in Young Adults. *J. Infect. Dis.* **2016**, *213*, 1115–1123. [CrossRef]

Received: 25 August 2020 | Revised: 9 November 2020 | Accepted: 5 January 2021

DOI: 10.1002/jmv.26789

SHORT COMMUNICATION

JOURNAL OF MEDICAL VIROLOGY WILEY

Antibody response to SARS-CoV-2 in infected patients with different clinical outcome

Gabriele Anichini[1] | Claudia Gandolfo[1,2] | Chiara Terrosi[1] | Simonetta Fabrizi[3] | Giovanni Battista Miceli[3] | Gianni Gori Savellini[1] | Shibily Prathyumnan[1] | Federico Franchi[4] | Maria Grazia Cusi[1,2]

[1]Virology Unit, Department of Medical Biotechnologies, University of Siena, Siena, Tuscany, Italy

[2]Microbiology and Virology Unit, Santa Maria alle Scotte University Hospital, Siena, Tuscany, Italy

[3]Preventive Medicine and Health Surveillance Unit, Santa Maria alle Scotte University Hospital, Siena, Tuscany, Italy

[4]Anesthesia and Intensive Care Unit, Department of Medicine, Surgery and Neuroscience, University of Siena, Siena, Tuscany, Italy

Correspondence
Maria Grazia Cusi, Virology Unit, Department of Medical Biotechnologies, University of Siena, Rettorato, via Banchi di Sotto 55, Siena 53100, Italy.
Email: mariagrazia.cusi@unisi.it

Abstract

Data regarding antibody responses to severe acute respiratory syndrome coronavirus-2 (SARS-CoV-2) in patients infected with COVID-19 are not yet available. In this study, we aimed to evaluate serum antibody responses in patients regardless of the outcome. We measured the circulating immunoglobulin G (IgG) antibody levels in 60 subjects with a certified history of SARS-CoV-2 infection by using immunoenzymatic, chemiluminescent, and Neutralization assays. Half patients had a severe infection, the other half were pauci-symptomatic. We analyzed their antibody response to see the trend of the humoral response. Our results showed a significant difference in circulating IgG level among the two groups. The neutralizing antibody response against SARS-CoV-2 was significantly higher among those who had severe disease. Furthermore, ten subjects from each group were screened twice, and a declining antibody trend was observed in pauci-symptomatic individuals. These findings provide evidence that humoral immunity against SARS-CoV-2 in pauci-symptomatic people is weak and may not be long-lasting. This may have implications for immunity strategy and prevention, since it is still not clear whether a time-dependent decrease of both circulating and neutralizing antibodies to nonprotective levels could occur in a longer time span and whether potential vaccines are able to induce a herd immunity and a durable response.

KEYWORDS
coronavirus, humoral immunity, neutralization

1 | INTRODUCTION

In December 2019, a cluster of patients with pneumonia of unknown cause was identified in Wuhan, Hubei Province, China.[1] On January 7, 2020, China centers for disease control and prevention identified a novel beta-coronavirus from lower respiratory tract samples of patients with pneumonia.[2] This novel coronavirus was later named "severe acute respiratory syndrome coronavirus-2" (SARS-CoV-2). As an emerging acute respiratory infectious disease, SARS CoV-2 primarily spreads through the respiratory tract, by droplets, respiratory secretions, and direct contact,[3] with a high human-to-human transmissibility.

Most adults or children with SARS-CoV-2 infection present mild flu-like symptoms; only a minority of patients have a severe outcome and rapidly develop acute respiratory distress syndrome, respiratory and multiple organ failure, bleeding and coagulation dysfunction, even death.[4] So far, the golden clinical diagnostic method of COVID-19 is nucleic acid detection in the nasopharyngeal swab or other lower respiratory tract samplings by real-time PCR, which can be further confirmed by next-generation sequencing.

Apart from RT-PCR testing, serological testing is an additional emerging option in COVID-19 diagnostics[5] primarily as a proof of past infection but also to support the diagnosis of suspected COVID-19 patients.[6,7] Serological assays for the evaluation of the humoral responses against Spike (S) and Nucleoprotein (N) in COVID-19 patients have been assessed, because of their high immunogenicity. Spike plays an important role in viral binding and entry into target cells,[8] while the Nucleoprotein in viral replication and assembly.[9] The kinetics of anti-N response has been described as similar to that of the anti-S, although N responses might appear earlier.[7] Anti-SARS-CoV-2 antibody titers seem to correlate with disease severity, likely reflecting higher viral replication rates and/or immune activation in patients with severe outcome.[10]

In hospitalized patients, seroconversion is typically detected between 5 and 14 days postsymptoms onset, with a median time of 5–12 days for anti-S immunoglobulin M and 14 days for immunoglobulin G (IgG), and immunoglobulin A.[6,7,11,11,12]

Neutralizing antibodies have been detected in symptomatic individuals[13,14] and their potency seems to be associated with high levels of circulating antibodies. On the other hand, despite representing the majority of SARS-CoV-2 infections, asymptomatic infections are currently poorly documented[15] and whether this immunity is mediated by neutralizing antibodies remains an outstanding question.[16]

Moreover, it is still unknown how long SARS-CoV-2 infected subjects could maintain long-term immunity and long-lasting protective antibodies, regardless of the outcome.

In this study, we measured the circulating IgG antibody levels in 60 subjects with a certified history of SARS-CoV-2 infection, by using three different assays based on different methods. Subjects were equally divided into two groups: those hospitalized, who had a severe outcome, and those pauci-symptomatic. We analyzed their antibody response to see the trend of the humoral response in individuals with different disease outcomes. Moreover, 10 patients of each group were screened a second time to evaluate the persistence of anti-SARS-CoV-2 antibody 2 months after symptoms onset.

2 | MATERIALS AND METHODS

2.1 | Study design and participants

The participants in this study were subjects with an assessed history of SARS-CoV-2 infection, between March and May 2020. Half of them were hospitalized in "Santa Maria alle Scotte" University Hospital, in Siena with a severe outcome. Instead, the other half consisted of pauci-symptomatic subjects reporting mild signs compatible with COVID-19 (fever, cough), who were placed in isolation at home. All infections were confirmed by RT-qPCR Test (nasopharyngeal swab) (in case of current infection) and/or by serological testing (for past infections). This research was carried out according to the principles of Helsinki declaration, with reference to BIOBANK-MIU-2010 document approved by the Ethics Committee with amendment No 1, on February 17, 2020 in terms of General Data Protection and Regulation. A total of 60 subjects, 30 who had a severe outcome and 30 who had mild infection were screened for the presence of anti-SARS-CoV-2 IgG antibodies. Moreover, 10 subjects selected from each group were screened twice, respectively, 30 and 60 days after symptoms, to evaluate the trend of their immune response.

2.2 | Cells and viruses

Vero E6 cells (ATCC CRL-1586^{M}) were cultured in Dulbecco's modified Eagle's medium (DMEM) (Euroclone) supplemented with 100 U/ml penicillin/streptomycin and 5% heat-inactivated fetal calf serum (Euroclone) at 37°C in a humidified 5% CO_2 atmosphere. SARS-CoV-2 virus (SARS-CoV-2/human/ITA/Siena-1/2020; GenBank: MT531537.2), isolated from a COVID infected patient in the Virology lab at "S. Maria alle Scotte" Hospital, was propagated on Vero E6 cells until a cytopathic effect (CPE) appeared. Viral stocks were prepared, titrated on Vero E6 cells, and stored at −80°C.

2.3 | SARS-CoV-2 IgG antibody detection

Subjects' sera were analyzed using two separate immunoassays. The Abbott SARS-CoV-2 IgG chemiluminescent microparticle immunoassay (CMIA) (Abbott Laboratories) was performed on an Abbott Architect i2000 (Abbott Diagnostics) according to the manufacturer's instructions. This method is a qualitative assay that detects IgG binding to an undisclosed epitope of the SARS-CoV-2 nucleocapsid protein, with the results expressed as relative light units. The other assay was the Enzywell SARS-CoV-2 IgG (DIESSE Diagnostica Senese; Monteriggioni), an enzyme-linked immunosorbent assay (ELISA)-based 96-well plate format assay which detects anti-SARS-CoV-2 IgG directed against the inactivated native virus, with the result given in optical density at 450 nm. The final interpretation of positivity was determined by the ratio above a threshold value, with positive ratio ≥1.4 or negative ratio less than 1.4 for CMIA assay, and a positive ratio ≥1.1, borderline ratio more than 0.9 and less than 1.1, or negative ratio less than 0.9 for the ELISA. Each value represented the mean of triplicate determinations.

2.4 | SARS-CoV-2 microneutralization test

SARS-CoV-2 virus neutralization assay was carried out on Vero E6 cells in a 96-well microplate. Twenty-five microliters of twofold serial dilutions (1:8–1:1024) of sera samples were added to an equal volume of the SARS-CoV-2 strain containing 150 $TCID_{50}$ and incubated for 90 min at 37°C. Finally, 50 μl of Vero E6 cells suspension (2×10^5 cells/ml) prepared in complete DMEM were added to each well. After incubation at 37°C, the cultures were daily examined at the microscope (Olympus IX51) for the presence of the CPE. The 50% end

point titer was calculated using the Reed-Muench method.[17] A positive and negative control serum were included in each assay. Geometric mean titers (GMTs) of the neutralization assay were calculated.

2.5 | Statistical analysis

The differences between age, time of blood sample collection, circulating IgG levels, and neutralizing titers were evaluated and the statistical significances assessed with two-tailed χ^2 test. Results were considered statistically significant at $p < .05$. Spearman's rank correlation coefficient was used to assess correlations of log-transformed continuous variables between the groups.

3 | RESULTS

3.1 | Study group

We analyzed sera from 60 subjects with a certified history of SARS-CoV-2 infection. Half of them had a severe infection and needed hospital recovery (H) and the other half was pauci-symptomatic with mild signs (fever and/or cough). Mean age was 66.1 years for the hospitalized (95% confidence interval [CI]: 61.0–71.0) and 45.0 for the pauci-symptomatic (95% CI: 38.6–51.4) subjects ($p < .0001$). All these subjects were screened for the presence of specific anti-SARS-CoV-2 IgG antibodies either by indirect ELISA or CMIA. Blood samples were collected about 30 days since symptoms onset (T_0). Finally, only 10 subjects of each group were screened twice (T_0 = average 30 days; T_1 = average 60 days) for the presence of both circulating IgG levels and specific anti-SARS-CoV-2 neutralizing antibodies.

3.2 | Anti-SARS-CoV-2 specific IgG

Results obtained by ELISA and CMIA, respectively, showed a significant difference in circulating IgG level among patients with a severe outcome and those with mild symptoms at T_0 ($n = 30$; 7.31 vs. 4.06; $p = .0018$ and 6.21 vs. 4.95; $p = .048$) (Table 1A).

Concerning those subjects who were screened twice ($n = 10+10$), no significant differences in IgG levels were found between the two samplings (T_0, T_1) of both the groups, using both ELISA and CMIA ($p > .05$), although a lower IgG level was noticed among those with mild symptoms (Table 1B).

On the contrary, regarding the neutralizing activity, an evident GMT difference was found between the two groups at T_0 (Figure 1); indeed, a higher titer was present in severe cases in comparison with those having mild disease (87.7 vs. 23.3; $p = .0002$). This difference was also confirmed for the patients tested twice ($p = .046$), although no significant difference in neutralizing antibody titer was found between the first and the second samples drawn 1 month apart from the same subjects, probably due to the limited number of samples (Table 1B). It is worthy mentioning that a different trend of antibody response was observed in the H group, where the tendency of neutralizing antibodies was increasing over time, while it was decreasing in pauci-symptomatic individuals.

3.3 | Neutralizing antibody titer and correlation with circulating IgG levels

We correlated the IgG titers obtained in the two serological assays, ELISA and CMIA, to the neutralizing antibody titers, to evaluate whether circulating IgG antibody levels could partly be associated to a neutralizing activity. As expected, we observed a moderate positive correlation between the neutralizing response and circulating IgG by using the whole virus proteins-based ELISA ($r = .60$) and a weak correlation using SARS CoV-2 N antigen-based CMIA ($r = .44$) (data not shown).

4 | DISCUSSION

In this study, we analyzed the titer of anti-SARS-CoV-2 IgG antibodies with three different serological assays in a cohort of subjects with a certified history of COVID-19, equally distributed with a severe outcome or mild symptoms.

Despite the limited number of subjects, the most remarkable finding of this study was the significantly lower antibody titer in patients who experienced mild infection with respect to those affected by a severe respiratory syndrome. Both ELISA and CMIA, although based on different antigens, such as all virus proteins in the first assay and the nucleoprotein in the second one, showed an antibody response, which was significantly higher in patients with severe disease than in pauci-symptomatic subjects in the same time frame since symptoms onset.

Previous studies on humoral response in SARS and MERS demonstrated that the humoral response could wane over time.[18,19] We do not know how long this immunity could last in individuals affected by COVID-19.[20] However, although the decay of total specific IgG was similar in both the groups, we noticed that the neutralizing antibodies, representing the protective response, only raised in severe cases 2 months after symptoms onset. On the contrary, the neutralizing response was very low in pauci-symptomatic individuals (GMT: 29.2) with an evident decrease after 2 months (GMT: 21.52). These data raise concern that humoral immunity against SARS-CoV-2 may not be long-lasting in people with mild illness, threatening their protective status. Moreover, neutralizing antibody titers from all study subjects did not show a good correlation with the level of circulating IgG antibodies evaluated in ELISA or CMIA. In particular, only a modest correlation ($r = .60$) was found with ELISA values, while weak correlation ($r = .44$) was shown with CMIA. This can be easily explained on the basis of the antigen used in each test. Indeed, ELISA was based on all the viral proteins,

TABLE 1 Serological analysis of the study population according to the clinical outcome in subjects screened once (Table 1A) and twice (Table 1B)

Table 1A	Severe cases (H) T_0 (30)	Pauci-symptomatic (P) T_0 (30)
CMIA IgG (S/SCO)	6.21 (5.47–6.95)	4.95 (3.97–5.93)
ELISA IgG (AU)	7.31 (5.82–8.80)	4.06 (2.81–5.31)
NT Ab (GMT)	87.7 (54.9–121.0)	23.3 (10.4–36.2)

Table 1B	Severe cases (H)		Pauci-symptomatic (P)	
	T_0 (10)	T_1 (10)	T_0 (10)	T_1 (10)
CMIA IgG (S/SCO)	5.63 (4.06–7.22)	5.54 (4.19–6.89)	6.46 (5.23–7.69)	4.94 (3.61–6.27)
ELISA IgG (AU)	6.16 (3.31–9.01)	6.28 (3.68–8.88)	5.01 (2.49–7.53)	3.23 (2.01–4.45)
NT Ab (GMT)	65.38 (0–254.0)	100.51 (14.6–186.0)	29.21 (8.61–49.8)	21.52 (0–45.4)

Note: 95% CI values were indicated below each result.

Abbreviations: AU, arbitrary units; CI, confidence interval; GMT, geometric mean titer; S/SCO, signal/signal cut off.

including the Spike protein, responsible for cell binding to the receptor and containing the sequence recognized by neutralizing antibodies. CMIA was only using the immunogenic nucleoprotein, to which the humoral response is promptly mounted in the host, but it is not involved in the neutralizing activity. The observational time considered in this study was quite short, but the preliminary results indicated that a part of the population, particularly young people who presented a very mild disease, developed a weak humoral response, mainly characterized by a low neutralizing activity that could wane over time. For this reason, patients with high levels of circulating antibodies, especially those who had a severe outcome, could be more likely protected, while subjects with a favorable outcome, who showed low levels of neutralizing antibodies, may not maintain a long-lasting response and be susceptible to reinfection. Therefore, it could be important to keep monitoring both kind of subjects and see whether a time-dependent decrease of both circulating and neutralizing IgG antibodies to nonprotective levels could occur in a longer time course.

This finding may have implications for immunity strategy and prevention, since it is still not clear whether the immunity is long-lasting and the potential vaccines, based on the spike antigen, are able to induce a durable response and herd immunity. Further studies are necessary to understand the role of cellular immune response and identify the correlates of protection for COVID-19.

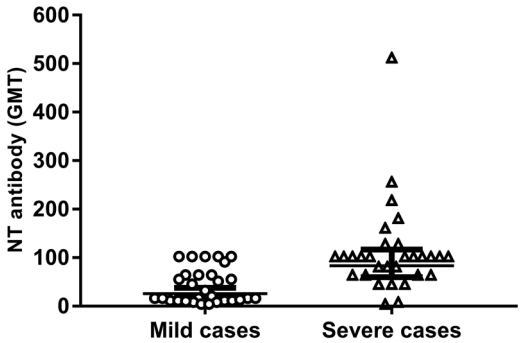

FIGURE 1 Differences in neutralizing antibody titers between SARS-CoV-2 infected patients with mild or severe outcome. The whiskers represent the values from the 5th to the 95th percentiles; the GMTs are depicted by the horizontal lines in the boxes. Individual data points are shown. The *p* value of the GMT between the two groups is 0.0002. GMT, Geometric mean titer; SARS-CoV-2, severe acute respiratory syndrome coronavirus-2

CONFLICT OF INTERESTS

The authors declare that there are no conflict of interests.

AUTHOR CONTRIBUTIONS

Conceptualization: Maria Grazia Cusi. Data curation: Maria Grazia Cusi, Gabriele Anichini. Investigation: Gianni Gori Savellini. Methodology: Gabriele Anichini, Claudia Gandolfo, Chiara Terrosi and Shibily Prathyumnan. Resources: Simonetta Fabrizi, Giovanni Battista Miceli and Federico Franchi. Supervision: Maria Grazia Cusi. Writing—original draft: Gabriele Anichini. Writing—review and editing: Maria Grazia Cusi. All authors revised and approved the final version of the manuscript.

ORCID

Maria Grazia Cusi http://orcid.org/0000-0001-8869-8164

REFERENCES

1. Zhu N, Zhang D, Wang W, et al. China novel coronavirus investigating and research team. A novel coronavirus from patients with pneumonia in China. *N Engl J Med*. 2020;382:727-733.
2. Lu R, Zhao X, Li J, et al. Genomic characterisation and epidemiology of 2019 novel coronavirus: implications for virus origins and receptor binding. *Lancet*. 2020;395:565-574.
3. Li X, Wang W, Zhao X, et al. Transmission dynamics and evolutionary history of 2019-nCoV. *J Med Virol*. 2020;92:501-511.

4. Lu H, Stratton CW, Tang YW. Outbreak of pneumonia of unknown etiology in Wuhan, China: the mystery and the miracle. *J Med Virol*. 92, 2020:401-402.
5. Patel R, Babady E, Theel ES, et al. Report from the American Society for Microbiology COVID-19 International Summit, 23 March 2020: value of diagnostic testing for SARS-CoV-2/COVID-19. *mBio*. 2020; 11:e00722-20.
6. Guo L, Ren L, Yang S, et al. Profiling early humoral response to diagnose novel coronavirus disease (COVID-19). *Clin Infect Dis*. 2020;71:778-785.
7. Zhao J, Yuan Q, Wang H, et al. Antibody responses to SARS-CoV-2 in patients of novel coronavirus disease. *Clin Infect Dis*. 2020:28ciaa344.
8. Ou X, Liu Y, Lei X, et al. Characterization of spike glycoprotein of SARS-CoV-2 on virus entry and its immune cross-reactivity with SARS-CoV. *Nat Commun*. 2020;11:1620.
9. Zeng W, Liu G, Ma H, et al. Biochemical characterization of SARS-CoV-2 nucleocapsid protein. *Biochem Biophys Res Commun*. 2020;527:618-623.
10. Long QX, Liu BZ, Deng HJ, et al. Antibody responses to SARS-CoV-2 in patients with COVID-19. *Nat Med*. 2020;26:845-848.
11. Amanat F, Stadlbauer D, Strohmeier S, et al. A serological assay to detect SARS-CoV-2 seroconversion in humans. *Nat Med*. 2020;26: 1033-1036.
12. Okba NMA, Müller MA, Li W, et al. Severe acute respiratory syndrome coronavirus 2-specific antibody responses in coronavirus disease patients. *Emerg Infect Dis*. 2020;26:1478-1488.
13. Wölfel R, Corman VM, Guggemos W, et al. Virological assessment of hospitalized patients with COVID-2019. *Nature*. 2020;581:465-469.
14. Wu F, Wang A, Liu M, et al. Neutralizing antibody responses to SARS-CoV-2 in a COVID-19 recovered patient cohort and their implications. *medRxiv*. 2020. https://doi.org/10.1101/2020.03.30.20047365
15. Li R, Pei S, Chen B, et al. Substantial undocumented infection facilitates the rapid dissemination of novel coronavirus (SARS-CoV-2). *Science*. 2020;368:489-493.
16. Grzelak L, Temmam S, Planchais C, et al. A comparison of four serological assays for detecting anti-SARS-CoV-2 antibodies in human serum samples from different populations. *Sci Transl Med*. 2020;12(559). https://doi.org/10.1101/2020.04.21.20068858
17. Reed LJ, Muench H. A simple method of estimating fifty per cent endpoints. *Am J Hyg*. 1938;27:493-497.
18. Cao WC, Liu W, Zhang PH, Zhang F, Richardus JH. Disappearance of antibodies to SARS-associated coronavirus after recovery. *N Engl J Med*. 2007;357:1162-1163.
19. Chang SC, Wang JT, Huang LM, et al. Longitudinal analysis of Severe Acute Respiratory Syndrome (SARS) coronavirus-specific antibody in SARS patients. *Clin Diagn Lab Immunol*. 2005;12:1455-1457.
20. Ibarrondo FJ, Fulcher JA, Goodman-Meza D, et al. Rapid decay of Anti-SARS-CoV-2 antibodies in persons with mild Covid-19. *N Engl J Med*. 2020;383:1085-1087NEJMc2025179.

How to cite this article: Anichini G, Gandolfo C, Terrosi C, et al. Antibody response to SARS-CoV-2 in infected patients with different clinical outcome. *J Med Virol*. 2021;1–5. https://doi.org/10.1002/jmv.26789